

Mean field theory of spin glasses

Francesco Zamponi

*Laboratoire de Physique Théorique,
École Normale Supérieure, 24 Rue Lhomond,
75231 Paris Cedex 05, France
<http://www.lpt.ens.fr/~zamponi>*

(Dated: September 23, 2014)

These lecture notes focus on the mean field theory of spin glasses, with particular emphasis on the presence of a very large number of metastable states in these systems. This phenomenon, and some of its physical consequences, will be discussed in details for fully-connected models and for models defined on random lattices. This will be done using the replica and cavity methods.

These notes have been prepared for a course of the PhD program in Statistical Mechanics at SISSA, Trieste and at the University of Rome “Sapienza”. Part of the material is reprinted from other lecture notes, and when this is done a reference is obviously provided to the original. I would like to warmly thank all the students and colleagues who read these notes, gave me their feedback and sent me their corrections, that allowed to fix many errors on the original manuscript. I also would like to thank SISSA and the University of Rome “Sapienza” for inviting me to give these lectures.

Contents

I. Introduction	3
A. Why study spin glasses?	3
B. Physical systems	3
C. Optimization problems	4
D. Models and universality classes	6
E. Frustration and quenched disorder	7
F. What is missing in these notes	8
II. Fully connected models	9
A. Free energy functional	9
1. The fully connected Ising ferromagnet	9
2. Metastable states in fully connected models	10
3. The general definition of the free energy functional	10
4. The Georges-Yedidia expansion	12
5. Free energy functional for a generic Ising model	13
6. Back to the fully connected ferromagnet	14
7. TAP equations for the SK model	15
8. Spherical p -spin model	15
9. Summary and remarks	16
B. Metastable states and complexity	17
1. The simplest example: the spherical p -spin glass model	17
2. The partition function	17
3. A method to compute the complexity	19
4. Replicated free energy of the spherical p -spin model	20
5. 1-step replica symmetry breaking	23
6. The phase diagram of the spherical p -spin model	24
7. Spontaneous replica symmetry breaking: the order parameter	26
C. The SK model: full replica symmetry breaking	26
1. The overlap distribution	27
2. The Parisi solution of the SK model	28
D. Susceptibilities	29
1. The ferromagnet	30
2. Spin glasses: linear susceptibilities	31
3. The static spin glass susceptibility	32

4. The dynamic spin glass susceptibility	33
E. Exercises	34
III. Diluted models and optimization problems	36
A. Definitions	36
1. Statistical mechanics formulation of optimization problems	36
2. Random optimization problems: random graphs and hypergraphs	37
3. Connectivity-temperature phase diagram	38
B. XORSAT: clustering and SAT/UNSAT transition	40
1. Bounds from the first and second moments methods	40
2. The leaf-removal algorithm	42
3. Clustering and SAT/UNSAT transitions.	45
4. On backbones	47
5. Summary	48
C. The replica symmetric cavity method	48
1. Recursions on a finite tree	49
2. From a tree to a random graph	50
3. Replica symmetric cavity equations in absence of local disorder	51
4. An alternative derivation	53
5. Fluctuations of the local environment: distributions of cavity probabilities	56
6. The zero temperature limit	57
7. On a factor graph	58
8. Summary	59
D. 1-step replica symmetry breaking	59
1. The auxiliary model	60
2. RS cavity equations for the auxiliary model: the 1RSB equations	61
3. Homogeneous 1RSB equations	62
4. Complications: spatial fluctuations, factor graphs	63
E. Phase transitions in q -COL	64
F. Exercises	65
IV. Conclusions and perspectives	70
References	71

I. INTRODUCTION

A. Why study spin glasses?

Spin glasses have been intensively studied since the seventies [1, 2]. The original motivation was to describe a class of magnetic alloys, but it was realized early on that they are representative of a much more general class of disordered systems. The concept of “disordered system” is obviously very generic. Disordered systems in fact display many different and interesting phenomena whose description might be the subject of a collection of monographs.

In these notes we will limit ourselves to discuss the main physical properties of spin glasses and list different systems that share the same properties. Spin glasses are very interesting for many reasons [3]:

- Spin glasses are the simplest example of *glassy systems*. Glassy systems are a class of disordered systems that share a common phenomenology, characterized by a very slow dynamics in the low temperature phase. In spin glasses, there is a highly non-trivial mean field approximation where one can study phenomena that have been discovered for the first time in this context, the most striking one being *the existence of many equilibrium states*¹.
- The study of spin glasses opens a very important window for studying the out-of-equilibrium behavior of glassy systems, i.e. their dynamic evolution when abruptly cooled into the low-temperature phase starting from high temperature. In this framework it is possible to derive some of the main properties of generic glassy systems, such as their history-dependent response [8–10]. This property, in the context of mean field approximation, is related to the existence of many equilibrium states. Aging and the related violations of the equilibrium fluctuation dissipation relations emerge in a natural way and can be studied within this simple setting [11–13].
- The theoretical concepts and the tools developed in the study of spin glasses are based on two logically equivalent although very different, methods: the algebraic broken replica symmetry method and the probabilistic cavity approach [9]. Both have a wide domain of applications. Some of the properties that appear in the mean field approximation, like ultrametricity, are unexpected and counterintuitive.
- Spin glasses also provide a testing ground for a more mathematically inclined probabilistic approach: the rigorous proof of the correctness of the solution of the mean field model came out after twenty years of efforts where new ideas, e.g. new variational principles [14], were at the basis of a recent rigorous proof (see [15] and [16] for a concise explanation of the main ideas) of the correctness of the mean field approximation in the case of the infinite range Sherrington-Kirkpatrick and p -spin models that we will introduce below.

B. Physical systems

Many physical systems have been described using methods and ideas borrowed from the spin glass physics. We list some of them below in order to illustrate the wide variety of physical situations. Details can be found in the references.

- Real spin glasses: these are typically metallic materials hosting magnetic impurities located at random positions. The spin polarization of the electrons around the magnetic impurity is oscillating at large distance,

$$S_{\text{ind}}(r) \sim \frac{\cos 2k_F r}{r^3} ; \quad (1)$$

these are called *Friedel oscillations* and are related to the existence of the Fermi surface (see chapter 2 of [10] for more details). Therefore, the coupling between two spins has random sign and intensity, because the distance between two spins is a random variable. The simplest idealization of the interaction between two spins S_i and S_j is a coupling term $-J_{ij}S_i \cdot S_j$ in the Hamiltonian, and J_{ij} is taken to be a random variable. In these materials the *disorder* (i.e. the values of the J_{ij}) is due to the doping with impurities, so in some sense it is put there “by hand” when preparing the sample (it is called *quenched disorder* in the literature).

¹ This sentence is too vague: one should discuss its precise mathematical meaning; although we will present later a physically reasonable definition, for a careful discussion see Refs. [4–7].

- Glass-forming liquids [17–19]: many liquids, when cooled fast enough, freeze in an amorphous state or *glass*. One may think for example to a system of hard spheres, or of point-like particles interacting via a Lennard-Jones potential. In a glass, the density profile is not uniform and the particles prefer to stay close to a set of sites that is not periodic, unlike in a crystal. In the glass case, the local environment of each particle is different. Yet no disorder is present in the original Hamiltonian because the interactions between the particles are deterministic. We may say instead that the disorder is *self-generated* by the system. In addition to hard-spheres and Lennard-Jones systems, many more complicated liquids like molecular liquids and polymeric liquids display a glass transition.
- Colloidal dispersions are typically made by mesoscopic particles dispersed in water or other solvents. The interaction between the particles can be tuned by adding different components to the solutions, and a wide variety of potentials, ranging from purely hard-core to long range interactions have been created. These systems usually display, at high enough concentration of particles, a dynamical arrest very similar to the one observed in glass forming liquids. Some ideas from glass physics have been applied to the study of these systems, mainly of their dynamics [20]. Note that, due to the wide variety of potentials that can be engineered, in some cases the underlying microscopic phenomenon might be very different, leading to different arrested phases such as gels, stripe phases, etc.
- Quantum glasses: there are many quantum systems that exhibit a glassy behavior. Obviously, one can consider spin glass materials in which quantum effects are important. But in addition, people have found an *electron (or Coulomb) glass* (see e.g. [21] and references therein) by considering a system of electrons close to the metal-insulator transition. The observation of an electronic glass phase has also been reported in high- T_c superconducting cuprates [22]. A particular glass phase (called *valence bond glass*) is present in a model of hopping electrons on a frustrated lattice [23]. Glass phases are expected also in systems of interacting bosons like cold atoms, see e.g. [24] and references therein. Recently, the observation of a superfluid-like response in disordered solid He^4 has motivated the study of superfluid glassy (*superglass*) phases [25].
- Random lasers: one can consider a cavity filled with a disordered system, e.g. a solution of mesoscopic particles in a liquid or glassy matrix with different refractive index. The particles act as a disordered set of scatterers for light; therefore the modes of the electromagnetic field into the cavity are disordered. If an amplifying molecule is present in the solution, coherent amplification of the modes can be realized and a lasing phenomenon is observed; many modes can be excited at the same time. The dynamics of the phases of the lasing modes can be described by an equation that closely resemble that of a spin glass model; this led to the prediction of a glassy phase for the system, manifested in a locking of the phases of the modes to random position. This phenomenon has been called *random mode locking* and is the disordered version of the standard mode-locking phenomenon that is observed in multimode laser cavities [26].
- Granular materials: these are ensemble of macroscopic particles, that, unlike in colloidal systems, are not dispersed in a solvent. Their mass is so large that the potential energy due to gravity ($\sim mgd$, with d the diameter of one particle) is much bigger than $k_B T$. Therefore in these systems thermal fluctuations are irrelevant, and their physics is dominated by gravity and frictional forces between the grains. A typical example is rice in a silos. In addition, the system might be agitated by an external force, like for nuts transported in a truck. The dynamics of these systems under external forces is very important for industrial applications. The configurations of the grains are typically amorphous, and some concepts borrowed from the physics of glasses have been applied to describe them, see e.g. [27].
- Biological systems: spin glass models have been used for a long time to describe several different biological systems. Probably the most successful example is that of neural networks [28]; in addition, other phenomena such as the folding of proteins have been studied using these methods [29–31]. Another important application of spin glass models is the inference of correlations hidden in biological data [32–36]. This field is now growing very quickly and there are many other applications that can be listed here.

C. Optimization problems

In addition to the above long list of physical systems, spin glass techniques have been applied to a large class of computer science problems, called “optimization problems”: this connection dates back from twenty years at least [9, 37]. In an optimization problem, one looks for a configuration of parameters minimizing some cost function (the length of a tour in the traveling salesman problem (TSP), the number of violated constraints in constrained satisfaction problems, etc.) [38].

As an example, consider a linear system of Boolean equations [37]: it is given a set of N Boolean variables x_i with indices $i = 1, \dots, N$. Any variable shall be False (F) or True (T). The sum of two variables, denoted by $+$, corresponds to the logical exclusive OR between these variables defined through,

$$\begin{aligned} F + T &= T + F = T \quad , \\ F + F &= T + T = F \quad . \end{aligned} \quad (2)$$

In the following we shall use an alternative representation of the above sum rule. Variables will be equal to 0 or 1 instead of F or T , respectively. The $+$ operation then corresponds to adding integer numbers, modulo two.

A linear equation involving three variables is for example $x_1 + x_2 + x_3 = 1$. Four among the $2^3 = 8$ assignments of (x_1, x_2, x_3) satisfy the equation: $(1, 0, 0)$, $(0, 1, 0)$, $(0, 0, 1)$ and $(1, 1, 1)$. A Boolean system of equations is a set of Boolean equations that have to be satisfied together. For instance, the following Boolean system involving four variables

$$\begin{cases} x_1 + x_2 + x_3 = 1 \\ x_2 + x_4 = 0 \\ x_1 + x_4 = 1 \end{cases} \quad (3)$$

has two solutions: $(x_1, x_2, x_3, x_4) = (1, 0, 0, 0)$ and $(0, 1, 0, 1)$. A system with one or more solutions is called satisfiable. Determining whether a Boolean system admits an assignment of the Boolean variables satisfying all the equations constitutes the XORSAT (exclusive OR Satisfaction) *decision* problem.

In spin language the problem can be reformulated as follows. We associate to each variable $x_i = 0, 1$ a spin $S_i = (-1)^{x_i}$. The equation $x_1 + x_2 = a$, where $a = 0, 1$, can be rewritten as $JS_1S_2 = 1$, where $J = (-1)^a$, and similarly for equations involving more variables². The system (3) can be rewritten as

$$-S_1S_2S_3 + S_2S_4 - S_1S_4 = 3 \quad . \quad (4)$$

Consider for simplicity a system of M equations, each involving two variables; it is equivalent to

$$H = - \sum_{(i,j)} J_{ij} S_i S_j = -M \quad , \quad (5)$$

where the sum is over all the pairs (i, j) that appear in one of the M equations³. The XORSAT decision problem is therefore equivalent to the following question: is the ground state energy of H equal to $-M$ or not?

In the decision problem one is asked to determine whether a given set of constraints can be satisfied or not. One can also consider the *optimization* version of the XORSAT problem, that consists in finding the ground state of H , or in other words of finding the maximum possible number of equations that can be simultaneously satisfied. The connection between (zero temperature) statistical mechanics and optimization should be clear from this example, and as we will see the Hamiltonian (5) is a typical spin glass Hamiltonian.

In spin glasses the J_{ij} are random variables. For instance, in the example (5), we can decide that each variable appears in *exactly* in z equations; the total number of equation is then $M = Nz/2$. Consider a graph such that each variable is a vertex and a link (i, j) correspond to an equation involving S_i and S_j . Then with this choice the model is defined on a graph such that each vertex has exactly z neighbors. We give equal probability to all graphs satisfying this constraint. For each equation (link) the corresponding coupling J_{ij} is taken as a random variable.

In computer science, random distribution of instances, such as the one we introduced above, have been used as a benchmark to test the behavior of *search algorithms*, i.e. algorithms that try to find a ground state of H (a solution of the problem). In physical language, a search algorithm correspond in some cases to a dynamical rule that, starting from a configuration of the spins, attempts to explore the configuration space while looking for the ground state. A typical example is Monte Carlo dynamics at very low temperature. The presence of a low-temperature “glassy” phase in the model, associated to slow dynamics, is clearly important for the performances of these algorithms. This is an important motivation to study the spin glass phases of such Hamiltonians.

Note that, despite the beautiful studies of the average properties of the TSP, Graph partitioning, Matching, etc., based on spin glass methods [9], a methodological gap between the field of statistical physics and that of computer

² An equation of length K , $x_1 + \dots + x_K = a$, is equivalent to $JS_1 \dots S_K = 1$.

³ For a generic system of M equations labeled by $a = 1, \dots, M$ one has $H = - \sum_{a=1}^M J_a S_{i_1^a} \dots S_{i_{K_a}^a} = -M$, where K_a is the length of equation a and $i_1^a, \dots, i_{K_a}^a$ is the set of variables belonging to equation a .

science is far from being bridged. In statistical physics statements are usually made on the properties of samples that are typical with respect to some disorder distribution (i.e. distribution of the J_{ij}). In optimization, however, one is interested in solving one (or several) particular instances of a problem, and needs efficient ways to do so, that is, requiring a computational effort growing not too quickly with the number of data defining the instance. Knowing precisely the typical properties for a given distribution of instances might not help much to solve practical cases. Unfortunately, statistical mechanics is for the moment unable to tell us precise properties for a given sample, i.e. for a given realization of the couplings.

Finally, note that the recent developments in quantum computing triggered some efforts to study the performances of quantum algorithms to solve these problems (see e.g. [39] for a review). Therefore, recently quantum versions of the problems (in which Ising spins are replaced by Pauli matrices and a transverse field is added) have been considered [40]. Understanding the properties of quantum spin glasses may also be important in this respect.

D. Models and universality classes

The simplest spin glass Hamiltonian has the form:

$$H = \sum_{i,k}^{1,N} J_{ik} S_i S_k, \quad (6)$$

where the J 's are *quenched* (i.e. time independent) random variables located on the links connecting two points of the lattice and the S 's are Ising variables (i.e. they are equal to ± 1). The total number of points is denoted with N and it goes to infinity in the thermodynamic limit. We will always assume that $J_{ii} = 0$, obviously, and $J_{ij} = J_{ji}$.

We can consider four models, whose solution is increasingly difficult to obtain [3]:

- The Sherrington-Kirkpatrick (SK, or *fully connected*) model [9, 41]: All J 's are random and different from zero, with a Gaussian or a bimodal distribution with variance $N^{-1/2}$. The coordination number $z = N - 1$ goes to infinity with N . In this case a mean field theory is valid in the infinite N limit [9].
- The Bethe lattice model [42–44]: The spins live on a random lattice such that each variable has z neighbors, therefore only $Nz/2$ J 's are different from zero: they have finite variance, it is convenient to choose $z^{-1/2}$ in order to have a good limit $z \rightarrow \infty$. In this case a modified mean field theory is valid. Note that this model correspond exactly to the XORSAT problem (5) if the distribution of the J is bimodal (up to a rescaling of H).
- The large range model [45]: The spins belong to a finite dimensional lattice of dimension D . Only nearest spins at a distance less than R interact and the variance of the J 's is proportional to $1/R^{D/2}$. If R is large, the corrections to mean field theory are small for thermodynamic quantities. They may, however, change the large distance behavior of the correlations functions and the nature of the phase transition, which may even disappear.
- The Edwards-Anderson (*finite dimensional*) model [1, 2]: The spins belong to a finite dimensional lattice of dimension D : only nearest neighbor interactions are different from zero and their variance is $D^{-1/2}$. In this case finite corrections to mean field theory are present, that are certainly very large in one or two dimensions, where no transition is expected. The Edwards-Anderson model corresponds to the limit $R = 1$ of the large range Edwards-Anderson model; both models are expected to belong to the same universality class. The large range Edwards-Anderson model provides a systematic way to interpolate between the mean field results and the short range model.

As far as the free energy is concerned, one can prove the following rigorous results:

$$\begin{aligned} \lim_{z \rightarrow \infty} \text{Bethe}(z) &= \text{SK} , \\ \lim_{R \rightarrow \infty} \text{Large range}(R) &= \text{SK} , \\ \lim_{D \rightarrow \infty} \text{Edwards-Anderson}(D) &= \text{SK} , \end{aligned} \quad (7)$$

The Sherrington-Kirkpatrick model is thus also a good starting point for studying the finite-dimensional case with short-range interactions, which is both the most realistic and the most difficult case to study. This starting point becomes worse and worse when the dimension decreases; for instance, it is not of any use in the limit where $D = 1$.

In the following we will mostly focus on the mean field theory of spin glasses, which gives the correct solution of the fully connected (SK) and Bethe lattice models. This theory is very complex and has already been the subject of several books and review papers [8, 9, 46]. Giving a complete account of the mean field theory of glasses is already a task that goes beyond the aim of these notes.

One of the main results of the theory is the existence of two distinct classes of models displaying a very different phenomenology:

1. The models defined above (except possibly the finite dimensional version) belong to a class of models called “full replica symmetry breaking” (fRSB). At high temperature they are in a paramagnetic phase akin to that of the ferromagnetic Ising model. Upon lowering the temperature, however, they undergo a transition to a spin glass phase. For these models, it is a second-order phase transition, to which are associated a diverging correlation length and power-law singularities controlled by critical exponents. Even in the mean field description, the low temperature phase is very complex. The equilibrium states are organized in an intricate hierarchical way, and the order parameter is a function. The mean field theory of fRSB models is reviewed in [8, 9].
2. A class of simpler models exist, where the (many) equilibrium states are organized in a much simpler way: different states are simply uncorrelated, in a sense that we will be made precise below. These models are called “one-step replica symmetry breaking” models (1RSB). The transition to the spin glass phase, in these models, is quite different from the fRSB case: although it is still second order from the thermodynamic point of view, the order parameter jumps at the transition, making it first order in some sense. In this case, the identification of a diverging correlation length and associated critical exponents is not evident. The simplest representative of this class of models is the spin glass Hamiltonian

$$H[S] = \sum_{i,j,k}^{1,N} J_{ijk} S_i S_j S_k, \quad (8)$$

which is called 3-spin glass. Again, we assume that J_{ijk} is zero when two or more indexes are equal, and that they are symmetric under permutations of the indexes. More generally one can consider $p > 2$ spin interactions, hence the name p -spin glass. As in the previous case, one can consider the fully connected, Bethe lattice, large range and finite dimensional versions of this model, and the relations (7) hold also in this case for the free energy. The mean field theory of 1RSB models is reviewed in [46].

The analysis of 1RSB models is fortunately much simpler than that of fRSB ones, and their phenomenology is also quite interesting and rich. Additionally, many interesting systems like fragile glasses and many optimization problems are conjectured to belong to this class. We will therefore start our analysis by studying p -spin glasses, and then describe (shortly) the solution of the more complicated SK model.

E. Frustration and quenched disorder

There are two common ingredients in all the models and physical systems we discussed above: *disorder* and *frustration*. The disorder, in some cases, is built in the Hamiltonian (the coupling J_{ij} are random); it represents for instance the random position of the impurities. Clearly, the impurities might diffuse throughout the sample, so J_{ij} should formally be considered as dynamical variables. Because the time scale of this evolution is much larger than any interesting time scale in the glass problem, however, we can consider the J_{ij} as essentially constant i.e. *quenched*.

When computing the partition function, we thus keep the J 's fixed,

$$Z_J(\beta) = \sum_S e^{-\beta H[S]}, \quad (9)$$

and from the partition function we can compute observables such as the energy, entropy, free energy, magnetization, etc. It is *these* quantities that should then be averaged over the distribution of the J 's. The average free energy must therefore be defined by a so-called *quenched* average over the disorder:

$$f = \overline{f_J} = -T \overline{\frac{1}{N} \log Z_J}. \quad (10)$$

In this way, the usual thermodynamic identities are satisfied: for instance, the average entropy is

$$s = -\frac{df}{dT} = -\overline{\frac{df_J}{dT}} = \overline{s_J}. \quad (11)$$

Ideally, we would like to know the properties of the system for each given realization of the J 's, that corresponds to a given physical sample. Fortunately, one can show that *intensive* quantities such as f , s , etc., are *self-averaging*, which means that in the large volume limit they converge with probability one (with respect to the distribution of the J 's) to the average defined above. As far as such observables are concerned, the average over the disorder is representative of the behavior of the typical sample. Yet, as discussed above, in some applications (mainly in computer science) one would like to know the properties of rare samples corresponding to particular choices of the J 's, or to have bounds that hold for any choice of the J 's. Unfortunately, these problems cannot be tackled using the methods described here.

In other cases, the disorder is self-generated by the system, as for glass-forming liquids. In these cases, clearly, the explicit average over the disorder is not needed.

Another crucial ingredient is *frustration*. In the examples above, this is due to the fact that the J 's have random signs. Therefore, a given spin is subject to fields due to their neighbors that have different signs. Some wants it to point up and others to point down. For this reason finding the ground state is not trivial and as we will see many degenerate ground states may be present. Note that this would not happen if all the J 's were negative: in this case the ground state, even in presence of disorder, would simply be a configuration where all spins are equal.

F. What is missing in these notes

It will be impossible to cover all the relevant issues about the complex physics of spin glasses. In the following, we will try to review some aspects of this problem, by alternating general discussions with some more technical sections where methods and techniques of general importance will be introduced.

We will focus more on *equilibrium* properties of *mean field* spin glasses, and a detailed investigation of the *dynamics* of spin glasses will not be done. Still, dynamics is very important and is probably the most relevant aspect for making contact with experiments. Excellent reviews can be consulted by readers who wish to dig deeper into this important subject [12, 46]. The notes are divided in two parts: the first is devoted to fully-connected models and the replica method, while the second to Bethe lattice models and the cavity method. We will not discuss finite dimensional models since the extension of these concepts to finite dimensional models is still debated; reviews and further references can be found in [18, 19] for 1RSB models and [6] for fRSB ones. Some exercises are proposed at the end of each section. Ideally they should be done while reading the notes; the appropriate moments are marked in the text by \Rightarrow **Ex. N.n.**

II. FULLY CONNECTED MODELS

We said in the introduction that frustration causes the existence of many thermodynamic states and that this is the main interesting property of glassy systems and in particular of spin glasses. The aim of this section is to make this statement more precise, by looking to the exact solution of fully connected models: the SK model belongs to the fRSB class and the spherical p -spin model belongs to the 1RSB class. Our aim here is to understand the nature of the transition and of the low temperature phase; to identify the symmetry that is broken (if any) and a correct order parameter; and to discuss what are the relevant susceptibilities that diverge signaling the transition.

A. Free energy functional

1. The fully connected Ising ferromagnet

Before turning to the more complicated case of spin glasses, we will here review very briefly the concept of *metastable state* for the familiar Ising ferromagnet. We will limit ourselves to the fully connected case where the definition is much simpler; for a general discussion see [47].

Let us then consider the fully connected Ising model, whose Hamiltonian is given by

$$H[S] = -\frac{J}{2N} \sum_{i,j}^{1,N} S_i S_j - \mathcal{B} \sum_{i=1}^N S_i = -\frac{NJ}{2} (m[S])^2 - N\mathcal{B}m[S], \quad (12)$$

where we defined $m[S] = \sum_{i=1}^N S_i / N$ as the magnetization per spin with $S_i = \pm 1$. The Hamiltonian $H[S]$, and consequently the Gibbs probability $P[S] \propto \exp -\beta H[S]$, depend only on the magnetization $m[S]$. The total probability that the system has magnetization $m[S] = m$ can thus be written as the product of the probability of a given configuration with $m[S] = m$ times the number of such configurations; the latter is a combinatorial factor counting the number of ways one can choose $N_+ = N(1+m)/2$ spins (out of N) to be equal to $+1$. We obtain

$$P(m) \propto e^{N[\beta J m^2 / 2 + \beta \mathcal{B} m]} \binom{N}{N_+} \sim e^{N[\beta J m^2 / 2 + \beta \mathcal{B} m + s_0(m)]} = e^{-\beta N f(m)}, \quad (13)$$

where

$$s_0(m) = \lim_{N \rightarrow \infty} \frac{1}{N} \log \binom{N}{N(1+m)/2} = -\frac{1+m}{2} \log \frac{1+m}{2} - \frac{1-m}{2} \log \frac{1-m}{2}. \quad (14)$$

The function $f(m)$ defined in Eq. (13) is the *large deviation function* associated to the magnetization m . If plotted as a function of m , it has a familiar form: at high temperature it is a convex function with a single minimum in $m = 0$, while below a *critical temperature* (in this case $T = 1$) there are two minima at $m = \pm m^*$ and a maximum in $m = 0$ and $f(m)$ is no more convex, see figure 1. In presence of a non-zero external field \mathcal{B} , one of the two minima has a lower $f(m)$ (a higher probability).

The function $f(m)$ is related to the probability, *at equilibrium*, to find the system in a configuration with magnetization m . This means that at low temperatures, there is high probability of finding the system with magnetization $\pm m^*$ (one of the two values will be preferred for $\mathcal{B} \neq 0$), while there is a low probability of finding an intermediate value of m , in particular $m \sim 0$. In other words, the system spends a lot of time close to configurations with $m = \pm m^*$, and much less time close to configurations with $m \sim 0$. Yet in order to go from $-m^*$ to $+m^*$, the magnetization must cross $m \sim 0$. The number of such transitions must be very small, or the probability of $m \sim 0$ would otherwise be large. The only possible solution is that the system stays for a long time close to $-m^*$, then performs a fast jump to m^* , stays a long time there, then performs a fast jump in the other direction, and so on.

To be more precise we should introduce a model of the dynamics and analyze it in details (\Rightarrow **Ex.II.1**). A nice and detailed discussion of this aspect by R. Monasson can be downloaded from <http://www.phys.ens.fr/~monasson/Appunti/ising.ps>. It turns out that the system stays close to $\pm m^*$ for large time intervals, whose length scales as $\tau_{\pm} \sim \exp N t_{\pm}$, while the rare jumps between these two states take a time that increases only polynomially with N , $\tau_{jump} \sim N^{\alpha}$. In other words, if prepared close to one of the two minima of the free energy, the system remains there with high probability, for a time that scales exponentially with N . This description is true for both minima, and in particular for the one with higher $f(m)$, which makes it less probable. This minimum is thus a classic example of a metastable state.

We are led to identify metastable states with the minima of a suitable free energy function $f(m)$. Before turning to a more general definition, it is useful to highlight some of its properties that will be important in the following. We know that $f(m)$ is an analytic function of *both* m and β . It does not show any singularity at the critical temperature. Yet we also know that for $\mathcal{B} = 0$ there is a phase transition at $T = 1$. The average magnetization is zero above $T = 1$ and non-zero below. The total free energy of the system is indeed given by

$$f = -\frac{T}{N} \log Z = -\frac{T}{N} \int dm e^{-\beta N f(m)} = \min_m f(m) . \quad (15)$$

The singularity of the thermodynamic observables (energy, magnetization, etc.) at the phase transition comes *from the bifurcation of the minima of $f(m)$* , i.e. by the minimization involved in the computation of f , and not by a singularity of $f(m)$ itself. This very peculiar property is characteristic of fully connected models. We will see that in more realistic models the situation is completely different. The fact that $f(m)$ is analytic in β at all β nonetheless suggests that we can compute it by a series expansion for small β (actually, in this case βf is just a linear function of β !). We will follow exactly this strategy in the next sections.

2. Metastable states in fully connected models

A general result of statistical mechanics (see e.g. [9, 48]) states that it is always possible to decompose the equilibrium probability distribution as a sum over *pure* states. In finite dimensional systems, pure states are defined by taking the thermodynamic limit with a given boundary condition [48]. If there are many pure states, one can select one of them by adding to the system a small field: the probability distribution of the pure state can be thought as the limit of zero field of the Gibbs measure in presence of the field.

In a fully-connected system such as the Ising model defined in (12), however, there is no space notion since all the spins interact with all others. There is therefore no boundary, and no boundary conditions can be applied to the system. The pure states can only be selected by using an external field. In this way we are able to define the Gibbs distribution restricted to one pure state, $P^\alpha(S_1, \dots, S_N)$. We can write the decomposition of the Gibbs measure as

$$P(S_1, \dots, S_N) = \frac{e^{-\beta H[S]}}{Z} = \sum_\alpha w_\alpha P^\alpha(S_1, \dots, S_N) , \quad (16)$$

where α is an index labeling the states and w_α is the weight of each state, $\sum_\alpha w_\alpha = 1$. In general, a pure state is specified by P^α , or equivalently by the full set of correlation functions $\langle S_{i_1} \dots S_{i_n} \rangle_\alpha$. A very important property of the probability distributions of pure states is the *clustering* property, i.e. the fact that connected correlation vanish at large distance [5]. Since for a fully connected model there is no space notion, the clustering property reads simply

$$P^\alpha(S_1, \dots, S_N) = \prod_{i=1}^N P_i^\alpha(S_i) . \quad (17)$$

In other words, spins are completely decorrelated within one state. The single-spin probability distribution is specified by the average magnetization of the spin S_i , $m_i^\alpha = \sum_S S P_i^\alpha(S)$; in fact for Ising spins we have

$$P_i^\alpha(S) = \frac{1 + m_i^\alpha S}{2} . \quad (18)$$

Thus, in a fully connected spin model, a *pure state* α is completely determined by the set of local magnetizations m_i^α , $i = 1, \dots, N$. Note that this result is valid *only* for these very special models.

3. The general definition of the free energy functional

In the case of the Ising model the two states are characterized by a uniform magnetization, $m_i^\alpha \equiv m^\alpha$. In a disordered system, for a given sample (realization of the J 's) each state is characterized by an amorphous magnetization or density profile. Therefore a good starting point to compute the properties of these states is the free energy as a functional of the magnetization/density profile⁴ [9, 49, 50]. It is a standard object in statistical mechanics, but it is useful to

⁴ In field theory it is the generating function of the irreducible correlation functions.

review here its definition and fix some notations. As we said above, in the general case the magnetization profile is not enough to determine a state since one should specify all the set of correlation function; however, the knowledge of m_i^α is already a good approximation. Therefore the definition of free energy functional that we will give in the following is an useful concept also for finite dimensional systems.

Consider a system of spins⁵ in which an external magnetic field⁶ b_i acts on the spin S_i ; the free energy is

$$-\beta F[b] = \log \sum_S e^{-\beta H[S] + \beta \sum_i b_i S_i} . \quad (19)$$

Here and in the following we omit the explicit dependence of the free energy on β . Note that $F[b]$ is extensive, i.e. proportional to N ; we will use capital letters for extensive quantities. The local magnetization in presence of these fields is

$$m_i[b] = \langle S_i \rangle_b = -\frac{d}{db_i} F[b] , \quad (20)$$

and the susceptibility is

$$\chi_{ij} = \frac{dm_i}{db_j} = -\frac{d^2 F[b]}{db_i db_j} = \beta \langle (S_i - m_i)(S_j - m_j) \rangle_b . \quad (21)$$

Note that χ_{ij} is a positive matrix⁷.

The free energy functional $\Gamma[m]$ is defined as the Legendre transform of $F[b]$:

$$-\beta \Gamma[m] = -\beta \max_b \left[F[b] + \sum_i b_i m_i \right] = \min_b \left[\log \sum_S e^{-\beta H[S] + \beta \sum_i b_i (S_i - m_i)} \right] ; \quad (22)$$

in this way $b = b[m]$ is a solution of (20), i.e. it is the set of local fields $b_i[m]$ that are needed to enforce the magnetizations m_i . The maximum condition comes from the fact that the susceptibility (21) is positive, hence the second derivative of $F[b] + \sum_i b_i m_i$ is negative.

Define, for fixed b_i and m_i , the average

$$\langle O \rangle = \frac{\sum_S O[S] e^{-\beta H[S] + \beta \sum_i b_i (S_i - m_i)}}{\sum_S e^{-\beta H[S] + \beta \sum_i b_i (S_i - m_i)}} ; \quad (23)$$

the field b is determined by the condition that the derivative with respect to b_i of the last expression in Eq. (22) vanishes. This condition can be written using the above definition as

$$\langle S_i - m_i \rangle = 0 . \quad (24)$$

The solution $b[m]$ is the derivative of $\Gamma[m]$:

$$b_i = \frac{d}{dm_i} \Gamma[m] , \quad \frac{db_i}{dm_j} = \frac{d^2 \Gamma[m]}{dm_i dm_j} = (\chi^{-1})_{ij} \geq 0 . \quad (25)$$

and the free energy $F[b]$ is the inverse Legendre transform of $\Gamma[m]$:

$$-\beta F[b] = -\beta \min_m \left[\Gamma[m] - \sum_i b_i m_i \right] ; \quad (26)$$

the stationarity implies that $m[b]$ is a solution of (25), and it must be a minimum since the second derivative of $\Gamma[m]$ is positive. This result leads to an important observation: if there are no external fields, $b_i = 0$, the free energy of the system is

$$F = -T \log \sum_S e^{-\beta H[S]} = \min_m \Gamma[m] . \quad (27)$$

⁵ For a system of particles replace the magnetic field by an external (chemical) potential.

⁶ We will use the letter b to denote external magnetic fields and the letter h to denote internal fields due to the other spins of the system.

⁷ We can write $\chi_{ij} = \langle \delta S_i \delta S_j \rangle$ or in matrix notation $\chi = \langle \delta S \delta S^T \rangle$. Then, for any vector v , we have $v^T \chi v = \langle (\delta S \cdot v)^2 \rangle \geq 0$. This result holds in particular for the eigenvectors of χ , and therefore the eigenvalues are all positive.

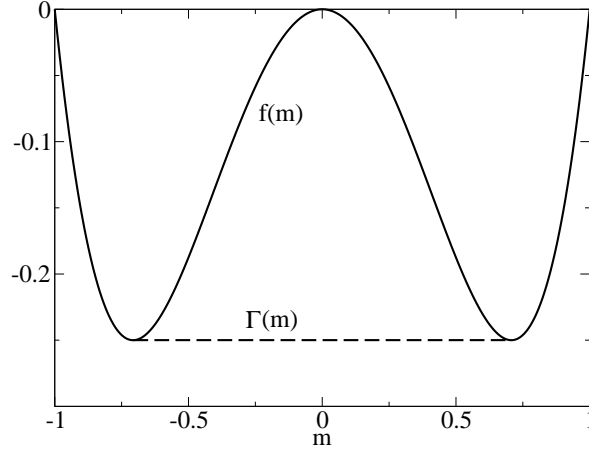


FIG. 1: The functions $f(m)$ and $\Gamma(m)/N$ for the fully connected Ising ferromagnet at $\mathcal{B} = 0$ and $T < 1$.

But we still have a problem: $\Gamma[m]$ is a convex function, hence it cannot have local minima, which is a problem if we want to use $\Gamma[m]$ to define metastable states. What is wrong? The problem can be easily understood by computing $F[b]$ and $\Gamma[m]$ for the fully connected Ising model. We consider a uniform field, $b_i = b$. Using the definition of $F[b]$ and the results of section II A 1:

$$F(b) = -T \log \int dm e^{-\beta N[f(m) - bm]} = N \min_m [f(m) - bm] . \quad (28)$$

Hence $F(b)$ is convex even if $f(m)$ is not convex; inverting the Legendre transform, we obtain that $\Gamma(m)$ is the convex envelope of $f(m)$, see figure 1.

We are therefore interested in $F(m) = Nf(m)$ and not really in $\Gamma(m)$. How can we define in general a non-convex functional $F[m]$, such that its minima are the metastable states? A way out of this problem is to compute the high temperature expansion of $\Gamma[m]$ defined above. The reason is that at $\beta = 0$ there is no interaction and $F[m] = \Gamma[m]$. When expanding around this limit, the convexity can be lost if metastable state appear. One can check explicitly that this gives the correct result for the Ising ferromagnet, which we will do at the end of the computation. Note that for finite dimensional systems, it is not possible to give a general definition of $F[m]$, and metastable states are more difficult to define. Still, expressions of $F[m]$ based on high temperature or low density expansions are often used to define metastable states in an approximate way. In the following, we will denote by $F[m]$ the functional obtained by a high temperature expansion of $\Gamma[m]$ defined in Eq. (22).

4. The Georges-Yedidia expansion

We will now derive a high temperature-small coupling expansion of this functional following the strategy of [51]; we will see that in fully connected models, where individual couplings vanish for $N \rightarrow \infty$, the expansion can be truncated after a finite number of terms, yielding a non-convex free energy functional $F[m]$ whose minima can be identified with the metastable states of the system.

To simplify the notation we define $A^\beta[m] = -\beta F[m]$ and $\lambda_i^\beta = \beta b_i$, and then

$$A^\beta[m] = \log \sum_S e^{-\beta H[S] + \sum_i \lambda_i^\beta (S_i - m_i)} , \quad (29)$$

where as discussed above λ^β is determined by setting $\langle S_i - m_i \rangle = 0$ (the average is on the measure defining A^β for fixed λ^β and m) and thus $\lambda_i^\beta = -\partial_{m_i} A^\beta[m]$. For $\beta = 0$ we can easily compute $A^0[m]$ because there is no interaction among the spins. We give explicit examples below.

We wish now to compute the derivatives of $A^\beta[m]$ at $\beta = 0$. By introducing the “observable”

$$U[S] = H[S] - \langle H \rangle - \sum_i \partial_\beta \lambda_i^\beta (S_i - m_i) \quad (30)$$

and recalling that $m_i = \langle S_i \rangle$ for all β , we get

$$\begin{aligned} \langle U \rangle &= 0 , \\ \frac{d}{d\beta} \langle O \rangle &= \left\langle \frac{\partial O}{\partial \beta} \right\rangle - \langle OU \rangle , \\ 0 &= \frac{dm_i}{d\beta} = \frac{d\langle S_i \rangle}{d\beta} = -\langle S_i U \rangle = -\langle (S_i - m_i)U \rangle . \end{aligned} \quad (31)$$

We then obtain

$$\begin{aligned} \frac{d}{d\beta} A^\beta[m] &= \left\langle -H[S] + \sum_i \partial_\beta \lambda_i^\beta (S_i - m_i) \right\rangle = -\langle H \rangle , \\ \frac{d^2}{d\beta^2} A^\beta[m] &= \langle HU \rangle = \langle U^2 \rangle , \\ \frac{d^3}{d\beta^3} A^\beta[m] &= -\langle U^3 \rangle + \left\langle 2U \frac{\partial U}{\partial \beta} \right\rangle = -\langle U^3 \rangle . \end{aligned} \quad (32)$$

and so on. To compute these derivatives at $\beta = 0$, we need to know $\partial_\beta \lambda_i^\beta(\beta = 0)$ that enters in U , and for the higher order derivatives, higher derivatives of λ^β also appear. The derivatives of λ^β at $\beta = 0$ can be computed recalling that $\lambda_i^\beta = -\partial_{m_i} A^\beta[m]$, so

$$\frac{d^n}{d\beta^n} \lambda_i^\beta = -\frac{\partial}{\partial m_i} \frac{\partial^n A^\beta[m]}{\partial \beta^n} . \quad (33)$$

For instance,

$$\begin{aligned} \frac{d}{d\beta} \lambda_i^\beta(\beta = 0) &= \frac{d}{dm_i} \langle H \rangle_0 , \\ \frac{d^2}{d\beta^2} \lambda_i^\beta(\beta = 0) &= -\frac{d}{dm_i} \langle U^2 \rangle_0 , \end{aligned} \quad (34)$$

and so on.

5. Free energy functional for a generic Ising model

As an example, we consider a model of Ising spins with Hamiltonian

$$H[S] = -\frac{1}{2} \sum_{i \neq j} J_{ij} S_i S_j - \mathcal{B} \sum_i S_i . \quad (35)$$

First we need to compute the zeroth order term:

$$\begin{aligned} A^0[m] &= \log \sum_S e^{\sum_i \lambda_i^0 (S_i - m_i)} = \sum_i \left[-\lambda_i^0 m_i + \log(2 \cosh \lambda_i^0) \right] , \\ \frac{dA^0[m]}{d\lambda_i^0} &= \langle S_i - m_i \rangle_0 = \tanh(\lambda_i^0) - m_i = 0 . \end{aligned} \quad (36)$$

Expressing λ_i^0 as a function of m_i we get

$$A^0[m] = \sum_i s_0(m_i) = -\sum_i \left(\frac{1+m_i}{2} \log \frac{1+m_i}{2} + \frac{1-m_i}{2} \log \frac{1-m_i}{2} \right) . \quad (37)$$

Note that at $\beta = 0$ the spins are uncorrelated, $\langle S_i S_j \rangle_0 = m_i m_j$, $\langle S_i S_j S_k \rangle_0 = m_i m_j m_k$, and so on, which allows us to compute

$$\begin{aligned} \left. \frac{d}{d\beta} A^\beta[m] \right|_{\beta=0} &= -\langle H \rangle_0 = \frac{1}{2} \sum_{i \neq j} J_{ij} m_i m_j + \mathcal{B} \sum_i m_i , \\ \left. \frac{d}{d\beta} \lambda_i^\beta \right|_{\beta=0} &= \frac{d}{dm_i} \langle H \rangle_0 = -\sum_{j(\neq i)} J_{ij} m_j - \mathcal{B} . \end{aligned} \quad (38)$$

Plugging the last equation into (30) we obtain

$$U_0 = -\frac{1}{2} \sum_{i \neq j} J_{ij} (S_i - m_i)(S_j - m_j) , \quad (39)$$

which allows us to compute the second and third derivatives of A^β . The result is

$$\begin{aligned} \left. \frac{d^2}{d\beta^2} A^\beta[m] \right|_{\beta=0} &= \langle U_0^2 \rangle_0 = \frac{1}{2} \sum_{i \neq j} J_{ij}^2 (1 - m_i^2)(1 - m_j^2) , \\ \left. \frac{d^2}{d\beta^2} \lambda_i^\beta \right|_{\beta=0} &= 2m_i \sum_{j(\neq i)} J_{ij}^2 (1 - m_j^2) , \\ \left. \frac{d^3}{d\beta^3} A^\beta[m] \right|_{\beta=0} &= -\langle U_0^3 \rangle_0 = 2 \sum_{i \neq j} J_{ij}^3 m_i (1 - m_i^2) m_j (1 - m_j^2) + \sum_{i \neq j \neq k} J_{ij} J_{ik} J_{jk} (1 - m_i^2)(1 - m_j^2)(1 - m_k^2) . \end{aligned} \quad (40)$$

Collecting these results, and going back to the original notation, we obtain the final result

$$\begin{aligned} -\beta F[m] &= -\sum_i \left(\frac{1+m_i}{2} \log \frac{1+m_i}{2} + \frac{1-m_i}{2} \log \frac{1-m_i}{2} \right) + \beta \frac{1}{2} \sum_{i \neq j} J_{ij} m_i m_j + \beta \mathcal{B} \sum_i m_i \\ &\quad + \frac{\beta^2}{4} \sum_{i \neq j} J_{ij}^2 (1 - m_i^2)(1 - m_j^2) + \frac{\beta^3}{6} \left[2 \sum_{i \neq j} J_{ij}^3 m_i (1 - m_i^2) m_j (1 - m_j^2) \right. \\ &\quad \left. + \sum_{i \neq j \neq k} J_{ij} J_{ik} J_{jk} (1 - m_i^2)(1 - m_j^2)(1 - m_k^2) \right] + O(\beta^4) , \\ \beta b_i[m] &= \text{atanh}(m_i) - \beta \left[\sum_{j(\neq i)} J_{ij} m_j + \mathcal{B} \right] + \beta^2 m_i \sum_{j(\neq i)} J_{ij}^2 (1 - m_j^2) + O(\beta^3) . \end{aligned} \quad (41)$$

In absence of external fields $b_i = 0$, the expressions simplify to the so-called Thouless-Anderson-Palmer (TAP) equations,

$$m_i = \tanh \beta h_i , \quad h_i = \mathcal{B} + \sum_{j(\neq i)} J_{ij} m_j - \beta m_i \sum_{j(\neq i)} J_{ij}^2 (1 - m_j^2) + O(\beta^2) , \quad (42)$$

where h_i is the effective magnetic field provided by the neighboring spins at site i .

6. Back to the fully connected ferromagnet

Before going to the more complicated SK model, it is instructive to look at the fully connected ferromagnet, where $J_{ij} = \frac{1}{N}$ for all ij . In this case the spins are all equivalent, so we expect that at the free energy minimum the magnetizations are all equal, $m_i = m$. Then it is easy to see that the terms of order β^2 and β^3 in the free energy expansion vanish for $N \rightarrow \infty$.

Keeping only the $O(\beta)$ term, the TAP equations simplify to the familiar mean-field result

$$m = \tanh[\beta(\mathcal{B} + m)] , \quad (43)$$

and the free energy is

$$f(m) = N^{-1} F[m] = -T s_0(m) - \frac{1}{2} m^2 - \mathcal{B} m , \quad (44)$$

which is the correct result, as we anticipated in Eq. (13). At this point it should be clear that $f(m)$ is not convex because we obtained it by neglecting higher order terms in β . The true function $\Gamma(m)$ is convex but non-analytic at low temperature (see Figure 1), so we cannot obtain it from a high-temperature expansion. This example suggests that the truncation of the high-temperature expansion has the effect of making the existence of *metastable states* manifest in $F[m]$. Note that obviously only the local minima of the TAP free energy, i.e. the solutions of the TAP equations with positive Hessian $\frac{d^2 F}{dm_i dm_j}$, can be interpreted as metastable states.

7. TAP equations for the SK model

In the SK model we set $\mathcal{B} = 0$ and the J_{ij} are Gaussian random variables with zero mean and variance $\overline{J_{ij}^2} = \frac{1}{N}$. The J_{ij} are thus typically of order of $1/\sqrt{N}$, so the terms $O(\beta^2)$ in the TAP free energy are now relevant. The terms $O(\beta^3)$ can, however, still be neglected because they vanish for $N \rightarrow \infty$.

Note that the term $\sum_{i \neq j} J_{ij} m_i m_j$ is a sum of a large number of terms; the signs of J_{ij} and m_i are random, but we expect the sign of m_i to be correlated with the sign of $h_i = \sum_{j(\neq i)} J_{ij} m_j$. This last quantity is the sum of N terms, each of order $1/\sqrt{N}$, and is therefore finite for large N . As the sign of m_i and h_i are correlated, we expect $\sum_{i \neq j} J_{ij} m_i m_j = \sum_i m_i h_i \sim N$.

Conversely, the term $O(\beta^2)$ in the free energy is a sum over a large number of terms, all of them positive. In this case fluctuations are therefore less important, so we can replace, for large N , J_{ij}^2 with its average value. Defining $q = \frac{1}{N} \sum_i m_i^2$, we get

$$\begin{aligned} -\beta F[m] &= \sum_i s_0(m_i) + \beta \frac{1}{2} \sum_{i \neq j} J_{ij} m_i m_j + N \frac{\beta^2}{4} (1 - q)^2, \\ h_i &= \sum_{j(\neq i)} J_{ij} m_j + \beta m_i (1 - q) \end{aligned} \quad (45)$$

the TAP equations for the SK model.

At high temperatures these equations have only the paramagnetic solution $m_i = 0$. We can study the stability of this solution upon lowering the temperature. The stability matrix for the paramagnet is obtained from (45):

$$\left. \frac{d^2 F[m]}{dm_i dm_j} \right|_{m_i=0} = (\beta + \beta^{-1}) \delta_{ij} - J_{ij}; \quad (46)$$

the stability condition is that all the eigenvalues should be positive. The spectrum of the matrix J_{ij} is known to be the Wigner semicircle defined in the interval $[-2, 2]$. For $T > 1$, one has $\beta + \beta^{-1} > 2$, and the paramagnet is stable. At $T = 1$, however, the spectrum touches zero, hence zero modes appear suggesting that below $T = 1$ the paramagnet becomes unstable.

Yet for $T < 1$, again $\beta + \beta^{-1} > 2$, so it seems that the paramagnet is stable for all temperatures. This strange result is in fact incorrect: the paramagnet is indeed unstable at low temperatures. A clear signature of this fact is obtained by considering its total free energy, $f_{\text{para}} = F[m = 0]/N = -\beta/4 - T \log 2$, and computing from it the entropy, $s_{\text{para}} = -df_{\text{para}}/dT = \log 2 - \beta^2/4$. This last quantity becomes negative for $T \leq 1/(2\sqrt{\log 2}) \sim 0.911$. This behavior is nonsensical because we are dealing with Ising spins, the states of the system are discrete and the entropy must be positive. The paramagnet actually becomes unstable at $T = 1$, but it is missed by the TAP equations (45) because of the approximations we made. There are different ways to understand this. For instance, one can look at the leading terms in the small β expansion; the resummation of these terms is divergent when $1 - \beta^2 J^2 (1 - q)^2 > 0$, which shows that the TAP equations (45) do not make sense for the paramagnet ($q = 0$) at $T < 1$ [50]. Alternatively, one can derive the same condition using the cavity method that we will discuss in the following [52]. This fact points out that the approximations we made in neglecting higher order terms and substituting others with their average are not completely harmless. In fact, while they are correct for stable states, they are not for unstable states and doing them blindly might stabilize solutions that are otherwise unstable.

What happens, then, below $T = 1$? At low temperatures the TAP equations have many solutions with $m_i \neq 0$ that we would like to interpret as (stable or metastable) thermodynamic states. The solution of the SK model is, however, rather complex, so we first investigate a much simpler model, the spherical p -spin model.

8. Spherical p -spin model

We will now compute the TAP free energy for the spherical p -spin model [53], which we will study in details. In order to obtain the p -spin model, we replace the Ising spins by real continuous variables σ_i , and include the constraint $\sum_i \sigma_i^2 = N$, i.e. the spins live on the N -dimensional sphere of radius \sqrt{N} . For this reason this is called a *spherical model*. Although this simplification is very convenient for analytical calculations, it is not useful for the SK model because the spherical version of the SK model is simply equivalent to a ferromagnet [54]. The p -spin model is therefore defined by the Hamiltonian

$$H[\sigma] = -\frac{1}{p!} \sum_{i_1 \dots i_p} J_{i_1 \dots i_p} \sigma_{i_1} \dots \sigma_{i_p} = - \sum_{i_1 < i_2 < \dots < i_p} J_{i_1 \dots i_p} \sigma_{i_1} \dots \sigma_{i_p}, \quad (47)$$

where the coupling constants J are again Gaussian random variables with zero mean and average

$$\overline{J_{i_1 \dots i_p}^2} = \frac{p!}{2N^{p-1}} . \quad (48)$$

Using the integral representation of the delta function, the zeroth order term is given by

$$\begin{aligned} e^{A^0[m]} &= \int d\sigma \delta \left(\sum_i \sigma_i^2 - N \right) e^{\sum_i \lambda_i^0 (\sigma_i - m_i)} = \int_{-i\infty}^{i\infty} \frac{d\mu}{2\pi} \int d\sigma e^{-\mu \sum_i \sigma_i^2 + \mu N + \sum_i \lambda_i^0 (\sigma_i - m_i)} \\ &= \int_{-i\infty}^{i\infty} \frac{d\mu}{2\pi} \exp \left[N\mu + \frac{N}{2} \log \left(\frac{\pi}{\mu} \right) + \frac{1}{4\mu} \sum_i (\lambda_i^0)^2 - \sum_i \lambda_i^0 m_i \right] . \end{aligned} \quad (49)$$

For large N we can evaluate the integral via a saddle point, and the stationarity condition for λ_i^0 gives $\lambda_i^0 = 2\mu m_i$, so

$$A^0[m] = N \text{st}_\mu \left[\mu(1-q) + \frac{1}{2} \log \left(\frac{\pi}{\mu} \right) \right] . \quad (50)$$

The stationarity condition for μ further gives $\mu = \frac{1}{2(1-q)}$, and finally

$$A^0[m] = N \frac{1}{2} \log(1-q) , \quad (51)$$

up to an irrelevant constant. By a similar computation one can show that the spins are uncorrelated up to $1/N$ corrections, i.e. $\langle \sigma_i \sigma_j \rangle = m_i m_j$. Note also that $\langle \sigma_i^2 \rangle = 1$ due to the spherical constraint. The $O(\beta)$ term is then simply $\frac{1}{p!} \sum_{i_1 \dots i_p} J_{i_1 \dots i_p} m_{i_1} \dots m_{i_p}$. The operator U_0 is therefore

$$U_0 = -\frac{1}{p!} \sum_{i_1 \dots i_p} J_{i_1 \dots i_p} [\sigma_{i_1} \dots \sigma_{i_p} - m_{i_1} \dots m_{i_p} - p(\sigma_{i_1} - m_{i_1}) m_{i_2} \dots m_{i_p}] . \quad (52)$$

To compute the $O(\beta^2)$, we assume as in the SK case that we can replace J^2 by its average. In computing the average of U_0^2 we must therefore only keep the terms with the same coupling, i.e. such that the indices $i_1 \dots i_p$ are equal up to a permutation. Otherwise, the two J have random sign and the contribution is of subleading order for large N . It is also useful to recall the relation $\langle U(\sigma_i - m_i) \rangle = 0$. We then get

$$\left. \frac{d^2}{d\beta^2} A^\beta[m] \right|_{\beta=0} = \langle U_0^2 \rangle_0 = \frac{N}{2} [1 - pq^{p-1} + q^p(p-1)] , \quad (53)$$

and the TAP free energy is [46]

$$f[m] = \frac{1}{N} F[m] = -\frac{1}{2\beta} \log(1-q) - \frac{1}{p!N} \sum_{i_1 \dots i_p} J_{i_1 \dots i_p} m_{i_1} \dots m_{i_p} - \frac{\beta}{4} [1 - pq^{p-1} + q^p(p-1)] . \quad (54)$$

9. Summary and remarks

In this section we computed the free energy functional for some spin glass models that we will discuss in the following sections. It is thus useful to summarize some important remarks that emerged during the discussion:

1. In performing the high-temperature expansion, we did not really define $F[m]$ by taking the maximum as in (22). Instead, we continued the $\beta = 0$ solution. This is not completely correct since the convexity of $F[m]$ is lost this way.
2. The “advantage” is that the local minima of $F[m]$ can be considered as *metastable states*, as we discussed in the case of the ferromagnet in external field. We will go back to this issue in the next section.
3. The approximations made in deriving $F[m]$ for disordered models can have important effects on the stability of the solutions, in particular they can stabilize solutions (e.g. the paramagnet) that are otherwise unstable.

Given these remarks, we now turn to the analysis of the solution of the TAP equations for the simplest case of the spherical p -spin.

B. Metastable states and complexity

1. The simplest example: the spherical p -spin glass model

In the last section we defined the spherical p -spin model [53]. It is the simplest spin glass for reasons that will soon be clear, and is thus a good starting point to understand the physics of spin glasses [46].

As we discussed above, the Gibbs measure can be decomposed in a set of pure states, that in fully connected models are completely determined by the set of local magnetizations m_i^α , $i = 1, \dots, N$. Note that the same holds for spherical spins because the distribution of a single spin is Gaussian with $\langle \sigma_i^2 \rangle = 1$ due to the spherical constraint, and therefore the only free parameter is the average m_i^α . The local magnetizations of pure states are the minima of the TAP free energy functional $F[m]$ in Eq. (54) [9, 49]. The weight w_α of state α is proportional to $\exp[-\beta N f_\alpha]$, where $f_\alpha = F[m_i^\alpha]/N$. In general the TAP free energy $F[m_i]$ depends explicitly on temperature, so the whole structure of the states may also depend strongly on temperature.

We derived the expression (54) of the TAP free energy for the fully connected p -spin models, from which the distribution of states can be computed. Here we will not perform the full computation, but it can be found in [46]. We will instead explain the result, and in the next section present a simpler method to obtain the same result.

It is convenient to start the description from very low temperature. In fact, a peculiar property of the spherical p -spin model –that greatly simplifies the description of the results of the TAP computation– is that the dependence of the free energy functional on T is very simple. The spin glass states (those with $m_i \neq 0$) are labeled by their intensive energy e at $T = 0$. The number of states of energy e is $\Omega(e) = \exp N \Sigma_0(e)$, where the function $\Sigma_0(e)$ is called *complexity*. It is a concave function that vanishes continuously at the ground state energy e_{\min} and goes discontinuously to 0 above some value e_{th} .

At finite temperatures, the minima are “dressed” by thermal fluctuations but they maintain their identity and one can follow their evolution at $T > 0$. At some temperature $T_{\max}(e)$, thermal fluctuations are so large that the states with energy e become unstable and disappear, until, at high enough temperature $T > T_{\text{TAP}}$, the last states (the ones with $f = f_{\min}$) disappear. The temperature evolution of the states is sketched in Fig. 2. At finite temperature, the number of spin glass states of a given free energy density f is $\Omega(f) = \sum_\alpha \delta(f - f_\alpha) = \exp N \Sigma(f)$, where $\Sigma(f) = \Sigma_0(e(f))$ and $e(f)$ is the $T = 0$ energy of the states of free energy f . Like its zero-temperature counterpart, the function $\Sigma(f)$ vanishes continuously at $f = f_{\min}$ and drops to zero above $f = f_{\text{th}}$. A qualitative plot of $\Sigma(f)$ is reported in Fig. 3.

In addition to the spin glass states with $m_i \neq 0$, the TAP equations always admit a paramagnetic solution with $m_i \equiv 0$. However, the paramagnetic state can be considered a pure state only for $T > T_d$. In fact, if one studies the equilibrium dynamics inside the paramagnetic state [46], one realizes that spin-spin dynamical correlation functions decay to their long-time value only for $T > T_d$. When $T < T_d$, the correlation remain larger than its equilibrium value even for infinitely long times. This means that starting from some equilibrium configuration in the paramagnetic state, the system cannot explore the whole paramagnetic state, which is therefore not a well defined ergodic component. Unfortunately for the moment one can realize this problem only through a dynamic calculation. One would like to see that $m_i = 0$ is not a pure state directly from the TAP computation, but how to do this is not clear for the moment. The dynamical TAP approach of [55] could help to clarify this issue.

In summary, p -spin models are characterized by the existence of a paramagnetic state for $T > T_d$, and by an *exponential number* of spin glass states for low temperatures $T < T_{\text{TAP}}$. The transition between the paramagnetic and the spin glass regime happens through a series of very interesting phase transitions that we now discuss.

2. The partition function

The partition function $Z_\alpha = e^{-\beta N f_\alpha}$ of a pure state α can be thought as the contribution of this state to the total partition function. Therefore, we can write the total contribution of the spin glass states to the partition function Z in the following way:

$$\begin{aligned} Z &= e^{-\beta N f_{\text{tot}}(T)} \sim \sum_\alpha e^{-\beta N f_\alpha} = \int df \sum_\alpha \delta(f - f_\alpha) e^{-\beta N f} \\ &= \int df \Omega(f) e^{-\beta N f} = \int_{f_{\min}}^{f_{\text{th}}} df e^{N[\Sigma(f) - \beta f]} \sim e^{N[\Sigma(f^*) - \beta f^*]}, \end{aligned} \quad (55)$$

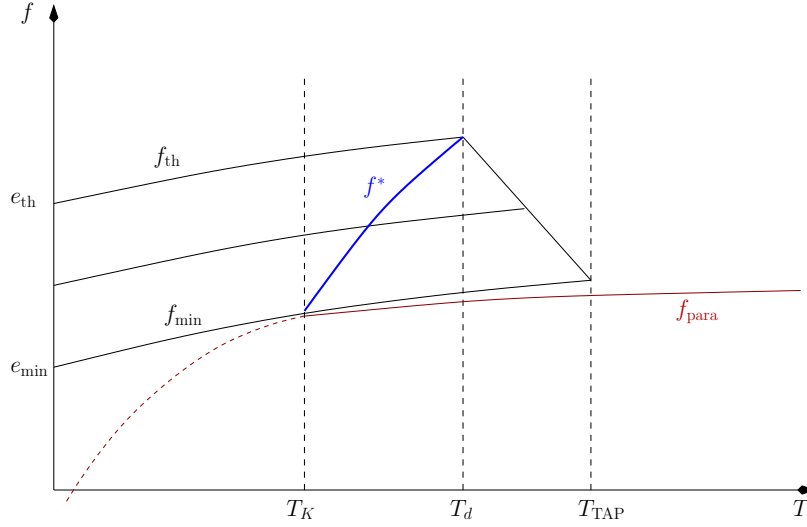


FIG. 2: Sketch of the evolution in temperature^a of the TAP states for the spherical p -spin model [13]. Each group of TAP states of free energy f can be followed in temperature until it becomes unstable and disappears. The complexity vanishes continuously at the ground state f_{\min} and goes abruptly to 0 above the maximum free energy f_{th} . The blue line is the free energy f^* of the states that dominate the partition function. Between T_d and T_K , the red line represents the equilibrium free energy $f^* - T\Sigma(f^*)$ that takes into account the entropic contribution of the degeneracy of the states and is equal to the free energy of the paramagnet.

^aNote that in the spherical p -spin model, because of the continuous variables, the entropy is *negative*, hence $df/dT = -s > 0$ and the free energy increases with temperature; in most models (and in all discrete models) instead the entropy is positive and the free energy decreases with temperature. This fact does not change the qualitative shape of the figure.

where $f^* \in [f_{\min}, f_{\text{th}}]$ is such that $f - T\Sigma(f)$ is minimum, i.e. it is the solution of

$$\frac{d\Sigma}{df} = \frac{1}{T}, \quad (56)$$

provided that it belongs to the interval $[f_{\min}, f_{\text{th}}]$. Starting from high temperatures, one encounters three distinct temperature regions:

- For $T > T_d$, the free energy density of the paramagnetic state is smaller than $f - T\Sigma(f)$ for any $f \in [f_{\min}, f_{\text{th}}]$, so the paramagnetic state dominates and coincides with the Gibbs state. Spin glass states exist for $T < T_{\text{TAP}}$ but they are irrelevant as their contribution to the total partition function is exponentially smaller than the one of the paramagnetic state.
- For $T_d \geq T \geq T_K$, a value $f^* \in [f_{\min}, f_{\text{th}}]$ is found, such that $f^* - T\Sigma(f^*)$ is exactly equal to f_{para} . In other words, the total free energy of all spin glass states coincides with the analytic continuation of the free energy of the paramagnetic state below T_d . This can be interpreted as follows. The paramagnetic state is obtained from the superposition of an *exponential number* of spin glass states of *higher* individual free energy density f^* . The Gibbs measure is split on this exponential number of contributions: however, no phase transition happens at T_d because of the equality $f^* - T\Sigma(f^*) = f_{\text{para}}$ which guarantees that the free energy is analytic on crossing T_d .
- For $T < T_K$, the partition function is dominated by the lowest free energy states, $f^* = f_{\min}$, with $\Sigma(f_{\min}) = 0$ and $f_{\text{tot}}(T) = f_{\min} - T\Sigma(f_{\min}) = f_{\min}$. At T_K a phase transition occurs; the free energy and its first derivatives are continuous but the second derivative of f_{tot} with respect to T (the specific heat) has a jump.

As we already discussed, the paramagnetic solution $m_i = 0$ disappears for $T < T_d$. In the range of temperatures $T_d > T > T_K$, the paramagnetic state is replaced by a strange state, in which the phase space of the model is disconnected in an exponentially large number of states, giving a contribution $\Sigma(T) \equiv \Sigma(f^*(T))$ to the total entropy of the system. The entropy $s(T)$ for $T_d > T > T_K$ can thus be written as

$$s(T) = \Sigma(T) + s_{\text{vib}}(T), \quad (57)$$

where $s_{\text{vib}}(T)$ is the individual entropy of a state of free energy f^* . The phase transition at T_K is signaled by the vanishing of the contribution $\Sigma(T)$. A similar “entropy crisis” scenario is realized in a very simple completely solvable model, the so-called Random Energy Model (\Rightarrow **Ex.II.2**).

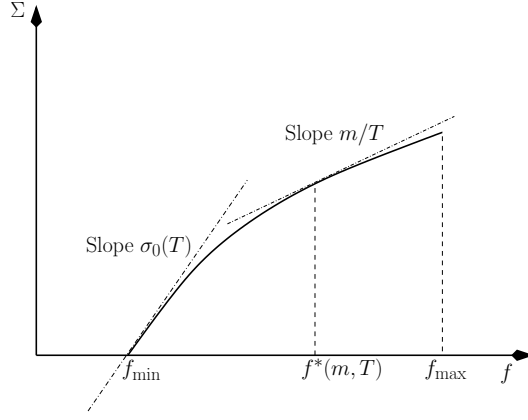


FIG. 3: A sketch of the complexity as a function of the free energy density for systems belonging to the p -spin class. The value $f^*(m, T)$, solution of $\frac{d\Sigma}{df} = \frac{m}{T}$, is also reported.

3. A method to compute the complexity

We presented the above picture as the result of a TAP computation that we did not describe explicitly. How can we compute the properties of the metastable states, for example the density of states $\Omega(f)$, without solving explicitly the TAP equations? For systems that present a structure of the free energy landscape similar to p -spin glasses, a general method to compute the complexity as a function of the free energy of the states has been proposed in [56]. The aim of this section is to present this method in some details.

The main problem we have to face is that, unlike in a ferromagnet, the states cannot be classified according to symmetry. In fact, the local magnetizations m_i^α are different and amorphous in each state. In principle, we should put an infinitesimal local magnetic field that is *different for each spin* in order to select a state. However, the local magnetizations of the states depend on the couplings J , so we must apply the small field *before* taking the average over the disorder and that field is itself correlated with the disorder. We therefore cannot study the states by selecting them according to an external field, as is usually done for standard phase transitions.

The idea of [56] is to bypass this problem by considering m copies of the original system that are coupled by a small attractive term. As we will show below, for $T < T_d$, it is possible to choose the small attractive coupling in such a way that *i*) the m copies are constrained to be in the same TAP state, and *ii*) they are uncorrelated within the TAP state. In this situation, the free energy of the m copies inside a TAP state is just m times f_α , because the m copies are independent in that state. Then, at low enough temperatures, the partition function of the replicated system is the sum over all states of the contribution of a single TAP state which is $e^{-\beta N m f_\alpha}$:

$$Z_m \sim \sum_{\alpha} e^{-\beta N m f_\alpha} = \int_{f_{\min}}^{f_{\text{th}}} df e^{N[\Sigma(f) - \beta m f]} \sim e^{N[\Sigma(f^*) - \beta m f^*]}, \quad (58)$$

where now $f^*(m, T)$ is such that $m f - T \Sigma(f)$ is minimum and satisfies the equation

$$\frac{d\Sigma}{df} = \frac{m}{T}. \quad (59)$$

As a result, we see that an additional weight m has been given to the term $-\beta f$ in (58). This is a crucial result: because of this, the full complexity function can be computed from the knowledge of the free energy of the replicated system. Defining

$$\Phi(m, T) = -\frac{T}{N} \log Z_m = \min_f [m f - T \Sigma(f)] = m f^*(m, T) - T \Sigma(f^*(m, T)), \quad (60)$$

it is indeed straightforward to show that

$$\begin{aligned} f^*(m, T) &= \frac{\partial \Phi(m, T)}{\partial m}, \\ \Sigma(m, T) &= \Sigma(f^*(m, T)) = m^2 \frac{\partial [m^{-1} \beta \Phi(m, T)]}{\partial m} = m \beta f^*(m, T) - \beta \Phi(m, T). \end{aligned} \quad (61)$$

The function $\Sigma(f)$ can then be reconstructed from the parametric plot of $f^*(m, T)$ and $\Sigma(m, T)$ by varying m at fixed temperature. From the knowledge of $\Sigma(f)$ all the information on the TAP states contained in Fig. 2 can be reconstructed.

Let us expand the complexity at low free energy as

$$\Sigma(f) = \Sigma(f_{\min}) + \sigma_0(T)(f - f_{\min}) + \dots \quad (62)$$

Hence $\sigma_0(T)$ is the slope of $\Sigma(f)$ at f_{\min} and we made its temperature dependence explicit. For $m = 1$, the glass transition happens when β equals $\sigma_0(T)$, or in other words T_K is the solution of $\sigma_0(T) = 1/T$. However, if m is allowed to assume real values by an analytical continuation and if $m < 1$, this condition is replaced by $\sigma_0(T) = m/T$. Because the temperature dependence of $\sigma_0(T)$ is usually mild, the glass transition is shifted to lower temperatures for $m < 1$, see Fig. 3. In other words, for any $T < T_K$ there exists a value $m_s(T) < 1$, such that for $m < m_s(T)$ the system is in the “high temperature” phase (where $f > f_{\min}$ and $\Sigma > 0$), while for $m > m_s(T)$ it is in the “low temperature” spin glass phase (where $f = f_{\min}$). The line $m_s(T)$ is defined by the condition $\sigma_0(T) = m_s(T)/T$, hence $m_s(T) = T\sigma_0(T)$. Because the free energy is always continuous and is *independent* of m in the spin glass phase (being simply the value $f_{\min}(T)$, such that $\Sigma(f_{\min}) = 0$), one can compute the free energy of the glass below T_K simply as $f_{\text{glass}}(T) = f_{\min}(T) = \Phi(m_s(T), T)/m_s(T)$. In this way we can compute the thermodynamic properties of the system. Note that by definition, at T_K we have $m_s(T_K) = T_K\sigma_0(T_K) = 1$.

In summary, this method allows us to compute the complexity $\Sigma(f)$ at any temperature, provided we are able to compute the free energy of m copies of the original system constrained to be in the same TAP state and to perform the analytical continuation to real m . In [57] this method was applied to the spherical p -spin system and it was shown that it reproduces the results obtained from the explicit TAP computation (see also [46] for a detailed discussion). In the next section we discuss this computation in detail.

4. Replicated free energy of the spherical p -spin model

In order to show explicitly how the method works, we perform here the explicit computation for the p -spin model following [57].

We wish to compute the free energy of m copies of the original system, coupled by an attractive term, the role of which will be discussed after the computation has been performed. To fix ideas, we might choose the following Hamiltonian for the m replicas:

$$H = H_J[\sigma_1] + \dots + H_J[\sigma_m] - \epsilon \sum_{a,b} \sum_{i=1}^N \sigma_i^a \sigma_i^b. \quad (63)$$

Note that the m copies all have the *same* couplings J . In principle we should compute $\Phi(m, T)$ for a given set of couplings, however, thanks to the self-averaging property, we can equivalently (in the thermodynamic limit) take the average over J of the free energy of the total system:

$$\Phi(m, T) = -\frac{T}{N} \log Z_m = -\frac{T}{N} \log \int D\sigma_1 \dots D\sigma_m e^{-\beta(H_J[\sigma_1] + \dots + H_J[\sigma_m]) + \beta\epsilon \sum_{a,b} \sum_{i=1}^N \sigma_i^a \sigma_i^b}. \quad (64)$$

To lighten the notation we include the spherical constraint in the integration measure, which we now denote $D\sigma$, i.e. $D\sigma = (\prod_i d\sigma_i) \delta(\sum_i \sigma_i^2 = N)$.

Let's forget for a moment about the coupling term and set $\epsilon = 0$. The main problem is that we have to perform the average of the logarithm of the partition function, which is not an easy task. Using the identity

$$\log x = \lim_{n \rightarrow 0} \partial_n x^n, \quad \Phi(m, T) = -\frac{T}{N} \lim_{n \rightarrow 0} \partial_n \overline{(Z_m)^n} \quad (65)$$

transforms the problem into that of calculating the average over the disorder of $(Z_m)^n$. Although this problem is difficult for real n , it can be solved for integer n . In fact, for integer n (and m) we get

$$\overline{(Z_m)^n} = \int D\sigma_1 \dots D\sigma_{nm} e^{-\beta(H_J[\sigma_1] + \dots + H_J[\sigma_{nm}])}, \quad (66)$$

where we now have a system of $m \times n$ copies or *replicas*. By convention we assume that replicas $\{1, \dots, m\}$ are the original ones (coupled), and $\{m+1, \dots, 2m\}$ are a copy of them (coupled), and so on. Note that there is no coupling

between replicas belonging to different blocks $\{1 + \ell m, \dots, (\ell + 1)m\}$. Labeling replicas by an index $a = 1, \dots, nm$, and dropping irrelevant normalization constants, we get

$$\begin{aligned} \overline{(Z_m)^n} &\propto \int D\sigma_i^a \prod_{i_1 < \dots < i_p} \int dJ_{i_1 \dots i_p} \exp \left[-J_{i_1 \dots i_p}^2 \frac{N^{p-1}}{p!} + \beta J_{i_1 \dots i_p} \sum_{a=1}^{mn} \sigma_{i_1}^a \dots \sigma_{i_p}^a \right] \\ &\propto \int D\sigma_i^a \prod_{i_1 < \dots < i_p} \exp \left[\frac{\beta^2 p!}{4N^{p-1}} \sum_{a,b}^{1,mn} \sigma_{i_1}^a \sigma_{i_1}^b \dots \sigma_{i_p}^a \sigma_{i_p}^b \right] \\ &= \int D\sigma_i^a \exp \left[\frac{\beta^2}{4N^{p-1}} \sum_{a,b}^{1,mn} \left(\sum_i^N \sigma_i^a \sigma_i^b \right)^p \right] = \int D\sigma_i^a \exp \left[N \frac{\beta^2}{4} \sum_{a,b}^{1,mn} \left(\frac{1}{N} \sum_i \sigma_i^a \sigma_i^b \right)^p \right]. \end{aligned} \quad (67)$$

Note that when taking the average over the J 's we had to take into account that they are symmetric under permutations, so the average must only be taken over $i_1 < \dots < i_p$.

We now see why the replica trick is useful. In fact, taking the average over the disorder for the replicated system, we eliminated the couplings J and introduced a coupling between replicas. The advantage is that once the disorder is eliminated, the replicated (and coupled) system becomes translationally invariant. Then, for a fully-connected model, the Hamiltonian becomes a function of a global quantity⁸, which in this case is the overlap between two different replicas of the system:

$$Q(\sigma^a, \sigma^b) = \frac{1}{N} \sum_i \sigma_i^a \sigma_i^b. \quad (68)$$

Note that $Q(\sigma^a, \sigma^a) = 1$ due to the spherical constraint. This quantity measures the extent to which the configurations of replica a and replica b are different.

A way to compute the replicated partition function starting from Eq. (67) is reviewed in [46]. Here we present a slightly different route, just to provide the reader with two different ways of doing the same computation. From Eq. (67) we can write

$$\begin{aligned} \overline{(Z_m)^n} &\propto \int D\sigma_i^a \int \prod_{a < b}^{1,mn} \left\{ dQ_{ab} \delta \left(Q_{ab} - \frac{1}{N} \sum_i \sigma_i^a \sigma_i^b \right) \right\} \exp \left[N \frac{\beta^2}{4} \sum_{a,b}^{1,mn} Q_{ab}^p \right] \\ &= \int dQ \exp \left[N \frac{\beta^2}{4} \sum_{a,b}^{1,mn} Q_{ab}^p \right] \int d\sigma_i^a \prod_{a \leq b}^{1,mn} \delta \left(N Q_{ab} - \sum_i \sigma_i^a \sigma_i^b \right) = \int dQ \exp \left[N \frac{\beta^2}{4} \sum_{a,b}^{1,mn} Q_{ab}^p \right] J(Q), \end{aligned} \quad (69)$$

where $dQ = \prod_{a < b} dQ_{ab}$ and in the second line we grouped the delta function that imposes the spherical constraint in $D\sigma$ with the other delta functions, hence adding the diagonal term for $a = b$ with $Q_{aa} = 1$.

We thus have to compute the Jacobian

$$J(Q) = \int d\sigma_i^a \prod_{a \leq b}^{1,mn} \delta \left(N Q_{ab} - \sum_i \sigma_i^a \sigma_i^b \right) = \int d\vec{\sigma}^a \delta(N Q_{ab} - \vec{\sigma}^a \cdot \vec{\sigma}^b), \quad (70)$$

where we think to σ_i^a as a N dimensional vector $\vec{\sigma}^a$ with $\vec{\sigma}^a \cdot \vec{\sigma}^b = \sum_i \sigma_i^a \sigma_i^b$. We note that Q is a symmetric real matrix and it can thus be diagonalized⁹. We have $Q = \Lambda^T D \Lambda$ where $\Lambda^{-1} = \Lambda^T$ is a $mn \times mn$ orthogonal matrix with $\det \Lambda = 1$, and D is a diagonal matrix, $D_{aa} = \lambda_a$ being the eigenvalues of Q . Calling σ a matrix composed by the collection of $\vec{\sigma}^a$, $\sigma = \{\vec{\sigma}^1 \dots \vec{\sigma}^{mn}\}$, we define $\mu = \sigma \Lambda^T$ and $\mu^T = \Lambda \sigma^T$, and we have

$$J(Q) = \int d\sigma \delta(N \Lambda^T D \Lambda - \sigma^T \sigma) = \int d\sigma \delta(N D - \Lambda \sigma^T \sigma \Lambda^T) = \int d\mu \delta(N D - \mu^T \mu), \quad (71)$$

⁸ We have already seen an example of the same property in the study of the Curie-Weiss model.

⁹ This way of performing the computation has been suggested by Pierfrancesco Urbani [58].

where all the manipulations above are possible because Λ is an orthogonal matrix and $\det \Lambda = 1$. We obtain

$$J(Q) = \int d\vec{\mu}^a \prod_{a=1}^{mn} \delta(N\lambda_a - \vec{\mu}^a \cdot \vec{\mu}^a) \prod_{a<b}^{1,mn} \delta(\vec{\mu}^a \cdot \vec{\mu}^b) \propto \int d\vec{\mu}^a \prod_{a=1}^{mn} \delta(\lambda_a - \vec{\mu}^a \cdot \vec{\mu}^a) \prod_{a<b}^{1,mn} \delta(\vec{\mu}^a \cdot \vec{\mu}^b), \quad (72)$$

where the factor N can be eliminated by rescaling the vectors $\vec{\mu}^a$, giving a proportionality constant that we neglect. We can now introduce polar coordinates where $\mu^a = |\vec{\mu}^a|$ and $\hat{\mu}^a$ is a unit N -dimensional vector that encodes the orientation of $\vec{\mu}^a = \mu^a \hat{\mu}^a$. We obtain

$$J(Q) \propto \int \prod_{a=1}^{mn} d\hat{\mu}^a d\mu^a (\mu^a)^{N-1} \prod_{a=1}^{mn} \frac{1}{\sqrt{\lambda_a}} \delta(\sqrt{\lambda_a} - \mu^a) \prod_{a<b}^{1,mn} \frac{1}{\sqrt{\lambda_a \lambda_b}} \delta(\hat{\mu}^a \cdot \hat{\mu}^b). \quad (73)$$

The angular integration gives a constant independent of the matrix Q (see [58] for an explicit computation) and we finally obtain

$$J(Q) \propto \prod_{a=1}^{mn} (\lambda_a)^{(N-1)/2} \prod_{a=1}^{mn} \frac{1}{\sqrt{\lambda_a}} \prod_{a<b}^{1,mn} \frac{1}{\sqrt{\lambda_a \lambda_b}} = \prod_{a=1}^{mn} (\lambda_a)^{(N-mn-1)/2} = (\det Q)^{(N-mn-1)/2} \sim (\det Q)^{N/2}, \quad (74)$$

where the last result holds for large N .

Plugging Eq. (74) in Eq. (69) we get¹⁰

$$\begin{aligned} \overline{(Z_m)^n} &\propto \int dQ_{ab} e^{NX(Q)}, \\ X(Q) &= \frac{\beta^2}{4} \sum_{ab} Q_{ab}^p + \frac{1}{2} \log \det Q. \end{aligned} \quad (75)$$

The advantage of this form of the integral is that we can use the saddle point (or Laplace, or steepest-descent) method, to solve it in the limit $N \rightarrow \infty$. This simplification is a consequence of the mean-field structure of the model, and results from decoupling the sites using the replica trick. The saddle-point method states that in the limit $N \rightarrow \infty$ the integral (75) is concentrated in the maximum of the integrand.

Note, however, that we have to be careful for two reasons. First, the free energy is given by

$$\Phi(m, T) = -T \lim_{N \rightarrow \infty} \frac{1}{N} \lim_{n \rightarrow 0} \partial_n \int dQ_{ab} \exp[NX(Q)] \quad (76)$$

and thus we should *first* take the limit $n \rightarrow 0$, and then $N \rightarrow \infty$. Unfortunately, we are unable to do so because X is not an explicit function of n and because we first need to send $N \rightarrow \infty$ to solve the integral. As a conclusion, we need to exchange the order of the two limits, solve the integral, find a parametrization of the matrix Q_{ab} , and finally take the $n \rightarrow 0$ limit. This operation is clearly quite dangerous from a strict mathematical point of view.

Second, we must pay attention to what is meant by the “maximum” of X . The problem is that the number of independent elements of Q_{ab} , $n(n-1)/2$, becomes negative in the limit $n \rightarrow 0$. It is hard to say what is the maximum of a function with a negative number of variables. There is, however, a criterion we can use to select the correct saddle point. The corrections to the saddle point result are given by the Gaussian integration around the saddle point itself. As a result, this integration gives the square root of the determinant of the second derivative matrix of X . In order to have a sensible result, we must have that the analytic continuation of all the eigenvalues of this matrix are negative. In other words, we have to select saddle points with a negative-defined second derivative of X [59].

¹⁰ The proportionality constant in Eq. (75) should be discussed a bit more carefully. At the leading exponential order in N , it gives a contribution of the form $\exp(mnNC)$ where C is a numerical constant. This can be argued because when $nm = 0$ the proportionality constant must be 1. This term shifts the free energy Eq. (76) by a multiple of mT , which corresponds to a constant shift of the entropy and can therefore be neglected. Other subleading corrections disappear in the large N limit. We conclude that the proportionality constant can really be neglected.

5. 1-step replica symmetry breaking

The saddle point equation for Q is complicated and cannot be solved in general. We need a simple *ansatz* on the form of the matrix Q in order to find the solution. How can we guess the form of Q ? At this point we have to reintroduce the coupling term. A quick look to the previous computation reveals that in presence of the coupling the nm replicas are divided in blocks of m replicas, such that each block is coupled while replicas in different blocks are not coupled. Let us label by B the blocks. Because the coupling term only depends on Q_{ab} , we can carry out the same computation and we find

$$X(Q) = \frac{\beta^2}{4} \sum_{ab} Q_{ab}^p + \frac{1}{2} \log \det Q + \beta \epsilon \sum_B \sum_{ab \in B} Q_{ab} . \quad (77)$$

We see that the coupling term *breaks explicitly* the replica symmetry.

The matrix element Q_{ab} , according to (68), measures the overlap of replicas a and b , i.e. how much the two replicas are close to each other. Therefore, it is very natural to assume that the replicas within a same block have high overlap due to the external coupling, while replicas in different blocks have much smaller overlap: in practice we can assume that their overlap is zero, as it would be for completely uncorrelated replicas. Moreover, we assume that the overlap between coupled replicas is the same for any pair of replicas $a \neq b$ belonging to the same block. This *ansatz*, which is the simplest possible, is called *1-step replica symmetry breaking* (1RSB) for reasons that will be made clear below. The 1RSB *ansatz* for Q reads, for $n = 2$ and $m = 3$:

$$Q = \begin{pmatrix} \begin{pmatrix} 1 & q & q \\ q & 1 & q \\ q & q & 1 \end{pmatrix} & 0 \\ 0 & \begin{pmatrix} 1 & q & q \\ q & 1 & q \\ q & q & 1 \end{pmatrix} \end{pmatrix} . \quad (78)$$

Note that here there is no spontaneous symmetry breaking: replica symmetry is broken explicitly by the coupling term, and Eq. (78) is the simplest *ansatz* that is compatible with the symmetries of the action $X(Q)$.

We can use the relation

$$\det \begin{pmatrix} 1 & q & q \\ q & 1 & q \\ q & q & 1 \end{pmatrix} = (1 - q)^{m-1} [1 + (m - 1)q] , \quad (79)$$

to get

$$\det Q = \{(1 - q)^{m-1} [1 + (m - 1)q]\}^n . \quad (80)$$

Substituting this *ansatz* in (77) we get

$$X(Q) = -\beta n m \phi_{1\text{RSB}}(m, q, T) + \beta \epsilon n m (m - 1) q \quad (81)$$

where the 1RSB free energy is

$$\phi_{1\text{RSB}}(m, q, T) = -\frac{1}{2\beta} \left\{ \frac{\beta^2}{2} [1 + (m - 1)q^p] + \frac{m - 1}{m} \log(1 - q) + \frac{1}{m} \log [1 + (m - 1)q] \right\} . \quad (82)$$

Note that this expression, which has been derived for integer m and n , is also perfectly well defined for real m and n , so that now we can perform the continuation to $n \rightarrow 0$ and real m . Finally

$$\Phi(m, T) = -\frac{T}{N} \lim_{n \rightarrow 0} \partial_n \exp \left[-\beta n m N \phi_{1\text{RSB}}(m, q^*, T) + N \beta \epsilon n m (m - 1) q^* \right] = m \phi_{1\text{RSB}}(m, q^*, T) - \epsilon m (m - 1) q^* , \quad (83)$$

and q^* is the stationary point of this expression.

An important remark is that, due to the simple structure of the saddle-point matrix Q , the result for $\Phi(m, T)$ is equivalent to the one that would be obtained by a direct computation of $-\frac{T}{N} \log \overline{Z_m}$ without introducing the n additional replicas. This is due to the fact that replicas in different blocks are completely uncorrelated, and therefore $X(Q)$ is simply proportional to n . This fact is very specific to the p -spin model and is false in most other cases. In

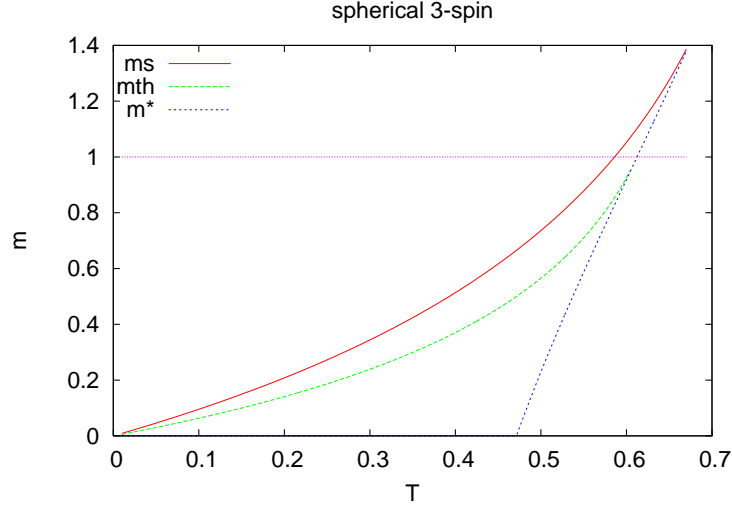


FIG. 4: Phase diagram of the 3-spin spherical model in the (m, T) plane.

these cases the calculation might be more complicated, but the general strategy outlined above remains valid. We will see an example later on, in \Rightarrow **Ex.III.1** (but it's too early to do the exercise at this point).

So, finally, we can discuss the role of the coupling ϵ . At low enough temperatures, three solutions of the stationary equation for q exist: two of them are minima (or maxima depending on m) and are separated by a minimum (maximum). Clearly, in this situation a large enough ϵ will always favor the large q solution. However, we do not want to perturb the TAP states, or in other words we want replicas to be uncorrelated within a state, and for this reason we must send $\epsilon \rightarrow 0$. While doing this, however, we want to maintain the high correlation between replicas. Hence, the prescription is to set $\epsilon = 0$ but always select the large q solution of the stationary condition, if it exists (see [57] for a more detailed discussion). Otherwise, if for $\epsilon = 0$ only the solution $q = 0$ exists, we get a trivial result: $\Phi(m, T) = -\frac{\beta m}{4} = m f_{\text{para}}$ and using Eq. (61) we find that the complexity vanishes.

6. The phase diagram of the spherical p -spin model

Let us summarize the previous discussion. We have assumed that replicas in different blocks are uncorrelated and have zero overlap, while replicas in the same block are correlated and so we assigned them an overlap q . This correlation is due to the external coupling ϵ , whose role is only to select the solution for q that has the highest overlap. Indeed, the free energy (83) at $\epsilon = 0$ and as a function of q always has a stationary point at $q = 0$, but for low enough temperatures a second stationary point appears at $q^* \neq 0$, and the coupling is only introduced to select this solution. This approach is very similar to what is usually done in first order phase transitions by selecting one state or the other using an infinitesimal external field (e.g. in a ferromagnet the states with positive or negative magnetization can be selected by an infinitesimal positive or negative magnetic field). Therefore, if we are interested in the partition function of m replicas *in the same state*, as we did in the previous section in order to compute the complexity, we should *always* take the solution with $q \neq 0$, if it exists.

The final result is that

$$\Phi(m, T) = m \phi_{\text{IRSB}}(m, q^*(m, T), T) . \quad (84)$$

From this, we can draw a “phase diagram” in the (m, T) plane, which is reported in Fig. 4 for the spherical 3-spin model (\Rightarrow **Ex.II.3, II.4 and II.5**). It results from a series of considerations:

- First of all we must identify the region where a solution with $q \neq 0$ is found. This region is delimited by the line $m^*(T)$. For $m < m^*(T)$, we have $q^*(m, T) = 0$, $\Phi(m, T)$ is trivial, and the complexity is zero. For $m > m^*(T)$, a non-trivial solution $q^*(m, T)$ is found: in this region we can compute, using Eq. (61), the complexity and free energy as a function of m :

$$\begin{aligned} \Sigma(m, T) &= m^2 \partial_m [m^{-1} \beta \Phi(m, T)] = m^2 \partial_m [\beta \phi_{\text{IRSB}}(m, q^*, T)] , \\ f^*(m, T) &= \partial_m \Phi(m, T) = \partial_m m \phi_{\text{IRSB}}(m, q^*, T) . \end{aligned} \quad (85)$$

These quantities are therefore defined *only* above the line $m^*(T)$. We can observe that the non-trivial solution $q^*(m, T)$ disappears at $m^*(T)$ by merging with another solution (a standard “bifurcation” of solutions). Because of this, a zero mode (the so-called “longitudinal” mode) in the stability matrix of the 1RSB solution appears at $m^*(T)$ (\Rightarrow **Ex.II.5**).

- Next, we analyze the behavior of $f^*(m, T)$ and $\Sigma(m, T)$. It turns out that starting from $m = \max\{0, m^*(T)\}$ and increasing m , both $f^*(m, T)$ and $\Sigma(m, T)$ first increase up to a maximum and then decrease upon further increasing m . This non-monotonicity leads to two branches of the parametric curve $\Sigma(f)$, of which only one is physical: the one that corresponds to *decreasing* f and Σ with m . Indeed, from Fig. 3 it should be clear that both f^* and Σ must decrease when increasing m . We then define a line $m = m_{\text{th}}(T)$ where $f^*(m, T)$ is maximum, which corresponds to the threshold values $f_{\text{th}}(T)$. The physical region is the one for $m \geq m_{\text{th}}(T)$. One can show in fact that for $m < m_{\text{th}}(T)$, the 1RSB solution is *unstable*: one of the eigenvalues of the stability matrix (the so-called “replicon” mode) becomes negative suggesting that a more complex matrix Q_{ab} should be considered (\Rightarrow **Ex.II.5**). However, one can show that no consistent solution can be constructed for $m < m_{\text{th}}(T)$ [60].
- Finally, we observe that at a fixed T , the complexity is finite for $m = m_{\text{th}}(T)$ and decreases on increasing m above $m_{\text{th}}(T)$, until it vanishes on a second line $m_s(T)$, that is also reported in Figure 4. Above this line, the complexity becomes negative, indicating that states do not exist anymore. States are therefore found for $m_s(T) > m > m_{\text{th}}(T)$, with $m_{\text{th}}(T)$ corresponding to $f_{\text{th}}(T)$ and $m_s(T)$ corresponding to $f_{\text{min}}(T)$.

Note that the two lines $m_{\text{th}}(T)$ and $m^*(T)$ merge at $m = 1$ and $T = T_d$. This is due to the fact that the longitudinal mode and the replicon mode coincide at $m = 1$. For $m > 1$, there is no line m_{th} because the 1RSB is stable in the whole interval $m_s(T) \geq m \geq m^*(T)$ (in other words, the longitudinal mode becomes unstable before the replicon mode). At yet higher temperatures the lines $m_s(T)$ and $m^*(T)$ touch: this is the temperature T_{TAP} above which only the paramagnetic state survives, see Figure 2.

From the previous discussion, in particular equations (55), (56) and (58), (59), $m = 1$ obviously corresponds to the equilibrium partition function of a single copy of the system. When the line $m_{\text{th}}(T)$ crosses $m = 1$, the saddle point in (55) is exactly equal to f_{th} , which is the point where the paramagnet breaks in many states. This crossing defines the temperature T_d . Similarly, the point where the line $m_s(T)$ crosses $m = 1$ corresponds to the point where the saddle point is equal to f_{min} , the complexity vanishes and a few states dominate, i.e. the phase transition T_K .

For $T < T_K$, the saddle point of (55) is always f_{min} , which can be computed by following the line $m_s(T)$. The analytic continuation above $m_s(T)$ is not correct: the complexity becomes negative above $m_s(T)$. In other words, the system of m replicas undergoes a glass transition on the line $m_s(T)$. However, we do not need to wonder about what happens above $m_s(T)$, because the discussion of Section II B 3 tells us that the value of the free energy $\Phi(m, T)$ on the line $m_s(T)$, which is $\Phi(m, T) = m f_{\text{min}}(T)$, is the one that persists up to the $m = 1$ line. Note that $m < 1$ and, recalling that $\Sigma = 0$ along m_s , from Eq. (61) one obtains:

$$f_{\text{min}}(T) = \left. \frac{\Phi(m, T)}{m} \right|_{m=m_s(T)} = \phi_{\text{1RSB}}(m_s(T), q^*(T), T). \quad (86)$$

This last result is very important. Indeed, for $T > T_K$ the free energy of the system is equal to the free energy of the paramagnet, corresponding simply to $\phi_{\text{1RSB}}(m = 1) = -\beta/4$. Below T_K , instead, the free energy of the system is given, comparing (86) and (85), by extremizing ϕ_{1RSB} with respect to *both* m and q . Actually, the extremum is a *maximum*, as can be seen by an explicit computation. Remarkably, the fact that the equilibrium spin glass free energy is the maximum of ϕ_{1RSB} with respect to m and q is the usual prescription of the replica method, and it can be rigorously proven to be correct [16].

In summary, the replica method allowed us to fully characterize the thermodynamics of the spherical p -spin model, by computing

- the free energy of the paramagnetic phase
- the free energy of the glass phase
- the distribution $\Sigma(f)$ of all the metastable states as a function of f and T

The main assumption we made in the derivation is that *the states are all equivalent*, with a self-overlap q and zero mutual overlap, i.e. they are randomly distributed in phase space. These properties are expressed by the 1RSB structure of the overlap matrix Q_{ab} where all nonzero entries, corresponding to the replicas in the same state, have the same value q . This behavior is exact for the spherical p -spin model, but it is somewhat exceptional. In particular it is not true for the SK model, where the states are organized in a very complicated structure.

As a final remark, it is important to stress that the vanishing of the replicon mode on the line m_{th} has an extremely important physical consequence: that the threshold states at f_{th} have a zero mode of their TAP stability matrix and they are therefore *marginal*. This is extremely important because one can show that this marginality property is intimately connected to many important properties of the out-of-equilibrium *aging* dynamics [11, 12, 60, 61]. For reasons of space, we cannot discuss these properties here and we refer the reader to [11, 12, 60, 61] and references therein.

7. Spontaneous replica symmetry breaking: the order parameter

To conclude this section, we will discuss now the concept of *spontaneous replica symmetry breaking*. Suppose that, ignoring completely the above discussion, we tried to compute directly the free energy of a *single copy* of the system. Then, using the replica method, we would write

$$f = -\frac{T}{N} \log Z = -\frac{T}{N} \lim_{\nu \rightarrow 0} \partial_{\nu} \overline{Z^{\nu}}. \quad (87)$$

Formally, this computation is completely identical to the one of the previous section, Eq. (66), with $\nu = mn$. This time, however, there is no external coupling that suggests us the structure (78) of the overlap matrix. The simplest guess would be simply to set $q = 0$, i.e. to assume that Q_{ab} is a diagonal matrix and that all the replicas are uncorrelated. Going through the rest of the computation would then give us the paramagnetic solution, which is wrong below T_K , and would miss the interesting structuring of configuration space below T_d . As guessed by Parisi [9], the correct solution is to assume the structure (78) also in the computation of (87), and consider m and q as variational parameters to be optimized. This solution is exactly what we obtained in Eq. (86), which shows that these two conceptually different strategies lead to the same result for the free energy of the glass (which is the correct one [16]). In this case, replica symmetry breaking is not imposed by an external field, but appears as a spontaneous symmetry breaking, which this was historically how it was introduced in order to find the correct solution.

The above discussion shows that q is the *order parameter* of the transition: it is zero in the paramagnetic phase, and it jumps to a nonzero value in the glass phase signaling the spontaneous breaking of replica symmetry. Alternatively, we can introduce an external field coupled to this order parameter in order to compute the properties of the low-temperature phase, analogously to a magnetic field for a ferromagnet. The transition is therefore first order from the point of view of the order parameter, but recall that it is second order from the thermodynamical point of view.

C. The SK model: full replica symmetry breaking

We can now go back to the SK model. In this case, the situation is much more complicated. The study of the TAP equations for the SK model was initiated in the original publication [49] (the reprints of this and other relevant papers can be found in [9]). The TAP equations for the SK model have many solutions, as is the case for the spherical p -spin model, but here the computation of their complexity is much more involved. It was started in [62], but a recent revival of interest led to a more complete understanding of the problem. It is reviewed in [63] and references therein.

There are two main reasons for this difficulty. First, the equilibrium states in the spin glass phase (i.e. the lowest energy states) *are not independently distributed*, unlike for the spherical p -spin model in which the different states have zero overlap. In the SK model, the mutual overlaps between equilibrium states are organized in a complicated pattern [9]. Second, the metastable states (whose free energy is larger than that of the equilibrium states) are not well-defined minima, again unlike for the spherical p -spin model. In the SK model, for finite N they come in pairs, one being a minimum and the other a maximum. The two coalesce in the $N \rightarrow \infty$ limit, forming a *saddle* point, i.e. a state with one zero mode.

In the SK model the existence of these marginally stable states is not important, as far as the equilibrium properties are concerned, because they do not appear in the computation of the partition function. The transition is from the high-temperature paramagnetic state to the low-temperature *equilibrium* states, and is second-order both thermodynamically and from the point of view of the order parameter. Indeed, the local magnetizations m_i are small close to T_c [49] and so are the overlaps [9].

Here we will only discuss the definition of the order parameter for the SK model and its solution using the replica method. For more details on the TAP approach see [9, 49, 62, 63].

1. The overlap distribution

As we already discussed, in presence of many pure states the Gibbs measure decomposes as $P[S] = \sum_{\alpha} w_{\alpha} P_{\alpha}[S]$, with $\sum_{\alpha} w_{\alpha} = 1$. We also said that each state is specified by its local magnetizations $m_i^{\alpha} = \langle S_i \rangle_{\alpha}$. We can define the *overlap* between two states

$$q_{\alpha\beta} = \frac{1}{N} \sum_i m_i^{\alpha} m_i^{\beta} = \frac{1}{N} \sum_i \langle S_i \rangle_{\alpha} \langle S_i \rangle_{\beta} . \quad (88)$$

In the case of the spherical p -spin model, we found that the natural order parameter was the overlap of two replicas defined in (68). The infinitesimal coupling forces the two replicas in the same state, so we have

$$q = \langle Q_{ab} \rangle = \sum_{\alpha} w_{\alpha} \frac{1}{N} \sum_i \langle S_i^a \rangle_{\alpha} \langle S_i^b \rangle_{\alpha} = \sum_{\alpha} w_{\alpha} \frac{1}{N} \sum_i m_i^{\alpha} m_i^{\alpha} = \sum_{\alpha} w_{\alpha} q_{\alpha\alpha} , \quad (89)$$

and the (thermal average of the) overlap is just the average self-overlap of a state α . Recall that for the spherical p -spin model we assumed that $q_{\alpha\alpha} \equiv q$, and that different states were uncorrelated, i.e. that $q_{\alpha\beta} = 0$ for $\alpha \neq \beta$.

In a more complicated situation we might be interested in the probability distribution of the overlap:

$$P(q) = \sum_{\alpha\beta} w_{\alpha} w_{\beta} \delta(q - q_{\alpha\beta}) ; \quad (90)$$

in general $P(q)$ will depend on the couplings J and we will then consider its average over the disorder, $\overline{P(q)}$. We wish now to work out a connection between this quantity and the matrix Q_{ab} that appears in the replicated free energy (75). Let us then consider the following quantity,

$$q^{(1)} = \frac{1}{N} \sum_i \overline{\langle S_i \rangle^2} , \quad (91)$$

where the average is over the Gibbs measure. By using the decomposition in pure states, we can rewrite $q^{(1)}$ as

$$q^{(1)} = \frac{1}{N} \sum_i \sum_{\alpha\beta} \overline{w_{\alpha} w_{\beta} \langle S_i \rangle_{\alpha} \langle S_i \rangle_{\beta}} = \sum_{\alpha\beta} \overline{w_{\alpha} w_{\beta} q_{\alpha\beta}} = \int dq \sum_{\alpha\beta} \overline{w_{\alpha} w_{\beta} \delta(q - q_{\alpha\beta})} q = \int dq \overline{P(q)} q \quad (92)$$

Therefore $q^{(1)}$ is the first moment of the overlap distribution, averaged over the disorder. By using the clustering property, we can easily find a generalization of this formula [9],

$$\begin{aligned} q^{(k)} &= \frac{1}{N^k} \sum_{i_1 \dots i_k} \overline{\langle S_{i_1} \dots S_{i_k} \rangle^2} = \frac{1}{N^k} \sum_{i_1 \dots i_k} \sum_{\alpha\beta} w_{\alpha} w_{\beta} \overline{\langle S_{i_1} \dots S_{i_k} \rangle_{\alpha} \langle S_{i_1} \dots S_{i_k} \rangle_{\beta}} \\ &= \frac{1}{N^k} \sum_{i_1 \dots i_k} \sum_{\alpha\beta} w_{\alpha} w_{\beta} \overline{\langle S_{i_1} \rangle_{\alpha} \dots \langle S_{i_k} \rangle_{\alpha} \langle S_{i_1} \rangle_{\beta} \dots \langle S_{i_k} \rangle_{\beta}} = \int dq \overline{P(q)} q^k \end{aligned} \quad (93)$$

The important fact is that we can also compute these quantities using the replica trick. In particular,

$$q^{(1)} = \frac{1}{N} \sum_i \overline{\langle S_i \rangle^2} = \frac{1}{Z^2} \sum_{S^1, S^2} e^{-\beta(H[S^1] + H[S^2])} \frac{1}{N} \sum_i S_i^1 S_i^2 = \lim_{n \rightarrow 0} \sum_{S^a} \frac{1}{N} \sum_i S_i^1 S_i^2 e^{-\beta \sum_a H(S^a)} , \quad (94)$$

where the last equation is obtained writing $Z^{-2} = \lim_{n \rightarrow 0} Z^{n-2}$. If we now go on with the calculation along the lines of the previous paragraphs, introducing the overlap matrix Q_{ab} , we get,

$$q^{(1)} = \int DQ_{ab} e^{-NX(Q_{ab})} Q_{12} = Q_{12}^{\text{SP}} e^{-NX(Q_{ab}^{\text{SP}})} = Q_{12}^{\text{SP}} \quad (95)$$

where Q_{ab}^{SP} is the saddle point value of the overlap matrix (from now on we will drop the suffix SP), and where we have exploited the fact that $S(Q_{ab})$ is of order n , and therefore does not contribute when $n \rightarrow 0$. Of course, there is something wrong about this formula, because replicas 1 and 2 cannot be different from the others. If we decided to call them 4 and 7, we would get a different result whenever Q_{ab} is not replica symmetric. To better understand

this point we note that if the saddle point overlap matrix is not symmetric, then there must be other saddle point solutions with the same free energy, but corresponding to matrices obtained from Q_{ab} by a permutation of lines and columns [9]. This result is general: when a saddle point breaks a symmetry corresponding to a given transformation, all the points obtained by applying the transformation to that particular saddle point, are equally valid. We must therefore average over all these saddle points, which is equivalent to symmetrizing the equation (95):

$$q^{(1)} = \lim_{n \rightarrow 0} \frac{2}{n(n-1)} \sum_{a>b} Q_{ab} \quad (96)$$

This result is already telling us that there is a connection between $q^{(1)}$ and the matrix of the overlap among replicas Q_{ab} . To go further, we can generalize (96) to get

$$q^{(k)} = \lim_{n \rightarrow 0} \frac{2}{n(n-1)} \sum_{a>b} Q_{ab}^k \quad (97)$$

Comparing with equation (93) gives that for a generic function $f(q)$

$$\int dq f(q) \overline{P(q)} = \lim_{n \rightarrow 0} \frac{2}{n(n-1)} \sum_{a>b} f(Q_{ab}) , \quad (98)$$

which, in particular, for $f(q) = \delta(q - q')$ finally provides the crucial equation connecting physics to replicas,

$$\overline{P(q)} = \lim_{n \rightarrow 0} \frac{2}{n(n-1)} \sum_{a>b} \delta(q - Q_{ab}) . \quad (99)$$

This equation shows that the average probability that two pure states of the system have overlap q is equal to the fraction of elements of the overlap matrix Q_{ab} equal to q . In other words, *the elements of the overlap matrix (in the saddle point) are the physical values of the overlap among pure states, and the number of elements of Q_{ab} equal to q is related to the probability of q .*

Before turning to a more precise computation for the SK model, it is useful to discuss some general properties of the overlaps. First of all, it is reasonable (and correct [9]) to assume that all the states have the same self overlap, $q_{\alpha\alpha} \equiv q_{\text{EA}}$, as in the spherical p -spin model. Then, for any two states α and β :

$$0 \leq \frac{1}{N} \sum_i (m_i^\alpha - m_i^\beta)^2 = q_{\alpha\alpha} + q_{\beta\beta} - 2q_{\alpha\beta} = 2(q_{\text{EA}} - q_{\alpha\beta}) \quad \Rightarrow \quad q_{\text{EA}} = \max\{q_{\alpha\beta}\} . \quad (100)$$

Additionally, it is convenient to remove the trivial symmetry $S \rightarrow -S$ that is present in the SK model and is reflected in $P(q) = P(-q)$. This can be done by adding an infinitesimal magnetic field that will favor one of the two states α and $-\alpha$ related by the symmetry. Once it is done, the overlaps are all positive and one obtains a distribution $P_+(q)$, such that $P(q) = (P_+(q) + P_+(-q))/2$. In the following we will drop the suffix $+$ and consider that the overlaps are all positive.

Finally, it is useful to define the function

$$x(q) = \int_0^q P(q') dq' \in [0, 1] , \quad \frac{dx}{dq} = P(q) . \quad (101)$$

As $P(q)$ is positive, $x(q)$ is a monotonically increasing function and so we can define its inverse $q(x)$. In particular we can write

$$q^{(1)} = \int_0^1 q P(q) dq = \int_0^1 q \frac{dx}{dq} dq = \int_0^1 q(x) dx . \quad (102)$$

2. The Parisi solution of the SK model

In the case of the SK model, one can again introduce replicas to average over the disorder, with again the result

$$\overline{Z^n} \sim \int dQ_{ab} e^{NX(Q_{ab})} . \quad (103)$$

The explicit form of $X(Q)$ can be found, for example, in [9], but it is not crucial for the rest of this discussion. The replica symmetric solution corresponds to $Q_{ab} = \delta_{ab} + q(1 - \delta_{ab})$ (in this case, we also allow for a finite overlap between replicas in different states). Remarkably, this solution predicts that $q = 0$ for $T > 1$, while $q \neq 0$ for $T < 1$, i.e. one finds a phase transition at $T = T_c = 1$. The entropy, however, becomes negative at low temperatures, and, as the SK model is formulated for discrete spins, this solution is clearly incorrect.

If one uses a 1RSB ansatz, as in (78), the situation is improved, in the sense that the entropy becomes negative at a much lower temperature and it is negative but small at $T = 0$. It is better to change notation, $q \rightarrow q_1$ in (78) and to replace the zeros by q_0 to be more general. Then, within the 1RSB ansatz, from (99) one has

$$\overline{P(q)} = \lim_{n \rightarrow 0} \frac{1}{n-1} [(n-m)\delta(q-q_0) + (m-1)\delta(q-q_1)] = m\delta(q-q_0) + (1-m)\delta(q-q_1), \quad (104)$$

meaning that two replicas have a probability m of being in the different states and a probability $1-m$ of being in the same state. Note that it follows from this interpretation that $m \leq 1$, as we found for the p -spin spherical model.

Parisi then introduced another level of replica symmetry breaking, by assuming that replicas are split into m_1 blocks, and that inside each block they are further split into $m_2 < m_1$ blocks. For $n = 8$, $m_1 = 4$ and $m_2 = 2$ the matrix Q would then read

$$Q = \begin{pmatrix} 1 & q_2 & q_1 & q_1 & q_0 & q_0 & q_0 & q_0 \\ q_2 & 1 & q_1 & q_1 & q_0 & q_0 & q_0 & q_0 \\ q_1 & q_1 & 1 & q_2 & q_0 & q_0 & q_0 & q_0 \\ q_1 & q_1 & q_2 & 1 & q_0 & q_0 & q_0 & q_0 \\ q_0 & q_0 & q_0 & q_0 & 1 & q_2 & q_1 & q_1 \\ q_0 & q_0 & q_0 & q_0 & q_2 & 1 & q_1 & q_1 \\ q_0 & q_0 & q_0 & q_0 & q_1 & q_1 & 1 & q_2 \\ q_0 & q_0 & q_0 & q_0 & q_1 & q_1 & q_2 & 1 \end{pmatrix}. \quad (105)$$

The 2RSB solution has a better entropy, that becomes negative at even lower temperatures and is now very small at $T = 0$. The $P(q)$ reads

$$\begin{aligned} \overline{P(q)} &= \lim_{n \rightarrow 0} \frac{1}{n-1} [(n-m_1)\delta(q-q_0) + (m_1-m_2)\delta(q-q_1) + (m_2-1)\delta(q-q_2)] \\ &= m_1\delta(q-q_0) + (m_2-m_1)\delta(q-q_1) + (1-m_2)\delta(q-q_2). \end{aligned} \quad (106)$$

The positivity of $P(q)$ requires $0 < m_1 < m_2 < 1$.

Iterating this procedure produces the correct solution. One ends up with a sequence of numbers $1 < m_K < m_{K-1} < \dots < m_2 < m_1 < n$, each one corresponding to blocks with overlap $q_0 < \dots < q_K$, and $K \rightarrow \infty$. The equality is reversed in the limit $n \rightarrow 0$, $m_0 = 0 < m_1 < m_2 < \dots < m_K < 1 = m_{K+1}$, and

$$\overline{P(q)} = \sum_{i=0}^K (m_{i+1} - m_i) \delta(q - q_i) \quad (107)$$

becomes a continuous functions with support in $[0, \max_i q_i]$. The function $x(q)$ is a piecewise constant function. In the limit $K \rightarrow \infty$ it becomes an arbitrary function that must satisfy only the constraint that $x \in [0, 1]$, $q \in [0, 1]$, and $\frac{dx}{dq} \geq 0$. The free energy becomes a functional of $x(q)$, and therefore $x(q)$ (or $P(q)$) is the order parameter of the transition for the SK model.

The Parisi solution has the following physical interpretation. Equilibrium states have self-overlap $q_K = q_{EA}$. They are arranged in clusters such that states inside a cluster have mutual overlap q_{K-1} , but such clusters are arranged in other (super)clusters, and states belonging to the same (super)cluster have mutual overlap q_{K-2} . Supercusters are arranged in supersuperclusters, etc.

The complicated mathematical structure of the Parisi solution, once correctly interpreted, led to a number of non-trivial predictions, that we cannot review here, but are discussed e.g. in [8, 9, 50]. At present, it has been proven that the free energy of the Parisi solution is correct, i.e. it is equal to the true free energy of the SK model below T_c [15]. This proof alone took twenty years of efforts, and most of the interesting properties of the solution, even if confirmed by numerical simulations, have not yet been rigorously proven.

D. Susceptibilities

It is interesting to discuss at this point the behavior of the magnetic susceptibilities that characterize the phase transitions we have investigated so far. We will first review the case of the ferromagnet, and then turn to the spin

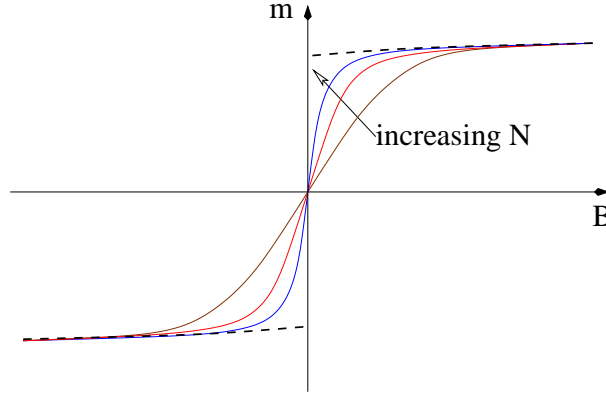


FIG. 5: Magnetization m as a function of magnetic field \mathcal{B} for a ferromagnetic system at $T < T_c$, for finite N and for $N \rightarrow \infty$.

glass. We will discuss explicitly the case of mean field models, but the discussion applies also to finite dimensional models, with minor modifications.

1. The ferromagnet

In a ferromagnet, the order parameter is the magnetization $m(T, \mathcal{B}; N) = \frac{1}{N} \sum_i \langle S_i \rangle$, or to be more precise

$$m^*(T) = \lim_{\mathcal{B} \rightarrow 0} \lim_{N \rightarrow \infty} m(T, \mathcal{B}; N). \quad (108)$$

The magnetization below T_c is given by $\pm m^*$ if $\mathcal{B} \rightarrow 0^\pm$ after $N \rightarrow \infty$. The behavior of $m(T, \mathcal{B}; N)$ is sketched in Fig. 5. At finite N , the magnetization is an analytic function of \mathcal{B} ; but in the limit $N \rightarrow \infty$, it becomes steep around $\mathcal{B} = 0$ where the singularity develops. The susceptibility

$$\chi(T, \mathcal{B}; N) = \frac{dm(T, \mathcal{B}; N)}{d\mathcal{B}} \quad (109)$$

calculated at $\mathcal{B} = 0$ is the slope of the curve at $\mathcal{B} = 0$ and diverges when $N \rightarrow \infty$ at all $T < T_c$. This quantity is not, however, the thermodynamic magnetic susceptibility, which is instead obtained by taking first the limit $N \rightarrow \infty$, and then $\mathcal{B} \rightarrow 0$, and which is finite as one can check from Fig. 5. The quantity $\chi(T, \mathcal{B}=0; N \rightarrow \infty)$ is the susceptibility in the full Gibbs measure, which is infinite below T_c because the Gibbs measure is unstable towards the decomposition in the two pure states with positive and negative magnetization. Note that because $\chi(T, \mathcal{B}=0; N)$ is analytic at finite N as a function of T , and diverges for all $T < T_c$, it follows that $\chi(T, \mathcal{B}=0; N \rightarrow \infty)$ must diverge for $T \rightarrow T_c^+$.

We can also compute the susceptibility at finite N in the Gibbs measure (i.e. in absence of external field) using the fluctuation dissipation relation

$$\chi(T, \mathcal{B} = 0; N) = \frac{dm}{d\mathcal{B}} = \frac{\beta}{N} \sum_{ij} \langle S_i S_j \rangle_c, \quad (110)$$

where $\langle S_i S_j \rangle_c = \langle S_i S_j \rangle - \langle S_i \rangle \langle S_j \rangle$ is the connected correlation function. For large enough N , we may think that the Gibbs measure is split between two states $\alpha = \pm$, each with weight $w_\alpha = 1/2$, so we have $\langle S_i \rangle = 0$. For the fully connected model, using the clustering property inside each state we get for $i \neq j$:

$$\langle S_i S_j \rangle_c = \langle S_i S_j \rangle = \frac{1}{2} [\langle S_i \rangle_+ \langle S_j \rangle_+ + \langle S_i \rangle_- \langle S_j \rangle_-] = \frac{1}{2} [(m^*)^2 + (-m^*)^2] = (m^*)^2, \quad (111)$$

and therefore

$$\chi(T, B = 0; N) = \beta(N-1)[m^*(T)]^2 + \beta, \quad (112)$$

which diverges for $N \rightarrow \infty$ in the low temperature phase. Note that this result is wrong, because for $T > T_c$ we obtain $\chi(T, B=0; N \rightarrow \infty) = \beta$, which does not diverge for $T \rightarrow T_c^+$.

Indeed, from the mean field equation $m = \tanh[\beta(\mathcal{B} + m)]$ (which holds only for $N \rightarrow \infty$) we get, taking the derivative of the equation with respect to \mathcal{B} ,

$$\chi = (1 - m^2)\beta(1 + \chi) \quad \Rightarrow \quad \chi(T, \mathcal{B}; N \rightarrow \infty) = \frac{\beta[1 - (m^*(T))^2]}{1 - \beta[1 - (m^*(T))^2]} , \quad (113)$$

and therefore for $T > T_c = 1$ we get $\chi(T, \mathcal{B}; N \rightarrow \infty) = \beta/(1 - \beta)$, which diverges for $T \rightarrow 1^+$. In order to get this result from the fluctuation-dissipation relation we need to take into account that the clustering properties only holds for $N \rightarrow \infty$. At finite N there are corrections of order $1/N$ to $\langle S_i S_j \rangle_c$. Because there are N^2 terms and a factor of $1/N$ in Eq. (110), these $1/N$ corrections affect the finite part of χ . Still, the calculation leading to (112) is correct for the divergent term¹¹.

In summary, the calculation of the leading term of χ in the Gibbs measure and at finite (but large) N can be done, using only the decomposition in pure states and the clustering property. This calculation shows that $\chi(T; \mathcal{B}=0; N)$ is divergent for $N \rightarrow \infty$ in the whole low temperature phase, which is to be expected from Fig. 5. But because χ is divergent for $T < T_c$, it must also diverge for $T \rightarrow T_c^+$. In this way we identify the susceptibility that diverges at the phase transition.

2. Spin glasses: linear susceptibilities

For a spin glass in absence of external field and for a symmetric distribution of J , $P(J_{ij}) = P(-J_{ij})$, one has $\overline{\langle S_i S_j \rangle_c} = 0$ for $i \neq j$. In fact, for $i \neq j$,

$$\overline{\langle S_i S_j \rangle} = \overline{\sum_{\alpha} w_{\alpha} m_i^{\alpha} m_j^{\alpha}} . \quad (114)$$

Due to the symmetry of the couplings, the probability (over the states α and the disorder) that the magnetizations m_i^{α} and m_j^{α} have the same or opposite signs are the same, and the average vanishes. The term $\overline{\langle S_i \rangle \langle S_j \rangle}$ vanishes because $\langle S_i \rangle$ and $\langle S_j \rangle$ have random signs. The total magnetic susceptibility is then given by

$$\chi = \beta \left(1 - \frac{1}{N} \sum_i \overline{\langle S_i \rangle^2} \right) = \beta(1 - q^{(1)}) . \quad (115)$$

This susceptibility is that one would measure if the system is prepared at equilibrium, then a small magnetic field is applied and the new equilibrium state is reached. A small magnetic field shuffles the free energy of the states, and therefore in general the new equilibrium states in presence of a field will be very different from the old ones. As a result, in order to observe the susceptibility (115) one has to wait a very long time for the system to reach the new equilibrium states.

One might also be interested in considering the linear susceptibility of a *single equilibrium state* α . This susceptibility is that one would observe if the system does not have time to escape its original state after the magnetic field is applied. Using the fluctuation-dissipation inside the state α we get, under the assumption $q_{\alpha\alpha} \equiv q_{\text{EA}}$,

$$\chi_{\alpha} = \beta \left(1 - \frac{1}{N} \sum_i \overline{\langle S_i \rangle_{\alpha}^2} \right) , \quad \chi_{\text{LR}} = \overline{\sum_{\alpha} w_{\alpha} \chi_{\alpha}} = \beta(1 - q_{\text{EA}}) . \quad (116)$$

The name χ_{LR} comes from the fact that this is the susceptibility associated to linear response inside a state. If $P(q)$ is not trivial, i.e. it is not a delta function, $q^{(1)} < q_{\text{EA}}$ and the two susceptibilities are different, in particular $\chi_{\text{LR}} < \chi$. This result is very reasonable. Once we switch on a small magnetic field \mathcal{B} , the system first responds by acquiring a small magnetization inside the state α , $m_{\text{LR}} \sim \chi_{\text{LR}} \mathcal{B}$. It will then escape from state α and find a better state in presence of \mathcal{B} , which will then give a larger magnetization $m \sim \chi \mathcal{B} > m_{\text{LR}}$. This last property of the spin glass phase is very important.

¹¹ In a short range system, the discussion is very similar. Clustering holds only for $|i - j| \rightarrow \infty$, but if the connected correlation is finite in this limit, the sum is dominated by the large values of $|i - j|$ and the result is the same as in (112).

Note that the time τ_N needed to change state diverges with N if there is a true phase transition. Then, we can define (at finite N) the dynamical magnetic susceptibility

$$\chi(t) = \frac{dm(t)}{d\mathcal{B}} = \beta \left(1 - \frac{1}{N} \overline{\sum_i \langle S_i(t) S_i(0) \rangle} \right), \quad (117)$$

where it is assumed that the system is in equilibrium in absence of field and the field is switched on at $t = 0$. For $1 \ll t \ll \tau_N$, the correlation function $\langle S_i(t) S_i(0) \rangle$ decorrelates inside the state α to which the initial configuration belongs, $\langle S_i(t) S_i(0) \rangle \sim \sum_\alpha w_\alpha \langle S_i \rangle_\alpha \langle S_i \rangle_\alpha$. Hence, we have

$$\chi(1 \ll t \ll \tau_N) = \beta \left(1 - \frac{1}{N} \overline{\sum_i \sum_\alpha w_\alpha \langle S_i \rangle_\alpha \langle S_i \rangle_\alpha} \right) = \chi_{\text{LR}}. \quad (118)$$

On the other hand, for $t \gg \tau_N$, the system decorrelates completely in the full Gibbs measure: $\langle S_i(t) S_i(0) \rangle \sim \langle S_i \rangle \langle S_i \rangle$, and $\chi(t \gg \tau_N) = \chi$, the equilibrium susceptibility. Recalling that τ_N diverges with N , we get

$$\begin{aligned} \lim_{N \rightarrow \infty} \lim_{t \rightarrow \infty} \chi(t) &= \chi, \\ \lim_{t \rightarrow \infty} \lim_{N \rightarrow \infty} \chi(t) &= \chi_{\text{LR}}. \end{aligned} \quad (119)$$

The behavior of $\chi(t)$ on a time scale t that diverges with N is more complicated, and its discussion is behind the scope of these notes.

In either case, *for spin glasses the magnetic susceptibilities are finite at the transition*. For a continuous transition, both χ and χ_{LR} show a cusp at T_c , when q_{EA} becomes non-zero. For a discontinuous 1RSB transition, χ_{LR} jumps at T_d where states appear. However, from (104) with $q_0 = 0$, we have $q^{(1)} = (1 - m)q_1 = (1 - m)q_{\text{EA}}$, so χ is analytic across T_d because $m = 1$ and $q^{(1)} = 0$, and has a cusp at T_K where $m \neq 1$.

3. The static spin glass susceptibility

The diverging susceptibility is more complicated in the spin glass case. In order to keep the discussion more general, we will avoid performing explicitly the average over the disorder and consider a single (large enough) sample, using the fact the susceptibilities are self-averaging quantities. In this way the following discussion can be extended straightforwardly to glassy systems without quenched disorder.

The analog of the magnetization for a spin glass system is the self-overlap $q_{\text{EA}} = q_{\alpha\alpha}$, which becomes non-zero when states appear. As we discussed in section II B 3, to compute q_{EA} we should put a coupling between replicas in order to force them to be in the same state. We consider two replicas and choose a coupling $\delta H = -\epsilon \sum_i S_i^1 S_i^2$. Then (108) becomes

$$q_{\text{EA}} = \lim_{\epsilon \rightarrow 0} \lim_{N \rightarrow \infty} \frac{1}{N} \sum_i \langle S_i^1 S_i^2 \rangle_\epsilon. \quad (120)$$

It is worth noting at this point that the quantity above is really the self-overlap of the states and not $q^{(1)}$, which is the thermodynamic average of $q_{\alpha\beta}$. The reason is the following. Suppose we are in a phase where the $P(q)$ is not trivial (for instance, we consider the SK model at $T < T_c$ or the p -spin model for $T < T_K$). In this case, the Gibbs measure is dominated by the set of states that have the lowest intensive free energy. The fluctuations in the weight are due to $1/N$ corrections to the free energy. We can write $f_\alpha = f_{\min} + \Delta f_\alpha/N$, and therefore

$$w_\alpha = \frac{e^{-\beta N f_\alpha}}{\sum_\alpha e^{-\beta N f_\alpha}} = \frac{e^{-\beta \Delta f_\alpha}}{\sum_\alpha e^{-\beta \Delta f_\alpha}}. \quad (121)$$

It can be shown [9] that these weights have finite fluctuations, and although the number of states with finite weights is infinite for $N \rightarrow \infty$, the number of states that are needed to cover a fraction $1 - \epsilon$ of the total weight is finite for any ϵ . The partition function of two replicas with the coupling discussed above can thus be written as

$$Z_\epsilon = e^{-2\beta N f_{\min}} \sum_{\alpha\beta} e^{-\beta(\Delta f_\alpha + \Delta f_\beta)} e^{\beta \epsilon N q_{\alpha\beta}}. \quad (122)$$

Clearly, because the number of relevant terms in the sum is finite, the weights are finite, and $q_{\text{EA}} = q_{\alpha\alpha} > q_{\alpha\neq\beta}$, the coupling term for any $\epsilon > 0$ makes the contribution of the terms with $\alpha = \beta$ exponentially bigger than that of $\alpha \neq \beta$. The replicas are therefore in the same state and the average overlap is given by q_{EA} . On the contrary, $q^{(1)}$ is related to a full average in the Gibbs measure in absence of any coupling¹².

The susceptibility associated to q_{EA} is therefore¹³ (at finite N and $\epsilon \rightarrow 0$, when the replicas are uncoupled):

$$\chi_{\text{SG}} = \frac{dq_{\text{EA}}}{d\epsilon} = \frac{\beta}{N} \sum_{ij} [\langle S_i^1 S_j^1 \rangle \langle S_i^2 S_j^2 \rangle - \langle S_i^1 \rangle \langle S_j^1 \rangle \langle S_i^2 \rangle \langle S_j^2 \rangle] . \quad (123)$$

Performing the decomposition in pure states and using the clustering property it is easy to show that

$$\chi_{\text{SG}} = \beta N \left[\sum_{\alpha\beta} w_\alpha w_\beta (q_{\alpha\beta})^2 - \sum_{\alpha\beta\gamma\delta} w_\alpha w_\beta w_\gamma w_\delta q_{\alpha\beta} q_{\gamma\delta} \right] = \beta N [q^{(2)} - (q^{(1)})^2] . \quad (124)$$

Then χ_{SG} is divergent in the spin glass phase where the $P(q)$ is not trivial and $q^{(k)} \neq 0$. This happens for $T < T_c$ in the SK model (and in all models with a second-order spin glass transition), and for $T < T_K$ in the spherical p -spin model (and in all models with a discontinuous transition). In all these cases the partition function is dominated by the low free energy states, so that an infinitesimal coupling suffices to force two replicas to be in the same state.

4. The dynamic spin glass susceptibility

The static spin glass susceptibility defined above does not diverge between T_d and T_K in the discontinuous case, as it should, because it is a thermodynamic quantity and we showed that the thermodynamics has no singularity at T_d . How can we obtain a susceptibility that diverges at the clustering transition? For this, we would like to probe each state separately and not the full Gibbs measure.

Similarly to what we did in Eq. (117), the solution is to consider a dynamical susceptibility. We define it as follows:

$$\chi_{\text{SG}}(t) = \frac{\beta}{N} \sum_{ij} [\langle S_i(t) S_j(t) S_i(0) S_j(0) \rangle - \langle S_i(t) S_i(0) \rangle \langle S_j(t) S_j(0) \rangle] . \quad (125)$$

Note that $\chi_{\text{SG}}(0) = 0$. Again, the time needed to change state, τ_N , diverges with N . For $t \gg \tau_N$ the system decorrelates in the full Gibbs measure and

$$\chi_{\text{SG}}(t \gg \tau_N) = \frac{\beta}{N} \sum_{ij} [\langle S_i S_j \rangle \langle S_i S_j \rangle - \langle S_i \rangle \langle S_i \rangle \langle S_j \rangle \langle S_j \rangle] = \chi_{\text{SG}} , \quad (126)$$

so that it reduces to the static spin glass susceptibility, and is finite between T_K and T_d .

In the region $1 \ll t \ll \tau_N$, the system is only able to decorrelate within one state, so the dynamical susceptibility is

$$\begin{aligned} \chi_{\text{SG}}(1 \ll t \ll \tau_N) &= \frac{\beta}{N} \sum_{ij} \left[\sum_a w_\alpha \langle S_i S_j \rangle_\alpha \langle S_i S_j \rangle_\alpha - \sum_\alpha w_\alpha \langle S_i \rangle_\alpha \langle S_i \rangle_\alpha \sum_\beta w_\beta \langle S_j \rangle_\beta \langle S_j \rangle_\beta \right] \\ &= \beta N \left[\sum_a w_\alpha q_{\alpha\alpha}^2 - \sum_{\alpha\beta} w_\alpha w_\beta q_{\alpha\beta}^2 \right] = \beta N [(q_{\text{EA}})^2 - q^{(2)}] = \chi_{\text{SG,LR}} . \end{aligned} \quad (127)$$

Now, $\chi_{\text{SG,LR}}$ also diverges in the discontinuous 1RSB case between T_d and T_K , where $q_{\text{EA}} \neq 0$ and $q^{(2)} = 0$.

In summary, we have $\chi_{\text{SG}}(0) = 0$ and

$$\begin{aligned} \lim_{N \rightarrow \infty} \lim_{t \rightarrow \infty} \chi_{\text{SG}}(t) &= \chi_{\text{SG}} , \\ \lim_{t \rightarrow \infty} \lim_{N \rightarrow \infty} \chi_{\text{SG}}(t) &= \chi_{\text{LR,SG}} . \end{aligned} \quad (128)$$

Note that in the cluster phase $T_K < T < T_d$, $\chi_{\text{SG}}(t)$ has a very peculiar behavior¹⁴: it grows up to a very large ($\sim N$) value for $t \sim \tau_N$, and then decays back to a finite value for really large times $t \gg \tau_N$. By contrast, in the thermodynamic spin glass phase, when $T < T_K$, $\chi_{\text{SG}}(t)$ is of order N for all times $t \gg 1$.

¹² By a similar argument one can show that $P(q) = \delta(q - q_{\text{EA}})$ for any $\epsilon > 0$

¹³ The factor β is sometimes omitted or replaced by β^2 in the literature.

¹⁴ This behavior has been recently observed in structural glasses, for which $\chi_{\text{SG}}(t)$ is usually called $\chi_4(t)$ in the literature.

E. Exercises

1. **Dynamics of the fully connected Ising model** - Write a program to simulate the Metropolis dynamics of the fully connected Ising model, Eq. (12). The dynamics is defined as follows. At each step try to flip a random spin, $S_i \rightarrow -S_i$. Draw a random number x uniformly in $[0, 1]$ and accept the move if $x < \exp[-\beta(H[S'] - H[S])]$, where S' is the configuration with S_i flipped. (Hint: in addition to the spins S_i , keep in memory the total magnetization $M = \sum_i S_i$, updating it at each step. Use it to compute the energy change.) Using the program, simulate the time evolution of a small number of spins in the low temperature phase. Check that the system jumps from one state to the other and try to observe the scaling of the persistence time with N .
2. **The Random Energy Model** - The Ising p -spin Hamiltonian (47) for Ising spins is, for a given configuration S (with $S_i = \pm 1$), a Gaussian random variable with zero average.

- Show that the covariance $\overline{H[S]H[S']} = \frac{1}{2}NQ(S, S')^p$, where $Q(S, S') = \frac{1}{N} \sum_i S_i S'_i$ is the overlap of S, S' .
- Deduce that for $p \rightarrow \infty$ the energy of a configuration is a Gaussian random variable with variance $N/2$ and that the energy of different configurations are uncorrelated (this is trivial).

Therefore in the large p limit the p -spin converges to the *Random Energy Model* (REM): there are 2^N configuration with energies E_i that are Gaussian and independent, with zero average and variance $N/2$.

- Compute the average number of configurations that have energy E , call it $\Omega(E)$; compute the complexity $\Sigma(e) = \frac{1}{N} \log \Omega(Ne)$ (the result is $\Sigma(e) = \log 2 - e^2$). Show that the complexity vanishes for $e < e_K$; compute e_K .
- The previous result implies that for $e > e_K$ the number of configurations is very large; conversely, for $e < e_K$ the probability of finding a configurations is exponentially small ($\Sigma < 0$) and we can assume that there are no configurations. Defining the partition function as

$$Z(T) = \sum_{i=1}^{2^N} e^{-E_i/T} \sim \int_{-N|e_K|}^{Ne_K} dE \Omega(E) e^{-E/T}, \quad (129)$$

compute the free energy $f(T)$ via a saddle point. Show that there is a phase transition at a certain temperature T_K , in particular that the second derivative of $f(T)$ (the specific heat) has a jump.

The REM has exactly the same phenomenology of the p -spin, except for the fact that in the REM *each configuration is a state* (we did not show it but it can be done for instance by showing that, for the p -spin model, the overlap in a state goes to 1 when $p \rightarrow \infty$). Therefore T_d does not exist since states are stable at all temperatures, and moreover the internal entropy $s(T)$ is identically zero. See [9, 64] for details.

3. **Zero-temperature complexity of the p -spin model** - Consider the zero-temperature limit of (82). Show that for $\beta \rightarrow \infty$ it has a finite limit at fixed $\mu = \beta m$ and with $q = 1 - \alpha T$, with α of order 1, given by

$$\phi_{\text{IRSB}} = -\frac{1}{4}(p\alpha + \mu) + \frac{1}{2\mu} \log \frac{\alpha}{\alpha + \mu}. \quad (130)$$

Deduce that α satisfies the equation $\alpha^2 + \mu\alpha - 2/p = 0$, and compute its positive solution (recall that $q \leq 1$). Now show that

$$\begin{aligned} e(\mu) &= \lim_{\beta \rightarrow \infty, \beta m = \mu} f(m, T) = \partial_\mu [\mu \phi_{\text{IRSB}}], \\ \Sigma(\mu) &= \mu^2 \partial_\mu \phi_{\text{IRSB}}, \end{aligned} \quad (131)$$

and compute their explicit expressions as function of μ . Check that the physical region corresponds, for $p = 3$, to $\mu \in [0.577, 0.884]$, that the threshold energy is $e_{th} = -\sqrt{4/3} \sim -1.155$ and that the ground state energy is $e_0 \sim -1.172$. Show that in general $e_{th} = -\sqrt{2(p-1)/p}$.

4. **Complexity of the 3-spin model** - Starting from Eq. (82), and using (61), compute $\Sigma(f)$ for the spherical 3-spin model at different temperatures, e.g. $T = 0.63 > T_d$, $T_d > T = 0.6 > T_K$, $T = 0.5 < T_K$ (it can be done by Mathematica¹⁵ or writing a program in C/Fortran/...). There are two possibilities to solve the equation for q : i) use that it is cubic and write the explicit solution; ii) write it as $q = f(q)$ and solve it iteratively.

¹⁵ A Mathematica sheet that does the job can be downloaded from <http://www.lpt.ens.fr/~zamponi>, section “Teaching”.

5. **Stability of the 1RSB solution for the 3-spin model** - The aim of this exercise is to obtain the lines m_{th} and m^* from the stability matrix of the 1RSB solution used in the previous exercise. Most of these results have been obtained in [61] which you can consult in case of difficulties. We consider m coupled replicas, in the limit of zero coupling. Following the discussion of section II B 4, the free energy is given by $X(Q)$ in Eq. (75) and the 1RSB ansatz corresponds in this language to choose $Q_{ab} = \delta_{ab} + q(1 - \delta_{ab})$. Furthermore, we have to consider the solution with the largest non-zero $q = q^* > 0$.

- Keep in mind that the matrix Q_{ab} is symmetric, $Q_{ab} = Q_{ba}$. Take the elements with $a < b$ as the independent ones. Show that the stability matrix of the second derivatives is

$$M_{a<b;c<d} = \frac{d^2 X}{dQ_{a<b}dQ_{c<d}} = \frac{\beta^2}{2} p(p-1) Q_{ab}^{p-2} (\delta_{ac}\delta_{bd} + \delta_{ad}\delta_{cb}) - Q_{ac}^{-1} Q_{bd}^{-1} - Q_{ad}^{-1} Q_{cb}^{-1} . \quad (132)$$

- Consider a small perturbation around the non-trivial 1RSB solution. Show that in this case

$$Q_{ab}^{-1} = \frac{1}{1-q} \left[\delta_{ab} - \frac{q}{1+(m-1)q} \right] \quad (133)$$

and the matrix M takes the form

$$\begin{aligned} M_{a<b;c<d} &= M_1 \frac{\delta_{ac}\delta_{bd} + \delta_{ad}\delta_{cb}}{2} + M_2 \frac{\delta_{ac} + \delta_{ad} + \delta_{bc} + \delta_{bd}}{4} + M_3 , \\ M_1 &= \beta^2 p(p-1) q^{p-2} - \frac{2}{(1-q)^2} , \\ M_2 &= \frac{4}{(1-q)^2} \frac{q}{1+(m-1)q} , \\ M_3 &= -2 \frac{1}{(1-q)^2} \left(\frac{q}{1+(m-1)q} \right)^2 . \end{aligned} \quad (134)$$

- Following [53, 65], show that the matrix above has three independent eigenvalues,

$$\begin{aligned} \lambda_R &= M_1 , \\ \lambda_L &= M_1 + (m-1)(M_2 + mM_3) , \\ \lambda_A &= M_1 + \frac{m-2}{2} M_2 . \end{aligned} \quad (135)$$

- Show that $\lambda_L \propto \frac{\partial^2 \phi_{\text{1RSB}}(m, q, T)}{\partial q^2}$. From this deduce that one must have $\lambda_L = 0$ on the line $m^*(T)$ where the non-trivial solution q^* disappears.
- Fix $p = 3$ and compute the three eigenvalues numerically. Check numerically that λ_L vanishes on the line m^* . Next, compute the line $m_{\text{th}}(T)$ corresponding to threshold states as the line where $\lambda_R = 0$. Show that you reproduce the results of figure 4.

III. DILUTED MODELS AND OPTIMIZATION PROBLEMS

A. Definitions

1. Statistical mechanics formulation of optimization problems

The theory of computational complexity [38] establishes a classification of constraint satisfaction problems (CSP) according to their difficulty in the worst case. For concreteness it is convenient to introduce three problems we shall use as running examples in the following:

- **k -XORSAT.** Find a vector \vec{x} of boolean variables satisfying the linear equations $A\vec{x} = \vec{b} \pmod{2}$, where each row of the 0/1 matrix A contains exactly k non-null elements, and \vec{b} is a given boolean vector.
- **q -coloring (q -COL).** Given a graph, assign one of q colors to each of its vertices, without giving the same color to the two extremities of an edge.
- **k -satisfiability (k -SAT).** Find a solution of a boolean formula made of the conjunction (logical AND) of clauses, each made of the disjunction (logical OR) of k literals (a variable or its logical negation).

Each of these problems admits several variants, for instance

- **Decision:** one has to assert the existence or not of a solution, for instance a proper coloring of a given graph.
- **Sampling:** one has to sample the solution according to a given distribution (e.g. uniform over all the solutions), and estimate for instance the total number of solution.
- **Optimization:** one has to discover optimal configurations; these are solutions, if present, or otherwise configurations minimizing the number of violated constraints: for instance colorings minimizing the number of monochromatic edges.

The decision variant of the three examples stated above fall into two distinct complexity classes: k -XORSAT is in the P class, while the two others are NP-complete for $k, q \geq 3$. This means that the existence of a solution of the XORSAT problem can be decided in a time growing polynomially with the number of variables, for any instance of the problem; one can indeed use the Gaussian elimination algorithm. On the contrary no fast algorithm able of solving every coloring or satisfiability problem is known, and the existence of such a polynomial time algorithm is considered as highly improbable.

A general statistical mechanics formulation of a CSP is the following. One is given N variables σ_i , $i = 1, \dots, N$, that might be Ising spins (Boolean variables) or Potts spins, real numbers, or more complicated variables. Then, one is given a set of M constraints labeled by $a = 1, \dots, M$; each constraint involves a certain set of variables that is denoted by $\sigma_a = (\sigma_{i_1}, \dots, \sigma_{i_{K_a}})$. The constraint is a function $\psi_a(\sigma_a)$ that is 0 when σ_a does not satisfy the constraint and 1 otherwise. In the following we will use also the words “clause” or “test” to denote a constraint.

The CSP consists in finding a configuration σ verifying the condition $\prod_a \psi_a(\sigma_a) = 1$; the number of solutions is

$$Z = \sum_{\sigma} \prod_a \psi_a(\sigma_a) . \quad (136)$$

The optimization version of the same problem is obtained by replacing the hard constraint ψ_a with a “soft” one, $\psi_a^\beta = e^{-\beta}$ if the constraint is not satisfied and $\psi_a^\beta = 1$ otherwise. This corresponds to a problem at finite temperature β such that the energy of a violated constraint is equal to 1. The optimization problem is that of finding the ground state, while the decision problem amount to decide whether a ground state with zero energy exists. In both cases we are interested in working at zero (or very small) temperature.

The three illustrative examples presented above admits a simple representation in this formalism:

- **k -XORSAT.** The degrees of freedom of this CSP are boolean variables that we shall represent, following the physics conventions, by Ising spins, $S \in \{-1, +1\}$. Each constraint involves a subset of k variables, $S_a = (S_{i_a^1}, \dots, S_{i_a^k})$, and reads $\psi_a(S_a) = \mathbb{I}(S_{i_a^1} \dots S_{i_a^k} = J_a)$, where here and in the following $\mathbb{I}(\cdot)$ denotes the indicator function of an event and $J_a \in \{-1, +1\}$ is a given constant. This is equivalent to the definition given in the introduction: defining $x_i, b_a \in \{0, 1\}$ such that $S_i = (-1)^{x_i}$ and $J_a = (-1)^{b_a}$, the constraint imposed by ψ_a reads $x_{i_a^1} + \dots + x_{i_a^k} = b_a \pmod{2}$, which is nothing but the a 'th row of the matrix equation $A\vec{x} = \vec{b}$. The addition modulo 2 of Boolean variables can also be read as the binary exclusive OR operation, hence the name XORSAT used for this problem.

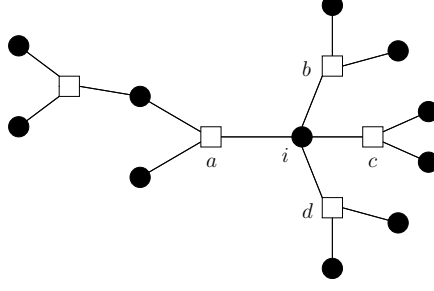


FIG. 6: An example of factor graph. The neighborhoods are for instance $\partial i = \{a, b, c, d\}$ and $\partial i \setminus a = \{b, c, d\}$

- q -COL. Here $\sigma \in \{1, \dots, q\}$ is the set of allowed colors on the N vertices of a graph. Each edge a connecting the vertices i and j prevents them from being of the same color: $\psi_a(\sigma_i, \sigma_j) = \mathbb{I}(\sigma_i \neq \sigma_j)$.
- k -SAT. As in the XORSAT problem one deals with Ising represented boolean variables, but in each clause the XOR operation between variables is replaced by an OR between literals (i.e. a variable or its negation). In other words a constraint a is unsatisfied only when all literals evaluate to false, or in Ising terms when all spins $S_a = (S_{i_a^1}, \dots, S_{i_a^k})$ involved in the constraint take their wrong values, that we denote $J_a = (J_{i_a^1}, \dots, J_{i_a^k})$: $\psi_a(S_a) = \mathbb{I}(S_a \neq J_a) = 1 - \mathbb{I}(S_a = J_a)$.

In all these cases we can define a Hamiltonian $H = \sum_{a=1}^M E_a(\sigma_a)$, such that $E_a = 0$ if the constraint is satisfied and $E_a = 1$ otherwise. Then, $\psi_a^\beta = \exp(-\beta E_a)$ and ψ_a corresponds to $\beta \rightarrow \infty$. For instance, in the case of the q -COL, the Hamiltonian corresponds to a Potts antiferromagnet $H = \sum_{(ij)} \delta(\sigma_i, \sigma_j)$. In the following we will often drop the explicit dependence on β to lighten the notation.

Factor graphs [66] provide an useful representation of a CSP. These graphs (see Fig. 6 for an example) have two kind of nodes. Variable nodes (filled circles on the figure) are associated to the degrees of freedom σ_i , while constraint nodes (empty squares) represent the clauses ψ_a . An edge between constraint a and variable i is drawn whenever ψ_a depends on σ_i . The neighborhood ∂a of a constraint node is the set of variable nodes (i_1, \dots, i_{K_a}) that appear in a . Conversely we will denote by ∂i the set of all constraints (a_1, a_2, \dots) in which variable i is involved. We shall conventionally use the indices i, j, \dots for the variable nodes, a, b, \dots for the constraints, and denote \setminus the subtraction from a set. The graph distance between two variable nodes i and j is the number of constraint nodes encountered on a shortest path linking i and j (formally infinite if the two variables are not in the same connected component of the graph).

Note that if the constraints only involve two variables i and j (as for instance in the SK model, in 2-XORSAT or in q -COL), then each constraint is equivalent to a link connecting i and j and the factor graph reduces to a standard graph.

2. Random optimization problems: random graphs and hypergraphs

The common notion of computational complexity, being based on worst-case considerations, could overlook the possibility that “most” of the instances of an NP problem are in fact easy and that the difficult cases are very rare. Random ensembles of problems have thus been introduced in order to give a quantitative content to this notion of typical instances; a property of a problem will be considered as typical if its probability (with respect to the random choice of the instance) goes to one in the limit of large problem sizes. Of course the choice of a distribution over the instances is arbitrary and could not reflect the properties of the instances that relevant for a given practical application. Still, the introduction of a distribution over the instances allows to formulate the problem in terms of the statistical mechanics of a spin-glass-like model. We will see that this formulation provides important insight in the properties of difficult instances of these problems.

An instance of a random CSP is defined by two objects: the underlying factor graph and, as in fully connected models, the set of *couplings* J appearing in the constraints (e.g. the right hand side of an equation in XORSAT). Both the factor graph and the couplings can be taken as random variables to define a probability distribution over instances. Recall that we have N variable nodes and M constraint nodes. In the statistical mechanics approach we will be interested in the thermodynamic limit of large instances where N and M both diverge with a fixed ratio $\alpha = M/N$.

Among many possible ensembles of graphs, two have been investigated in great detail:

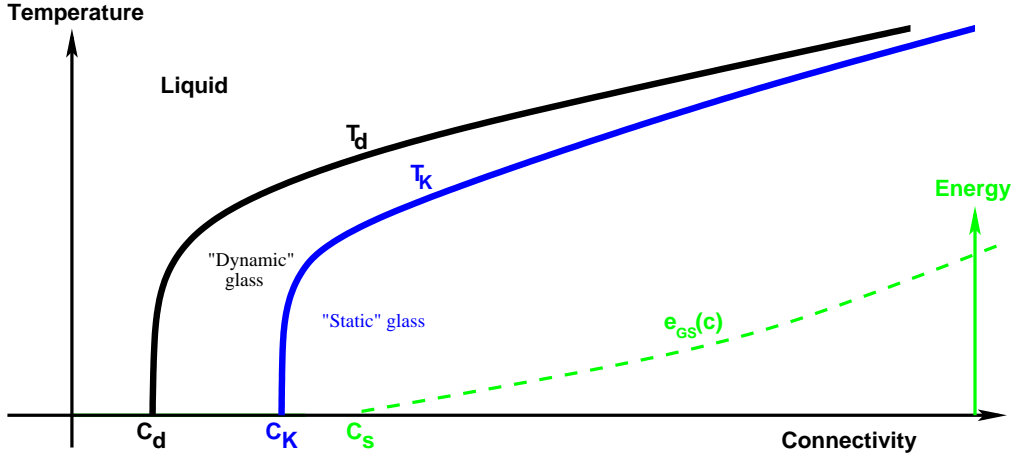


FIG. 7: Sketch of the phase diagram in the coloring problem at finite temperature (from [68]). At T_d , the system falls out of equilibrium (“dynamic” transition). At T_K the system undergoes a “static” glass transition. e_{GS} represents the ground state energy, which is nonzero above the connectivity c_s .

- *Random regular graphs* (or fixed connectivity) [67]: each constraint involves k distinct variables (k is a free parameter for (XOR)SAT and $k = 2$ for COL), and each variable enters in *exactly* c different constraints. Uniform probability is given to all graphs satisfying this property. Note that one must have $Mk = Nc$, i.e. $c = kM/N = k\alpha$.
- *Erdős-Rényi random graphs* [66]: For each of the M clauses a a $k(\geq 2)$ -uplet of distinct variable indices (i_a^1, \dots, i_a^k) is chosen uniformly at random among the $\binom{N}{k}$ possible ones. For large N, M the degree of a variable node of the factor graph converges to a Poisson law of average αk . To compare with regular graphs we shall use the notation $c = k\alpha$ for the average connectivity.

In principle one might allow also the connectivity of the constraints to be a random variable but we do not discuss such case here. Note that the limit $c \rightarrow \infty$ with a proper scaling of the couplings gives back the fully connected model. In this limit, the fluctuations of c in Erdős-Rényi graphs can be neglected and the two ensembles of graph are equivalent.

Random (hyper)graphs have many interesting properties in this limit [66]. In particular, picking at random one variable node i and isolating the subgraph induced by the variable nodes at a graph distance smaller than a given constant L yields, with a probability going to one in the thermodynamic limit, a (random) tree. This tree can be described by a Galton-Watson branching process: the root i belongs to l constraints, where l is a Poisson random variable of parameter αk (or $l = \alpha k$ in the fixed connectivity case). The variable nodes adjacent to i give themselves birth to new constraints, in numbers which are independently Poisson distributed with the same parameter. This reproduction process is iterated on L generations, until the variable nodes at graph distance L from the initial root i have been generated.

The algorithm to construct Erdős-Rényi graphs is trivial, because it is given by the definition. Fixed connectivity graphs can be constructed as follows: first one attach to each variable node a number c of links, thus obtaining Nc links. These links have to be connected to the $Mk = Nc$ links attached to constraint nodes. To do this, one simply numbers the links from 1 to Nc and then pick up a random permutation of these numbers in order to decide which of the variable links has to be attached to a given constraint link. The resulting graph however might have variables that are connected twice or more to the same node. In this case the permutation is discarded and a new one is picked until a good graph is reached. In practice the probability of such event is small if N is large and c not too large, so that the procedure converges quickly to a good graph.

3. Connectivity-temperature phase diagram

In the previous sections we discussed the appearance of an exponential number of states as a function of the temperature, therefore focusing on the free energy f of the states. In the case of a random CSP, the control parameters are the temperature T and the connectivity of the underlying graph c (or equivalently the ratio of constraints per variable $\alpha = c/k$), and we are mostly interested in the $T = 0$ limit.

We anticipate that the typical phase diagram of a random CSP looks like the one in figure 7. The fully connected case corresponds to the limit of large c . In this case, as a function of temperature, we have shown that there is a “clustering” transition at T_d and a spin glass transition at $T_K < T_d$. Both T_d and T_K depend on c and they vanish at some given values of c , c_d and c_K respectively. Therefore we expect that for connectivities below c_d , there is a unique cluster of ground states of zero energy (solutions), while for $c > c_d$ these ground states are arranged in many clusters, each cluster being characterized by the number of solutions \mathcal{N}_{in} belonging to it. We call “internal entropy” of a cluster the logarithm $s = \frac{1}{N} \log \mathcal{N}_{in}$, and again we call complexity Σ the logarithm of the number of clusters.

In the case of the p -spin model we used the modified partition function (58) in order to compute the complexity. We now comment briefly on the way this general formalism is applied to constraint satisfaction problems (CSP). First we split the free energy of a state in $f = e - Ts$, and we introduce a complexity as a function of e and s , $\Sigma(e, s) = \frac{1}{N} \log \mathcal{N}(e, s)$. Then we rewrite (58) as

$$Z_m = \int de ds e^{N[\Sigma(e, s) - \beta m(e - Ts)]} . \quad (137)$$

It would have been useful to introduce two parameters, one conjugated to energy and the other to entropy; however, in general the partition function above, that contains only m , is easier to compute (e.g. using replicas as we already discussed). Therefore, since we have only one parameter m , we cannot reconstruct the full $\Sigma(e, s)$ via a double Legendre transform. The point we want to discuss now is that depending on how we take the $T \rightarrow 0$ limit, we can obtain information on the entropy or the energy of the states.

For a satisfiable instance of a CSP, the law defined in (136) is the uniform distribution over the solutions of the CSP, and the partition function counts the number of such solutions. If we take the limit $\beta \rightarrow \infty$ at fixed m of (137), the term $\exp[-N\beta me]$ restricts the integral to $e = 0$ and we get

$$Z_m = \int ds e^{N[\Sigma_s(s) + ms]} , \quad (138)$$

where $\Sigma_s(s) = \Sigma(e = 0, s)$. We can define a “free entropy”

$$\mathcal{S}(m) = \frac{1}{N} \log Z_m = \max_s [\Sigma_s(s) + ms] , \quad (139)$$

from which we can compute $\Sigma_s(s)$ by a Legendre transform. This “entropic” method allows to obtain information on the distribution of the entropies of the zero energy states, when they exist. This approach is however ill-defined for unsatisfiable instances. In this case Eq. (137) gives

$$\mathcal{S}(m) = \max_{s, e} [\Sigma(s, e) + m(s - \beta e)] . \quad (140)$$

If one takes now the limit $\beta \rightarrow \infty$ in the region where $e > 0$, the complexity term becomes subdominant and we do not get much information.

In order to obtain a meaning result, one has to take the limit $m \rightarrow 0$ and $\beta \rightarrow \infty$ simultaneously, in such a way that the product βm , usually denoted y , remains finite. One therefore obtains

$$\mathcal{S}_e(y) = \max_e [\Sigma_e(e) - ye] , \quad \Sigma_e(e) \equiv \max_s \Sigma(s, e) . \quad (141)$$

This “energetic” cavity approach allows to obtain the distribution $\Sigma_e(e)$ of the energies of the states (irrespective of their entropy) and allows in particular to compute the ground state energy of the problem [69, 70].

We expect (and it can be verified by the explicit solution of these models) that the static value $m_s(T, c)$, that results from optimization of the free energy, will be 1 in the “liquid” (or “paramagnetic”) high temperature phase. Then $m_s(T = 0, c) = 1$ on the $T = 0$ line below c_d . On increasing c above c_d , $m_s(T = 0, c)$ will become smaller than one and decrease, still remaining finite. Only at $c = c_s$, $m_s(T = 0, c_s) = 0$, signaling the transition to the unsatisfiable phase. Above c_s , $m_s(T, c)$ vanishes linearly in T for $T \rightarrow 0$, defining the corresponding y . For this reason, the entropic cavity method is mostly appropriate below c_s , while the energetic cavity method is mostly appropriate above c_s .

Both methods can be used to detect c_s . Indeed, c_s is the point where solutions at $e = 0$ disappear, hence $\max_s \Sigma_s(s) = \max_s \Sigma(e = 0, s)$ vanishes at c_s . In the entropic method, $\Sigma_s(s)$ is computed directly and its maximum corresponds to $m = 0$. In the energetic method, in the satisfiable region, we can take a second limit $y \rightarrow \infty$ (after $\beta \rightarrow \infty$ at fixed $y = \beta m$) to concentrate on the states with $e = 0$. The complexity computed in this limit is $\Sigma_e(0) = \max_s \Sigma(s, e = 0)$, so that it gives back the maximum of the entropic complexity. In other words the procedure $y \rightarrow \infty$ after $\beta \rightarrow \infty$ is equivalent to perform the entropic computation with a Parisi parameter $m = 0$, i.e. to weight all the pure states in the same way, irrespectively of their sizes, which is the correct way to determine

the satisfiability threshold c_s . The determination of the clustering transition is more subtle. A calculation of c_d using the energetic method was first performed in [69, 70]; this corresponds to the appearance of a solution of the 1RSB equations with $m = 0$. Later it has been shown that the calculation of c_d at $m = 1$ can be performed using the entropic cavity method [71]; this is the equilibrium clustering threshold, which can be related to a dynamical transition at zero temperature as a function of c .

B. XORSAT: clustering and SAT/UNSAT transition

Before discussing the cavity method, we would like to analyze in some detail the XORSAT problem. We will focus on the XORSAT problem defined on Erdős-Rényi random graphs, and with couplings $J_a = \pm 1$ (equivalently $b_a = 0, 1$) with probability $1/2$. We will refer to this distribution as “random XORSAT” in this section. Similarly to the fully connected p -spin model, random XORSAT can be fully analyzed at zero temperature and the phase diagram can be understood in detail. These results have been originally derived in [72, 73]. A very nice review on phase transition in optimization problems, from which this section is reprinted, is [37].

1. Bounds from the first and second moments methods

Let \mathcal{N} be a random variable taking values on the positive integers (it will be the number of solution of an instance drawn from the assigned probability distribution), and call $p_{\mathcal{N}}$ its probability. We denote by $\langle \mathcal{N} \rangle$ and $\langle \mathcal{N}^2 \rangle$ the first and second moments of \mathcal{N} (assumed to be finite), and write

$$P_{SAT} = p(\mathcal{N} \geq 1) = \sum_{\mathcal{N}=1,2,3,\dots} p_{\mathcal{N}} = 1 - p_0 \quad (142)$$

the probability that \mathcal{N} is not equal to zero. Our aim is to show the inequalities

$$\frac{\overline{\mathcal{N}^2}}{\overline{\mathcal{N}^2}} \leq p(\mathcal{N} \geq 1) \leq \overline{\mathcal{N}}. \quad (143)$$

The right inequality, called “first moment inequality”, is straightforward:

$$\overline{\mathcal{N}} = \sum_{\mathcal{N}} \mathcal{N} p_{\mathcal{N}} = \sum_{\mathcal{N} \geq 1} \mathcal{N} p_{\mathcal{N}} \geq \sum_{\mathcal{N} \geq 1} p_{\mathcal{N}} = p(\mathcal{N} \geq 1). \quad (144)$$

Consider now the linear space made of vectors $\mathbf{v} = (v_0, v_1, v_2, \dots)$ whose components are labelled by positive integers, with the scalar product

$$\mathbf{v} \cdot \mathbf{v}' = \sum_{\mathcal{N}} p_{\mathcal{N}} v_{\mathcal{N}} v'_{\mathcal{N}}. \quad (145)$$

Choose now $v_{\mathcal{N}} = \mathcal{N}$, and $v'_0 = 0, v'_{\mathcal{N}} = 1$ for $\mathcal{N} \geq 1$. Then

$$\mathbf{v} \cdot \mathbf{v} = \overline{\mathcal{N}^2}, \quad \mathbf{v} \cdot \mathbf{v}' = \overline{\mathcal{N}}, \quad \mathbf{v}' \cdot \mathbf{v}' = p(\mathcal{N} \geq 1). \quad (146)$$

The left inequality in (143) is simply the Cauchy-Schwarz inequality for \mathbf{v}, \mathbf{v}' : $(\mathbf{v} \cdot \mathbf{v}')^2 \leq (\mathbf{v} \cdot \mathbf{v}) \times (\mathbf{v}' \cdot \mathbf{v}')$. If \mathcal{N} represents the number of solution of a given XORSAT instance, we can use these bounds to obtain bounds on $P_{SAT} = p(\mathcal{N} \geq 1)$.

Figure 8 shows the probability that a random 3-XORSAT formula is satisfiable as a function of α for increasing sizes N . It appears that formulas with ratio $\alpha < \alpha_c \simeq 0.918$ are very likely to be satisfiable in the large N limit, while formulas with ratios beyond this critical value are almost surely unsatisfiable. Use of the first and second moment inequalities (143) for the number \mathcal{N} of solutions provides us with upper and lower bounds to the Sat/Unsat ratio α_s .

To calculate the first moment of \mathcal{N} remark that an equation is satisfied by one half of the configurations. When we average over the possible choices of the second member of the equation, we have that two equations are satisfied simultaneously by $1/4$ of the configurations, and M equations are satisfied simultaneously by $1/2^M$ of the configurations. The average number of solutions is thus $2^N/2^M$, from which we get

$$P_{SAT} \leq \overline{\mathcal{N}} = 2^{N(1-\alpha)}. \quad (147)$$

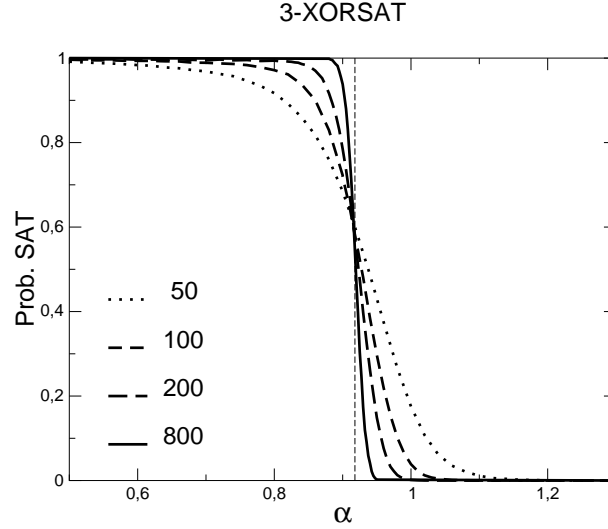


FIG. 8: Probability that a random 3-XORSAT formula is satisfiable as a function of the ratio α of equations per variable, and for various sizes N . The dotted line locates the threshold $\alpha_s \simeq 0.918$.

The first moment vanishes for ratios larger than unity, showing that

$$\alpha_c \leq 1. \quad (148)$$

This upper bound is definitely larger than the true threshold from the numerical findings of Figure 8. Close to $\alpha = 1$ formulas are unsatisfiable with probability one (when $N \rightarrow \infty$), yet the average number of solutions is exponentially large! The reason is that the average result is spoiled by rare, satisfiable formulas with many solutions.

As for the lower bound we need to calculate the second moment $\overline{\mathcal{N}^2}$ of \mathcal{N} . We use here the representation in terms of bits and we denote by $X = \{x_1, \dots, x_N\}$ the configuration of the N bits. For a given instance, $\mathcal{N} = \sum_X \mathbb{I}(X) = \sum_X \prod_a \mathbb{I}_a(X)$, where $\mathbb{I}(X)$ is the indicator function of the event that X is a solution to that instance, and $\mathbb{I}_a(X)$ is the indicator of X being a solution to clause a . As equations are independently drawn

$$\overline{\mathcal{N}^2} = \overline{\sum_{X,Y} \mathbb{I}(X)\mathbb{I}(Y)} = \sum_{X,Y} \overline{\prod_a \mathbb{I}_a(X)\mathbb{I}_a(Y)} = \sum_{X,Y} \prod_a \overline{\mathbb{I}_a(X)\mathbb{I}_a(Y)} = \sum_{X,Y} p(X,Y)^M \quad (149)$$

where the sum is carried out over the pairs X, Y of configurations of the N variables, and $p(X, Y)$ is the probability that both X and Y satisfies the same randomly drawn equation. The latter can be easily expressed in terms of the Hamming distance (per variable) d between X and Y , defined as the fraction of variables having opposite values in X and Y . The general expression for k -XORSAT is¹⁶

$$p(d) = \frac{1}{4}(1 + (1 - 2d)^k). \quad (150)$$

Going back to (149) we can sum over Y at fixed X , that is, over the distances d taking multiple values of $\frac{1}{N}$ with the appropriate binomial multiplicity, and then sum over X with the result

$$\overline{\mathcal{N}^2} = 2^N \sum_d \binom{N}{Nd} p(d)^M = \exp(N \max_{d \in [0;1]} A(d, \alpha)) \quad (151)$$

in the large N limit, where

$$A(d, \alpha) = \log 2 - d \log d - (1 - d) \log(1 - d) + \alpha \ln p(d). \quad (152)$$

¹⁶ The equation is satisfied by X with probability $1/2$. Given that X is a solution, it is satisfied also by Y if the number of variables entering the equation and taking opposite values in Y as in X is even. By definition of d the probability (over its index i) that a variable takes different value in X and Y is d . To construct the equation one has to extract k independent indexes i , then the probability that the extracted variables are equal in X and Y is $\binom{k}{0} d^0 (1 - d)^{k-0}$. Similarly the probability to have two different variables is $\binom{k}{2} d^2 (1 - d)^{k-2}$, and so on. The sum of all even numbers gives expression (150) for $p(d)$. See [37] for details.

The absolute maximum of the function $A(d, \alpha)$ is located in $d^* = \frac{1}{2}$ when $\alpha < \alpha_2 \simeq 0.889$, and $d^* < \frac{1}{2}$ when $\alpha > \alpha_2$. In the latter case $\overline{N^2}$ is exponentially larger than \overline{N}^2 , and the second moment inequality (143) does not give any information about P_{SAT} . In the former case $\overline{N^2}$ and \overline{N}^2 are equivalent to exponential-in- N order. It is shown in [37], by computing the saddle point corrections to (151), that their ratio actually tends to one as $N \rightarrow \infty$. We conclude that formulas with ratios of equations per variable less than α_2 are satisfiable with high probability in the infinite size limit, or, equivalently,

$$\alpha_c \geq \alpha_2 \simeq 0.889 . \quad (153)$$

Unfortunately the lower and upper bounds do not match and the precise value of the threshold remains unknown at this stage. We explain in the next section how a simple preprocessing of the formula, before the application of the first and second moment inequalities, can close the gap, and shed light on the structure of the space of solutions.

2. The leaf-removal algorithm

We now sketch how clustering in the random 3-XORSAT problem may be analyzed rigorously. The techniques used are borrowed from the analysis of algorithms, and probability theory.

Let \mathcal{S} be a randomly drawn 3-XORSAT system. A crucial remark is that removal of an equation containing a single-occurrence variable preserves the satisfiability, or unsatisfiability of \mathcal{S} . Consider for instance $x_1 + x_2 + x_3 = b$. Clearly if x_1 appear only in this equation, for any value of x_2 and x_3 the equation can be satisfied by choosing the appropriate value of x_1 . Therefore if the system of the remaining solution is satisfiable, the same will be for the full system.

This procedure can be iterated to further simplify \mathcal{S} until no single-occurrence variable is left. The output of the procedure is \mathcal{S}' , the largest subsystem of \mathcal{S} where variables appear at least twice¹⁷. In the following, we analyze:

- the procedure which allows us to extract system \mathcal{S}' from \mathcal{S} ;
- the statistical properties of \mathcal{S}' , and their consequences in terms of satisfiability for \mathcal{S} ;
- how the solutions of the original system \mathcal{S} can be reconstructed from the solutions of \mathcal{S}' , and how clustering emerges from this reconstruction process.

Intuition on single-occurrence variable removal is made easier once we introduce the graphical representation of Boolean systems in terms of factor graphs discussed above.

Removal of a single-occurrence variable and of its attached equation from the system \mathcal{S} is equivalent to removal of a leaf variable and its attached constraint from the factor graph. Removal of a leaf may “uncover” vertices and produce new leaves. The process may therefore be iterated well after all leaves present in the original hypergraph have been removed. How can we quantitatively track the reduction of the hypergraph as removal goes on? Let us call step of the procedure the action of choosing a leaf and removing it together with its constraint, and ℓ -vertex a vertex of connectivity ℓ , i.e. which appears in ℓ distinct constraints (with $\ell \geq 0$). Removed leaves will be considered as 0-vertices in order to conserve the total number of vertices. The number of ℓ -vertices after T steps is a stochastic variable, depending upon the system \mathcal{S} and the sequence of leaves removed by the procedure, denoted by $N_\ell(T)$. Obviously, for all T ,

$$\sum_{\ell \geq 0} N_\ell(T) = N \quad \text{and} \quad \sum_{\ell \geq 0} \ell N_\ell(T) = 3(M - T) \quad , \quad (154)$$

as a result of the conservation of the total number of vertices and constraints respectively. Removal goes on as long as $N_1(T) \geq 1$. Denote $\mathbf{N}(T)$, and call population the set $\{N_\ell(T), \ell \geq 0\}$ of all numbers of ℓ -vertices. Knowledge of the population is generally not sufficient to unambiguously determine the hypergraph produced by T steps of the removal procedure. Indeed, many hypergraphs have the same population $\mathbf{N}(T)$. An essential observation is, however, that the output of T steps of the removal procedure is equally distributed among the set of all hypergraphs having population $\mathbf{N}(T)$. In other words, a complete statistical information about hypergraphs is obtained from the knowledge of the population.

¹⁷ From this definition, it is clear that \mathcal{S}' is unique and independent of the order in which equations with single-occurrence variable are removed.

Let us now see how this population $\mathbf{N}(T)$ is modified during step $T \rightarrow T+1$. The variations of the N_ℓ are stochastic variables due to the randomness in the system \mathcal{S} and the choice of the leaf to be removed, with conditional expectations with respect to $\mathbf{N}(T)$ given by

$$\mathbf{E}[N_\ell(T+1) - N_\ell(T)|\mathbf{N}(T)] = -\delta_{\ell 1} + \delta_{\ell 0} + 2p_{\ell+1}(T) - 2p_\ell(T) \quad . \quad (155)$$

When a constraint is removed, a 1-vertex disappears ($-\delta_{\ell 1}$ term in (155)) to become a 0-vertex ($\delta_{\ell 0}$). This constraint is attached to two other vertices. The numbers ℓ, ℓ' of occurrences of each of these two vertices are distributed with probability

$$p_\ell(T) = \frac{\ell N_\ell(T)}{3(M-T)} \quad , \quad (156)$$

and are diminished by one once the constraint is taken away¹⁸. From (155), the expectation values of N_ℓ vary by a quantity of the order of unity at each time step, and the expected densities of ℓ -vertices, defined through

$$n_\ell(T) = \frac{\mathbf{E}[N_\ell(T)]}{N} \quad , \quad (157)$$

undergo changes of the order of $1/N$ only. We are naturally led to conclude that densities are function of a much longer “time scale”, $t = T/N$. In other words, given $t \in [0, 1]$, $n_\ell([tN])$ and $n_\ell([tN] + o(N))$ are equal to within $o(1)$ terms as N tends to infinity, and we denote by $n_\ell(t)$ their common limit. Assuming that the densities $n_\ell(t)$ are differentiable functions of this time, we obtain from evolution equation (155) a set of coupled first order differential equations¹⁹,

$$\frac{dn_\ell}{dt}(t) = -\delta_{\ell 1} + \delta_{\ell 0} + \frac{2}{3(\alpha - t)} [(\ell + 1) n_{\ell+1}(t) - \ell n_\ell(t)] \quad . \quad (158)$$

Resolution of these equations require to assign the initial conditions. At time $t = 0$, that is, prior to any removal of constraint, densities are Poisson distributed with parameter 3α ,

$$n_\ell(0) = e^{-3\alpha} \frac{(3\alpha)^\ell}{\ell!} \quad , \forall \ell \quad , \quad (159)$$

as we discussed above.

Solutions of equations (158) with initial conditions (159) read

$$\begin{aligned} n_0(t) &= e^{-3\alpha b(t)^2} + 3\alpha b(t)^2 (1 - b(t)) \quad , \\ n_1(t) &= 3\alpha b(t)^2 \left(e^{-3\alpha b(t)^2} + b(t) - 1 \right) \quad , \\ n_\ell(t) &= e^{-3\alpha b(t)^2} \frac{(3\alpha b(t)^2)^\ell}{\ell!} \quad , \quad \forall \ell \geq 2 \quad , \end{aligned} \quad (160)$$

where

$$b(t) \equiv \left(1 - \frac{t}{\alpha} \right)^{1/3} \quad . \quad (161)$$

These equations are valid as long as n_1 is positive, since the procedure stops when no leaf is left. The density $n_1(t)$ of 1-vertices is showed on Fig. 9 for various initial ratios α of equations per variable. The shape of the curve reflects the competition between two opposite effects: the annihilation of 1-vertices due to leaf removal and their creation as a result of reduction of 2-vertices to 1-vertices. At small ratios e.g. $\alpha = 0.7$, the former mechanism dominates and n_1 is a decreasing function of time. For slightly larger ratios, the density n_1 does not monotonously decrease with time any longer, but still vanishes at time $t^* = \alpha$ i.e. when no constraint is left.

¹⁸ The probability p_1 of picking a variable, say, x_1 , is equal to the number ℓ_1 of its occurrences divided by the total number of occurrences of variables in the system, $3(M - T)$. The probability of picking any variable with occurrence ℓ is p_1 multiplied by the number $N_\ell(T)$ of such variables, hence (156). Equation (154) ensures that p_ℓ is properly normalized.

¹⁹ The left hand side of (155) reads $N[n_\ell(t + 1/N) - n_\ell(t)] = dn_\ell/dt + O(1/N)$ through a Taylor expansion.

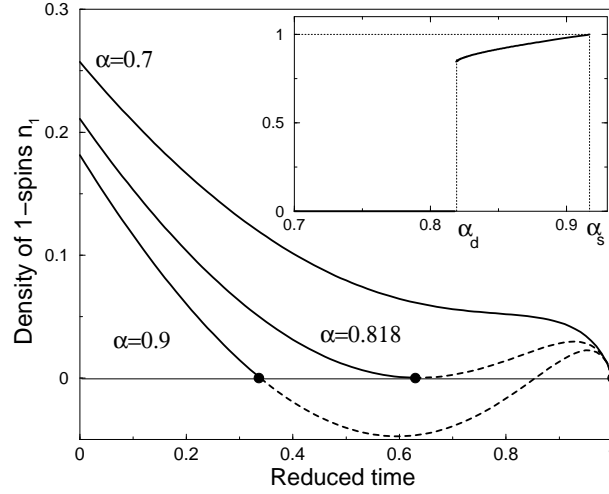


FIG. 9: (From [37]) Evolution of the density of 1-vertices, $n_1(t)$, under the operation of the leaf removal procedure as a function of the reduced time t/α . For $\alpha < \alpha_d \simeq 0.818$, $n_1(t)$ remains positive until all the constraints are eliminated at $t^* = \alpha$. For $\alpha > \alpha_d$ the procedure stops at the time t^* for which n_1 vanishes (black dots), and becomes negative for $t > t^*$ (dashed part of the curves). Notice that t^* discontinuously jumps down at $\alpha = \alpha_d$. In the inset, α' defined in Eq. (165) is plotted as a function of α .

According to the solution (160) of the equation of motion, this statement holds for ratios α for which the equation

$$b = 1 - e^{-3\alpha b^2} \quad , \quad (162)$$

has no strictly positive root. When α is larger than

$$\alpha_d = \min_{0 < b < 1} \left[-\frac{\ln(1-b)}{3b^2} \right] \simeq 0.818469... \quad , \quad (163)$$

there exist non zero real solutions to (162), and we denote by b^* the largest one. As shown in Fig. 9, the density of 1-vertices decreases and vanishes at time $t^* < \alpha$ where $b(t^*)$, given in Eq. (161), reaches b^* . The output of the procedure is a non-empty subset \mathcal{S}' of \mathcal{S} with $M' = N(\alpha - t^*)$ equations, such that any of the

$$N' = N \sum_{\ell \geq 2} n_\ell(t^*) \quad (164)$$

variables present in \mathcal{S}' appears at least twice. The ratio of equations per variable in \mathcal{S}' is given by

$$\alpha' = \frac{M'}{N'} = \frac{\alpha b^{*2}}{1 - 3\alpha b^*(1 - b^*)} \quad , \quad (165)$$

and is shown in the inset of Fig. 9.

Let us briefly sum up the outcome of the above analysis. There exists a critical ratio α_d (163) for the original system \mathcal{S} such that

- if $\alpha < \alpha_d$, the leaf removal procedure succeeds in eliminating all variables and equations, thus \mathcal{S}' is empty;
- if $\alpha > \alpha_d$, the output of the procedure is a non-empty subset \mathcal{S}' , with ratio of equation per variables equal to α' (165).

The reader could feel concerned about fluctuations around those average results. Equation of motion (158) is indeed true for the average density of vertices only. Fortunately, one can show that, for large sizes N , the numbers of ℓ -vertices are highly concentrated around their average values,

$$N_\ell(T) = N n_\ell\left(\frac{T}{N}\right) + o(N) \quad , \quad (166)$$

whatever the initial instance \mathcal{S} and the sequence of choices done by the removal procedure. Therefore, the evolution of the population cannot deviate from the average behaviour when $N \rightarrow \infty$ [37].

3. Clustering and SAT/UNSAT transitions.

As before, we consider a system \mathcal{S} with ratio α and apply the leaf removal procedure. The output is the subsystem \mathcal{S}' . Can we reconstruct the solutions of \mathcal{S} from the ones of \mathcal{S}' ? The answer is positive, and the reconstruction process permits us to characterize the structure of the set of solutions in an accurate way.

Assume that we have, in the course of the removal procedure, stored all removed equations on top of each other in a stack. Let X' be a solution of \mathcal{S}' . The length of X' , that is, the number of variables it includes is N' defined in (164). Through a relabelling of variables we can always assume that X' specifies the values of the first N' variables x_i . We are now going to reinsert in \mathcal{S}' the equations that were removed from \mathcal{S} following a Last-In-First-Out unstacking order.

Consider the first reinserted *i.e.* on top of stack equation,

$$x_i + x_j + x_k = v \quad , \quad (167)$$

where $v = 0, 1$ is the second member, and (i, j, k) a triplet of distinct integers comprised between 1 and N . Call ν_1 the number of these integers strictly larger than N' . That this equation was eliminated by the leaf removal procedure and was the last one to be so tells us that $\nu_1 \geq 1$: at least one of the three variables in (167) is not assigned by the particular solution X' . If ν is precisely equal to unity, we have, say, $i, j \leq N'$ and $k \geq N' + 1$. Then the values of x_i, x_j are known for X' , and there is a unique way to assign x_k to satisfy (167). If $\nu_1 = 2$, we know, say, x_i from X' , and have two possible combinations of x_j, x_k fulfilling (167). Therefore we can construct two distinct solutions of the system $\mathcal{S}'_1 = \mathcal{S}' +$ reinserted equation. The reasoning is straightforwardly extended to the last $\nu_1 = 3$ case, with the general result that $2^{\nu_1 - 1}$ distinct solutions can be reconstructed from X' . Then, after reinsertion of the second-to-top equation, we reconstruct $2^{\nu_2 - 1}$ solutions from any of the solutions of \mathcal{S}'_1 where ν_2 is the number of new variables *i.e.* present in the reinserted equation and not fixed by \mathcal{S}'_1 . Iterating this procedures up to the reinsertion of all $M - M'$ equations permits us to obtain (labeling R the reinsertion “time”)

$$\mathcal{N}_{rec} = \prod_{R=1}^{M-M'} 2^{\nu_R - 1} \quad (168)$$

solutions of $\mathcal{S}'_{M-M'} = \mathcal{S}' +$ all the reinserted equations. Notice that solutions of $\mathcal{S}'_{M-M'}$ do not quite coincide with the ones of the original system \mathcal{S} . Variables that were absent from equations in \mathcal{S} (*i.e.* that had zero connectivity) are still undetermined from \mathcal{S}'_M , and can be freely chosen, giving an extra multiplicative factor to the total number of solutions of \mathcal{S} that can be reconstructed from X' ,

$$\mathcal{N}_{in} = 2^{N_0} \mathcal{N}_{rec} = 2^{N_0} \prod_{R=1}^{M-M'} 2^{\nu_R - 1} \quad , \quad (169)$$

where N_0 is the number of 0-occurrence variables. This set of solutions and X' are respectively called *cluster of solutions* and *seed of the cluster*. Taking the logarithm of (168) and dividing by N , we obtain the following expression for the entropy of the reconstructed cluster from seed X' ,

$$\frac{s}{\log 2} = \frac{1}{N} \log_2 \mathcal{N}_{in} = \frac{N_0}{N} + \frac{1}{N} \sum_{R=1}^{M-M'} (\nu_R - 1) \quad . \quad (170)$$

The average value of this entropy can be calculated from the knowledge of the average values of the ν_{RS} . Note that time R of the reconstruction process corresponds to time $T = 1 + M - M' - R$ of the leaf removal process. As equations were carefully introduced in opposite order to their removal, the expectation value of $\nu_R - 1$ (conditioned to population $\mathbf{N}(T)$, at time $T = 1 + M - M' - R$) can be estimated from the analysis of the previous section and is equal to $2p_1(1 + M - M' - R)$ with p_1 given in (156). Changing variable from R back to T and taking the limit $N \rightarrow \infty$ we end up with

$$\frac{s}{\log 2} = e^{-3\alpha} + \int_0^{t^*} dt \frac{2n_1(t)}{3(\alpha - t)} \quad , \quad (171)$$

where the first term comes from the contribution $n_0(0)$ (159) of absent variables, and t^* is the time at which the leaf removal procedure halts.

For small ratios α , \mathcal{S}' is empty, and so is X' . The halt time $t^* = \alpha$ and integration of (171) with the help of (160) leads to the simple result $s(\alpha) = (1 - \alpha) \log 2$. As we have reconstructed all possible solutions of \mathcal{S} from the empty

X' , s coincides with the total entropy s_{tot} of solutions, that in this case coincides with $\frac{1}{N} \log \overline{\mathcal{N}}$. At such small ratios the fluctuations of \mathcal{N} are not important.

On the contrary, for $\alpha > \alpha_d$ the leaf removal procedure stops at $t^* < \alpha$, and has not succeeded in eliminating all equations and variables. The average entropy associated to a cluster reconstructed from one seed is

$$\frac{s(\alpha)}{\log 2} = 1 - \alpha - b^* - \alpha b^{*2} (2b^* - 3) \quad , \quad (172)$$

where b^* is, as before, the largest positive root of (162).

To complete our description of clusters, some statistical knowledge about their seeds is required. The number \mathcal{N}' of solutions of \mathcal{S}' can be analyzed by means of the first and second moments method (143), giving respectively some upper and lower bound to the probability $\text{Prob}[\mathcal{N}' \geq 1]$ of existence of solutions. The first moment is easy to calculate: as the second members of the various equations are uncorrelated, we find

$$\overline{\mathcal{N}'} = 2^{N'} \times \left(\frac{1}{2}\right)^{M'} = 2^{N'(1-\alpha')} \quad . \quad (173)$$

The overbar denotes here the unbiased expectation value over all instances with N' variables, M' equations such that any variable appears at least twice. The second moment calculation is made more difficult by the existence of constraints on the minimal number (two) of occurrences of variables in \mathcal{S}' . It requires a combinatorial analysis of the number of systems \mathcal{S}' *i.e.* ways of choosing equations, having a given pair of configurations for solutions. This calculation is beyond the scope of these notes and was done by Dubois and Mandler [74]. The outcome is that, at large N , the second moment $\overline{(\mathcal{N}')^2}$ is asymptotically equal to the first moment squared, $(\overline{\mathcal{N}'})^2$, when $\alpha' < 1$ and exponentially larger when $\alpha' > 1$. This result has two important consequences.

First, from (143), we conclude that $\alpha' = 1$ is at the same time an upper and a lower bound to the exact value of the threshold for \mathcal{S}' . Therefore $\alpha' = 1$ is the location of the sat-unsat threshold for reduced subsystems. Using (165), we see that $\alpha' = 1$ is reached for an initial ratio equal to

$$\alpha_s \simeq 0.917936... \quad , \quad (174)$$

as shown in Fig. 9. Remarkably, while the moments method directly applied to \mathcal{S} gave lower and upper bounds to the threshold separated by a finite gap only, the outcome is much better when applied to \mathcal{S}' . The concentration of \mathcal{N}' contrasts with the (instance-to-instance) fluctuations exhibited by \mathcal{N} , and suggests that the latter thus essentially comes from fluctuations in the numbers N_0 and N_1 of 0- and 1-vertices eliminated by the leaf removal algorithm. This comes as no surprise since variations of N_0 and N_1 induce drastic changes on the number of solutions e.g. the presence of a 0-vertex multiply the number of GS by two. Conversely, in \mathcal{S}' , variables appear at least twice and are more interconnected, giving rise to weaker fluctuations for \mathcal{N}' .

Secondly, when $\alpha' < 1$, the number of solutions of \mathcal{S}' is, with high probability, given by (173)²⁰. This is the number of seeds each of which gives a cluster of solutions for \mathcal{S} . The number of clusters of solutions is therefore

$$\mathcal{N}_{clu} = 2^{N'(1-\alpha')} = e^{N \Sigma} \quad , \quad (175)$$

where the entropy of clusters is defined as

$$\frac{\Sigma(\alpha)}{\log 2} = \frac{N'}{N} (1 - \alpha') = b^* - 3\alpha b^{*2} + 2\alpha b^{*3} \quad . \quad (176)$$

From the reconstruction process it is clear that two different seeds cannot give twice the same solutions. Therefore the total entropy of solutions of \mathcal{S} is

$$s_{tot}(\alpha) = \Sigma(\alpha) + s(\alpha) = (1 - \alpha) \log 2 \quad , \quad (177)$$

as obtained when summing (176) and (172). This is exactly the analytic continuation of the entropy of the unclustered phase. We have now established that $s_{tot} = (1 - \alpha) \log 2$ for all ratios $\alpha < \alpha_s$. The entropies of solutions in a cluster, s , and of clusters, Σ , are shown in Fig. 10.

²⁰ This statement comes, again, from the fact that the second moment is equal to the squared first moment, and therefore fluctuations of \mathcal{N}' around the average value are extremely rare.

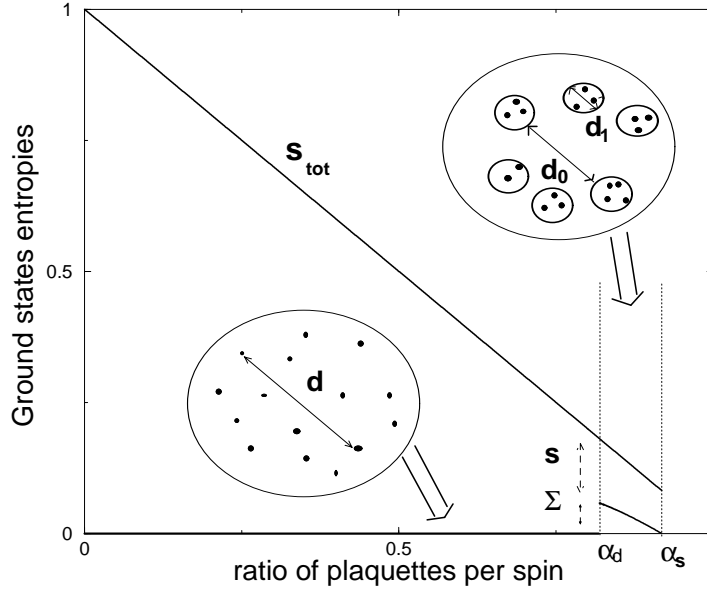


FIG. 10: (From [73]: entropies are in units of $\log 2$) Ground state structure and entropies as a function of the ratio α of equations per spin. The total entropy (logarithm of the number of unfrustrated ground states per spin, or solutions) is $s_{tot} = (1 - \alpha) \log 2$ for $\alpha < \alpha_s \simeq 0.918$. For $\alpha < \alpha_d \simeq 0.818$, solutions are uniformly scattered on the N -dimensional hypercube, with a typical normalized Hamming distance $d = 1/2$. At α_d , the solution space discontinuously breaks into disjoint clusters: the Hamming distance $d_1 \simeq 0.14$ between solutions inside a cluster is much smaller than the typical distance $d_0 = 1/2$ between two clusters (RSB transition). The entropy of clusters, s , and of solutions in each cluster, Σ , are such that $\Sigma + s = s_{tot}$. At α_s , the number of clusters ceases to be exponentially large ($\Sigma = 0$). Above α_s , ground states are frustrated, i.e. there are no solutions.

What we are left with is merely justifying the cluster denomination used above. The reconstruction process allows a complete characterization of solutions, in terms of an extensive number of (possibly overlapping) blocks made of few variables, each block being allowed to flip as a whole from a solution to another. When $\alpha < \alpha_d$, with high probability, two randomly picked solutions differ over a fraction $d = 1/2$ of variables, but are connected through a sequence of $O(N)$ successive solutions differing over $O(1)$ variables only. For $\alpha_d < \alpha < \alpha_s$, flippable blocks are juxtaposed to a set of seed-dependent frozen variables. For picture 10 to be true, we must establish that different clusters do not overlap or, more precisely, that any two solutions belonging to two different clusters are far away from each other. A lower bound to the Hamming distance d between these two solutions is the Hamming distance d_s between the seeds of their respective clusters. A lower bound d_s , as a function of α , can in turn be estimated using again the first moment method *i.e.* from the vanishing condition of the expectation number $\overline{\mathcal{N}^{\prime 2}(d_s)}$ of solutions of \mathcal{S}' lying apart at distance $\leq d_s$. An explicit calculation shows that $d_s > 0$ for all $\alpha > \alpha_d$ [72, 73].

4. On backbones

The reconstruction procedure helps us to interpret equation (162) as a self-consistent equation for the size of the backbone of a cluster of solutions. Let X' be a solution of \mathcal{S}' , and \mathcal{B} the set of variables taking the same value in all solutions of the cluster associated to seed X' . The cardinality of \mathcal{B} divided by N is the backbone b . Obviously, the variables assigned by X' are elements of \mathcal{B} , thus

$$b \geq \sum_{\ell \geq 2} n_{\ell}(t^*) = b^*(1 - 3\alpha b^*(1 - b^*)) \quad , \quad (178)$$

showing that the backbone is strictly positive. So far no proof of the equality between b and b^* has been obtained in literature, though this could, in principle, be inferred from the analysis of the removal and reconstruction procedures described above. The following is a hand-waving argument supporting the interpretation of b^* as the cluster backbone [75].

We want to estimate the probability that a variable, say, x_1 does not belong to the backbone *i.e.* that x_1 takes value 0 on some solutions and 1 on others. x_1 appears in ℓ equations, where ℓ is a Poisson variable with parameter

3 α . Consider one of these equations,

$$x_1 + x_j + x_k = v \quad . \quad (179)$$

If either x_j or x_k does not belong to \mathcal{B} , neither does x_1 . Thus the probability that the above equation does not constrain x_1 to take the same value on all solutions is $1 - b^2$. This expression assumes that the events “ $x_j \in \mathcal{B}$ ” and “ $x_k \in \mathcal{B}$ ” are independent, a literally wrong assumption which, however, apparently becomes asymptotically true for large system sizes (this is the basis of the cavity method that we will discuss in the next section). Similarly, under the assumption that the above events are independent from equation to equation, we obtain

$$\text{Prob}[x_1 \in \mathcal{B}|\ell] = 1 - (1 - b^2)^\ell \quad . \quad (180)$$

Summing over ℓ , we have

$$\text{Prob}[x_1 \in \mathcal{B}] = \sum_{\ell=0}^{\infty} e^{-3\alpha} \frac{(3\alpha)^\ell}{\ell!} [1 - (1 - b^2)^\ell] = 1 - e^{-3\alpha b^2} \quad . \quad (181)$$

As the l.h.s. of the above equation is precisely the size of the backbone, b , we see that b fulfills (162) and is equal to b^* as announced.

5. Summary

Unfortunately, the method discussed in this section can be applied only to the XORSAT problem. In fact, the clusters in this problem have a very simple structure: they are built around a seed (solution of the reduced system S') by adding back the leaves. This has a number of peculiar consequences:

1. *In all clusters there is a finite fraction of “frozen” variables (backbone):* these are the variables in the seed that are constrained to take the same value in all the solutions belonging to the cluster; and some of the leaves, those that belong to equations where both other variables belong to the seed (see the discussion in the last section).
2. *All the clusters have the same internal entropy:* this is because adding back the leaves, the fraction of “free” variables is determined only by the topology of the graph and not by the particular “seed” that defines the cluster. Moreover, all these variables (those that are not in the backbone) are completely free to be ± 1 with probability 1/2. Therefore, the internal entropy is determined only by the topology of the graph (the size of its backbone) and does not depend on the cluster.
3. *The SAT/UNSAT transition coincides with the point where Σ vanishes:* this is because when $\Sigma = 0$ the reduced system becomes UNSAT.

As we will see the structure of other optimization problems is more complicated: the internal entropy may fluctuate from cluster to cluster, and a backbone is not always present. In these cases we need a different method, that we explain in the next section. Before turning to that, it is useful to reproduce the results obtained above by mean of the replica method [75] (\Rightarrow **Ex.III.1**).

C. The replica symmetric cavity method

The cavity method, initially invented to deal with the Sherrington Kirkpatrick model of spin glasses [9], is a powerful method to compute the properties of ground states in many condensed matter and optimization problems. It is in principle equivalent to the replica method, but it turns out to have a much clearer and more direct interpretation, that allows in practice to find solutions to some problems which remain rather difficult to understand in the replica formalism: the replica approach is very elegant and compact, but it is more difficult to get an intuitive feeling of what is going on. Also, the cavity approach deals with usual probabilistic objects, and can lend itself to rigorous studies [15]. We shall present it here at two successive levels of approximation. The first one, corresponding in replica language to the replica symmetric (RS) solution, is an easy one and has already been studied a lot. The one corresponding to one step replica symmetry breaking (1RSB) is more involved and has been fully understood only very recently [43, 44, 71, 76–78].

1. Recursions on a finite tree

The key properties of random graphs that is exploited by the cavity method is that loops are very large in the thermodynamic limit, as we discussed in the introduction to this section. Therefore, locally random graphs look like trees. Before studying the cavity method, we must understand how to solve statistical mechanics models defined on trees. This can be done by a generalization of the transfer matrix methods that are used to solve models in one dimension (which is indeed the special case of a regular tree with connectivity $c = 2$). We will for the moment restrict to consider models where the clauses have connectivity $k = 2$: for these models, one does not need a factor graph representation, since interactions can be represented by a standard graph with vertices $i = 1, \dots, N$ representing variables σ_i and links $\langle i, j \rangle$ representing interactions $\psi_{ij}(\sigma_i, \sigma_j)$. We shall repeatedly use in the following the same notation we used for factor graphs, specialized to the $k = 2$ case: therefore we use ∂i for the set of vertices adjacent to a given vertex i , i.e. for the sites which interact with i , and $\partial i \setminus j$ for those vertices around i distinct from j .

Let us then consider the case where the interaction graph is a finite tree. In this case the computation can be organized in a very simple way, taking benefit of the natural recursive structure of a tree. We define the quantity $Z_{i \rightarrow j}(\sigma_i)$, for two adjacent sites i and j , as the partial partition function for the subtree rooted at i , excluding the branch directed towards j , with a fixed value of the spin variable on the site i . We also introduce $Z_i(\sigma_i)$, the partition function of the whole tree with a fixed value of σ_i . These quantities can be computed according to the following recursion rules, see Fig. 11 for an example,

$$Z_{i \rightarrow j}(\sigma_i) = \prod_{k \in \partial i \setminus j} \left(\sum_{\sigma_k} Z_{k \rightarrow i}(\sigma_k) \psi_{ik}(\sigma_i, \sigma_k) \right), \quad Z_i(\sigma_i) = \prod_{j \in \partial i} \left(\sum_{\sigma_j} Z_{j \rightarrow i}(\sigma_j) \psi_{ij}(\sigma_i, \sigma_j) \right). \quad (182)$$

It will be useful for the following discussion to rewrite these equations in terms of normalized quantities which can be interpreted as probability laws for the random variable σ_i , namely $\eta_{i \rightarrow j}(\sigma_i) = Z_{i \rightarrow j}(\sigma_i) / \sum_{\sigma'} Z_{i \rightarrow j}(\sigma')$ and $\eta_i(\sigma_i) = Z_i(\sigma_i) / \sum_{\sigma'} Z_i(\sigma')$. The quantity $\eta_{i \rightarrow j}(\sigma_i)$ is the marginal probability law of variable σ_i in a modified system where the link $\langle i, j \rangle$ has been removed. The recursion equations read in these notations

$$\eta_{i \rightarrow j}(\sigma_i) = \frac{1}{z_{i \rightarrow j}} \prod_{k \in \partial i \setminus j} \left(\sum_{\sigma_k} \eta_{k \rightarrow i}(\sigma_k) \psi_{ik}(\sigma_i, \sigma_k) \right), \quad \eta_i(\sigma_i) = \frac{1}{z_i} \prod_{j \in \partial i} \left(\sum_{\sigma_j} \eta_{j \rightarrow i}(\sigma_j) \psi_{ij}(\sigma_i, \sigma_j) \right), \quad (183)$$

where $z_{i \rightarrow j}$ and z_i are normalization constants:

$$z_{i \rightarrow j} = \sum_{\sigma_i} \prod_{k \in \partial i \setminus j} \left(\sum_{\sigma_k} \eta_{k \rightarrow i}(\sigma_k) \psi_{ik}(\sigma_i, \sigma_k) \right), \quad z_i = \sum_{\sigma_i} \prod_{j \in \partial i} \left(\sum_{\sigma_j} \eta_{j \rightarrow i}(\sigma_j) \psi_{ij}(\sigma_i, \sigma_j) \right), \quad (184)$$

Since the leaves are isolated when the link connecting them is removed, one has $Z_{i \rightarrow j}(\sigma_i) = \text{const.}$ and $\eta_{i \rightarrow j}(\sigma_i) = \text{const.}$ for leaves. However, one can also choose to put an arbitrary $\eta_{i \rightarrow j}(\sigma_i)$ on the leaves: this might represent an external field acting on them, or the effect of a given boundary condition. Moreover the quantity $\eta_i(\sigma_i)$ is exactly the marginal probability law of the Gibbs-Boltzmann distribution, hence the local magnetizations can be computed as $m_i = \langle \sigma_i \rangle = \sum_{\sigma} \eta_i(\sigma) \sigma$. Finally, it is useful to define the object

$$z_{ij} = \sum_{\sigma_i, \sigma_j} \eta_{j \rightarrow i}(\sigma_j) \eta_{i \rightarrow j}(\sigma_i) \psi_{ij}(\sigma_i, \sigma_j) = \frac{z_j}{z_{j \rightarrow i}} = \frac{z_i}{z_{i \rightarrow j}}, \quad (185)$$

where the last two equalities are easily derived using Eqs. (183).

We can now write the free energy of the system. Clearly, for any spin σ_i the total partition function is $Z = \sum_{\sigma_i} Z_i(\sigma_i)$. Note that using Eqs. (183) and (184), we obtain

$$z_i = \sum_{\sigma_i} \prod_{j \in \partial i} \left(\sum_{\sigma_j} \eta_{j \rightarrow i}(\sigma_j) \psi_{ij}(\sigma_i, \sigma_j) \right) = \sum_{\sigma_i} \prod_{j \in \partial i} \left(\sum_{\sigma_j} \frac{Z_{j \rightarrow i}(\sigma_j)}{\sum_{\sigma'} Z_{j \rightarrow i}(\sigma')} \psi_{ij}(\sigma_i, \sigma_j) \right) = \frac{\sum_{\sigma_i} Z_i(\sigma_i)}{\prod_{j \in \partial i} \sum_{\sigma_j} Z_{j \rightarrow i}(\sigma_j)}, \quad (186)$$

and along the same steps

$$z_{j \rightarrow i} = \frac{\sum_{\sigma_j} Z_{j \rightarrow i}(\sigma_j)}{\prod_{k \in \partial j \setminus i} \sum_{\sigma_k} Z_{k \rightarrow j}(\sigma_k)}. \quad (187)$$

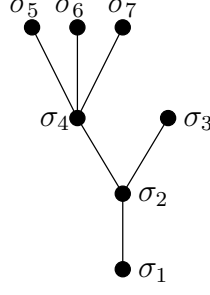


FIG. 11: Example of an Ising tree model on 7 vertices. The definition of $Z_{2 \rightarrow 1}$ and its recursive computation reads here: $Z_{2 \rightarrow 1}(\sigma_2) = \sum_{\sigma_3, \dots, \sigma_7} \psi_{23}(\sigma_2, \sigma_3) \psi_{24}(\sigma_2, \sigma_4) \psi_{45}(\sigma_4, \sigma_5) \psi_{46}(\sigma_4, \sigma_6) \psi_{47}(\sigma_4, \sigma_7) = \sum_{\sigma_3, \sigma_4} Z_{3 \rightarrow 2}(\sigma_3) Z_{4 \rightarrow 2}(\sigma_4) \psi_{23}(\sigma_2, \sigma_3) \psi_{24}(\sigma_2, \sigma_4)$.

So we can start from an arbitrary spin i and

$$Z = \sum_{\sigma_i} Z_i(\sigma_i) = z_i \prod_{j \in \partial i} \left(\sum_{\sigma_j} Z_{j \rightarrow i}(\sigma_j) \right) = z_i \prod_{j \in \partial i} \left(z_{j \rightarrow i} \prod_{k \in \partial j \setminus i} \sum_{\sigma_k} Z_{k \rightarrow j}(\sigma_k) \right), \quad (188)$$

and we can continue to iterate this relation until we reach the leaves of the tree. Using Eq. (185), we finally obtain

$$Z = z_i \prod_{j \in \partial i} \left(z_{j \rightarrow i} \prod_{k \in \partial j \setminus i} z_{k \rightarrow j} \dots \right) = z_i \prod_{j \in \partial i} \left(\frac{z_j}{z_{ij}} \prod_{k \in \partial j \setminus i} \frac{z_k}{z_{jk}} \dots \right) = \frac{\prod_i z_i}{\prod_{\langle i, j \rangle} z_{ij}} \quad (189)$$

and the free energy is

$$\begin{aligned} F &= -T \log Z = \sum_i f_i - \sum_{\langle i, j \rangle} f_{ij}, \\ f_i &= -T \log z_i, \\ f_{ij} &= -T \log z_{ij}. \end{aligned} \quad (190)$$

The advantage of this expression of F is that it does not depend on the arbitrary choice of the initial site i we made above.

On a given tree, the equations (183) for the $\eta_{i \rightarrow j}$ for all directed edges of the graph have a single solution, which is easily found by propagating the recursion from the leaves of the graph. From this solution, one can compute the free energy using Eq. (190). If the connectivity of the tree is bounded, then the number of steps required to compute F is proportional to the number of nodes N in the tree when $N \rightarrow \infty$. Note that in the particular case of a “tree” with connectivity two (in other words, a one dimensional chain with open boundaries) the above equations are exactly equivalent to the transfer matrix method (\Rightarrow **Ex.III.2**).

2. From a tree to a random graph

The reasoning of section IIIC1 was made under the assumption that the interaction graph was a tree, and we arrived on the recursion (183). Suppose now that we are on a random graph, and we cut a link $\langle i, j \rangle$; then we produce two “cavity” variables on sites i and j , whose connectivity has been decreased by one. As before, we define the quantity $\eta_{i \rightarrow j}(\sigma_i)$ as the marginal probability law of variable σ_i in a modified system where the link $\langle i, j \rangle$ has been removed. We can write an exact equation:

$$\eta_{i \rightarrow j}(\sigma_i) = \frac{1}{z_{i \rightarrow j}} \sum_{\{\sigma_k\}, k \in \partial i \setminus j} \eta_{(\partial i \setminus j) \rightarrow i}(\{\sigma_k\}) \prod_{k \in \partial i \setminus j} \psi_{ik}(\sigma_i, \sigma_k), \quad (191)$$

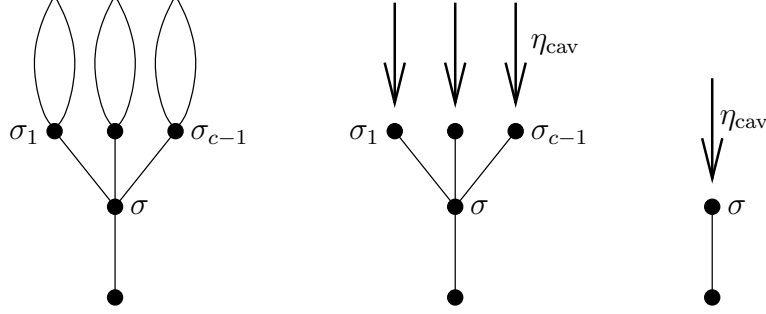


FIG. 12: Pictorial representation of Eq. (194). The bubbles on the first panel represent subtrees of the graph; their effect on the spins $\sigma_1, \dots, \sigma_{c-1}$ is summarized by η_{cav} , represented as a bold arrow in the second panel. Tracing over these $c - 1$ spins leads to the third panel.

where we introduced a multi-spin cavity field $\eta_{(\partial i \setminus j) \rightarrow i}(\{\sigma_k\}, k \in \partial i \setminus j)$ that describes the joint distribution of the spins in $\partial i \setminus j$ in absence of the links that connect them to i . The problem obviously is that in these way the equations are not closed. We can close the equations if we assume that the cavity variables are uncorrelated and write

$$\eta_{(\partial i \setminus j) \rightarrow i}(\{\sigma_k\}, k \in \partial i \setminus j) = \prod_{k \in \partial i \setminus j} \eta_{k \rightarrow i}(\sigma_k), \quad (192)$$

which gives back Eqs. (183). Now, Eqs. (183) have to be interpreted as a set of coupled equations for the unknown $\eta_{i \rightarrow j}$. Contrary to the tree, on a graph with loops they cannot be solved by recursion. Still the number of equations is clearly equal to the number of unknown and we can hope for a unique solution.

The replica symmetric cavity method corresponds to the use of the local recursion equations (183) derived under the assumption (192) to compute the free energy of models defined on sparse random graphs, that are locally tree-like.

How can we justify assumption (192)? The key observation is that, as we already discussed, random graphs converge locally to trees in the thermodynamic limit. Loops have typically length $\sim \log(N)$. Therefore, if we cut the links between variables in $\partial i \setminus j$ and variable i , in the modified system variables in $\partial i \setminus j$ are very far away. *If there is a single pure state*, then correlations in the Gibbs measure decay quickly with distance and Eq. (192) becomes asymptotically correct for $N \rightarrow \infty$. In summary, the assumption of the existence of a single pure state implies that the effect of the loops does not spoil the existence of a unique solution to the local recursions (183). Their presence simply provides self-consistent boundary conditions. We conclude that Eqs. (183) provide an exact description of a disordered model on a random graph for $N \rightarrow \infty$, in a phase where there is a single pure state.

Note that one can look for a solution of the recursion equations (183) on any graph, even in the presence of short loops. Although this procedure is not exact in general, it might provide a good approximation to the true solution of the problem. This approach is known as Belief Propagation in inference problems [79], and corresponds to the Bethe approximation of statistical mechanics [80].

3. Replica symmetric cavity equations in absence of local disorder

To become more familiar with the cavity method, we now consider the simplest possible case. We specialize to a model such that

1. The underlying graph is a random regular graph: the connectivity of the constraints is $k = 2$, so we do not need a factor graph representation, and the connectivity of the variables is fixed to c . We have therefore N variables and $M = Nc/2$ links (constraints).
2. There is no disorder in the Hamiltonian, i.e. the constraints are all equal to a deterministic function of the involved variables.

Simple example of models in this class are

1. The Ising ferromagnet/antiferromagnet: $H = - \sum_{(ij)} JS_i S_j$;

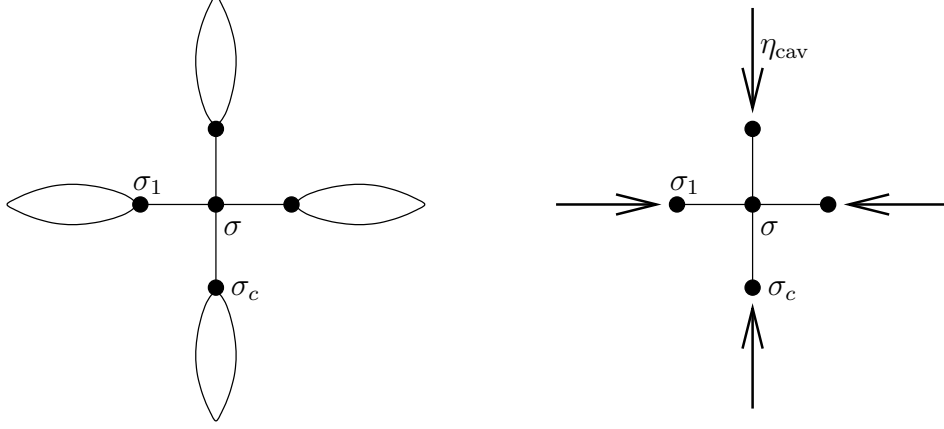


FIG. 13: Illustration of Eq. (195); the local magnetization of one site is computed by taking into account all the c neighbors.

2. The Potts antiferromagnet $H = \sum_{(ij)} \delta(\sigma_i, \sigma_j)$, that corresponds to q -COL.

3. A model of hard spheres, defined by $n_i \in \{0, 1\}$ (occupation numbers) and local constraints that impose that if a site is occupied ($n_i = 1$) at least some of the neighboring sites cannot be occupied [81].

Therefore this class is already rich enough to show some interesting features and structures: actually, q -COL already contains the richest 1RSB structure and further complications do not add much to the physical picture [76].

The main simplification in these models is that *all sites are statistically equivalent*, i.e. the local environment is tree-like (with probability 1 for $N \rightarrow \infty$) without fluctuations of the connectivity or of the local interactions. The latter have the form $\psi_{ij}(\sigma_i, \sigma_j) = \psi(\sigma_i, \sigma_j)$ for a fixed function ψ . Notice that in these systems, the frustration and the disorder (if any) are due to the presence of loops, and thus occur only on large scales ($\sim \log N / \log(c-1)$).

Consider a site i and the region around this site. For $N \rightarrow \infty$, this region will be a tree with probability 1 and we can use the recursion (183) to compute everything inside the tree. The problem is that in this case the “leaves” are connected to the rest of the graph, which provides a boundary condition that has to be determined. Suppose that we are in a phase that is not frustrated. Then, we expect the system to be homogeneous. Suppose then that each of the leaves feel the same external field due to the rest of the graph. We initiate then the recursion with the same $\eta_0(\sigma)$ for all the leaves. Then, at each iteration, the η ’s remain identical and satisfy the recursion:

$$\eta_{g+1}(\sigma) = \frac{1}{z_g} \sum_{\sigma_1, \dots, \sigma_{c-1}} \eta_g(\sigma_1) \dots \eta_g(\sigma_{c-1}) \psi(\sigma, \sigma_1) \dots \psi(\sigma, \sigma_{c-1}) . \quad (193)$$

Since the tree region around site i can be arbitrarily large, we have to iterate this recursion for a very large number of times, and it is natural to assume that we will converge to a fixed point²¹ η_{cav} which satisfies the relation

$$\eta_{\text{cav}}(\sigma) = \frac{1}{z_{\text{cav}}} \sum_{\sigma_1, \dots, \sigma_{c-1}} \eta_{\text{cav}}(\sigma_1) \dots \eta_{\text{cav}}(\sigma_{c-1}) \psi(\sigma, \sigma_1) \dots \psi(\sigma, \sigma_{c-1}) = \frac{1}{z_{\text{cav}}} \left(\sum_{\sigma'} \eta_{\text{cav}}(\sigma') \psi(\sigma, \sigma') \right)^{c-1} , \quad (194)$$

with z_{cav} is the normalization constant. A pictorial representation of this equation can be found in Fig. 12. The local magnetization is then computed as

$$\langle \sigma \rangle = \sum_{\sigma} \eta(\sigma) \sigma , \quad \eta(\sigma) = \frac{1}{z(s)} \sum_{\sigma_1, \dots, \sigma_c} \eta_{\text{cav}}(\sigma_1) \dots \eta_{\text{cav}}(\sigma_c) \psi(\sigma, \sigma_1) \dots \psi(\sigma, \sigma_c) , \quad (195)$$

²¹ In presence of spontaneous symmetry breaking, for instance for a ferromagnetic system at low temperature, there might be several fixed points. In ordered systems, one can usually select one of them by adding a suitable small external field to break explicitly the symmetry and obtain a system with a single pure state.

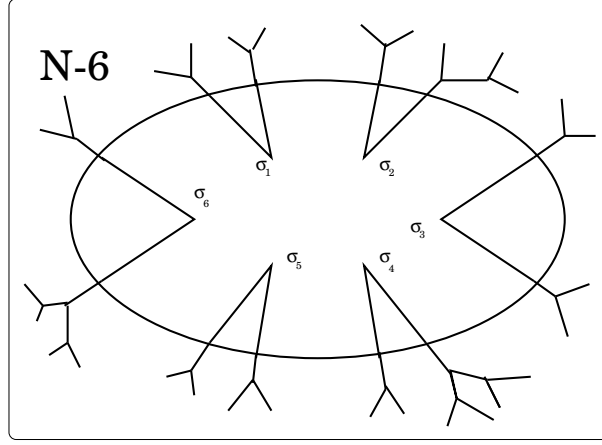


FIG. 14: An example, for the case $c = 3$, of a $\mathcal{G}_{N,6}$ cavity graph where $q = 6$ randomly chosen cavity variables have $c - 1 = 2$ neighbours only. All the other $N - 6$ spins outside the cavity are connected through a random graph such that every spin has $c = 3$ neighbours.

including the c neighbors of a central site as represented in Fig. 13. Although we fixed a particular site i at the beginning, this reasoning is clearly independent of the site in the thermodynamic limit, since in that limit all sites have the same environment around them. Therefore, we expect that in this limit all the fields $\eta_{i \rightarrow j}$ (or equivalently η_g) will converge to η_{cav} , solution of (194), and all the fields $\eta_i(\sigma)$ will converge to $\eta(\sigma)$ defined in (195).

We can now compute the free energy of the system. We start from Eq. (190) together with (184) and (185). We observe that, under the homogeneity assumption made above, all $z_i = z^{(s)}$ and $z_{ij} = z^{(l)}$ are equal with

$$\log z^{(l)} = \log \sum_{\sigma_1 \sigma_2} \eta_{\text{cav}}(\sigma_1) \eta_{\text{cav}}(\sigma_2) \psi(\sigma_1, \sigma_2) . \quad (196)$$

and

$$\log z^{(s)} = \log \sum_{\sigma, \sigma_1, \dots, \sigma_c} \eta_{\text{cav}}(\sigma_1) \cdots \eta_{\text{cav}}(\sigma_c) \psi(\sigma, \sigma_1) \cdots \psi(\sigma, \sigma_c) = \log \sum_{\sigma} \left(\sum_{\sigma'} \eta_{\text{cav}}(\sigma') \psi(\sigma, \sigma') \right)^c . \quad (197)$$

Recall that for a random regular graph the number of links is $Nc/2$. Then we get

$$\begin{aligned} f &= \frac{F}{N} = f^{(s)} - \frac{c}{2} f^{(l)} , \\ f^{(s)} &= -T \log z^{(s)} , \\ f^{(l)} &= -T \log z^{(l)} . \end{aligned} \quad (198)$$

The cavity method (here presented for an homogeneous state of a model without disorder on a random regular graph) consists in solving Eq.(194) and using then Eq. (198) to compute the free energy. Obviously, any other observable can be computed from the free energy by adding suitable external fields.

4. An alternative derivation

Before moving to more complicated cases, it is useful to present an alternative derivation of the cavity method, that also explain the historical origin of its name. This derivation was the original one of [43] and this section is reprinted from that paper.

Let us introduce an intermediate object which is a model with N variables, on a slightly different random lattice, where q randomly chosen “cavity” variables have only $c - 1$ neighbours, while the other $N - q$ spins all have c neighbours (see fig.14). We call such a graph a $\mathcal{G}_{N,q}$ “cavity graph”. The cavity variables are characterized by some joint probability distribution $\eta_{\text{cav}}(\sigma_1, \dots, \sigma_q)$.

While our primary interest is in $\mathcal{G}_{N,0}$ graphs, the intermediate construction of $\mathcal{G}_{N,q}$ is helpful. The basic operations which one can perform on cavity graphs are the following:

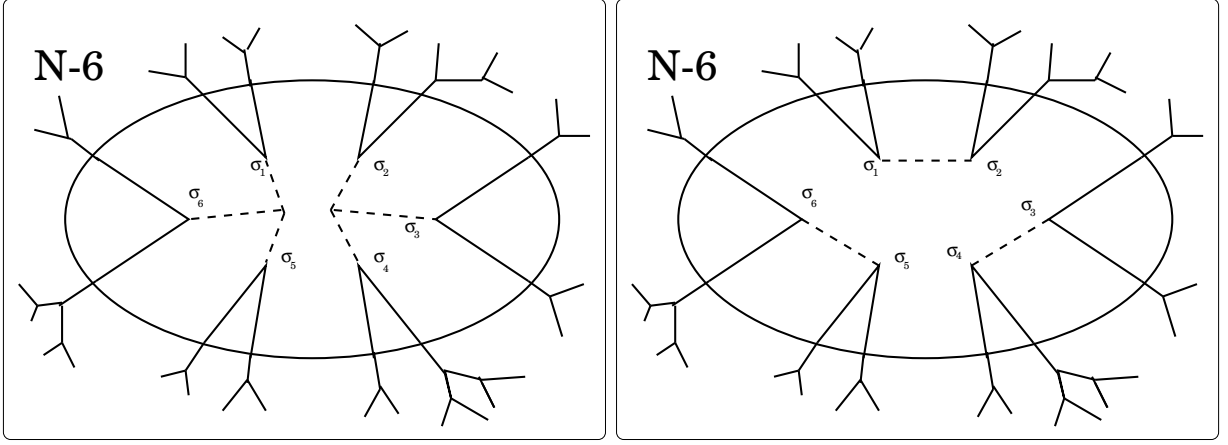


FIG. 15: Starting from the $\mathcal{G}_{N,6}$ cavity graph, one can either add two sites (left figure) and create a $\mathcal{G}_{N+2,0}$ graph, or add three links (right figure) and create a $\mathcal{G}_{N,0}$ graph.

- *Iteration:* By adding a new spin σ_0 into the cavity, connecting it to $c-1$ of the cavity spins, say $\sigma_1, \dots, \sigma_{c-1}$, one changes a $\mathcal{G}_{N,q}$ into a $\mathcal{G}_{N+1,q-c+2}$ graph:

$$\Delta N = 1, \quad \Delta q = -c + 2. \quad (199)$$

- *Link addition:* By adding a new link between two randomly chosen cavity spins σ_1, σ_2 , one changes a $\mathcal{G}_{N,q}$ into a $\mathcal{G}_{N,q-2}$ graph:

$$\Delta N = 0, \quad \Delta q = -2. \quad (200)$$

- *Site addition:* By adding a new spin σ_0 into the cavity, connecting it to c of the cavity spins say $\sigma_1, \dots, \sigma_c$, one changes a $\mathcal{G}_{N,q}$ into a $\mathcal{G}_{N+1,q-c}$ graph:

$$\Delta N = 1, \quad \Delta q = -c. \quad (201)$$

In particular, if one starts from a $\mathcal{G}_{N,2c}$ cavity graph and perform c link additions, one gets a $\mathcal{G}_{N,0}$ graph, i.e. our original problem with N variables. Starting from the same $\mathcal{G}_{N,2c}$ cavity graph and performing 2 site additions, one gets a $\mathcal{G}_{N+2,0}$ graph, i.e. our original problem with $N+2$ variables. Therefore the variation in the free energy when going from N to $N+2$ sites ($F_{N+2} - F_N$) is related to the average free energy shifts $\Delta F^{(s)}$ for a site addition, and $\Delta F^{(l)}$ for a link addition, through:

$$F_{N+2} - F_N = 2\Delta F^{(s)} - c\Delta F^{(l)}. \quad (202)$$

Using the fact that the total free energy is asymptotically linear in N , the free energy is finally

$$f = \lim_{N \rightarrow \infty} F_N/N = \frac{F_{N+2} - F_N}{2} = \Delta F^{(s)} - \frac{c}{2}\Delta F^{(l)}. \quad (203)$$

An intuitive interpretation of this result (for even c) is that in order to go from N to $N+1$ one should remove $c/2$ links (the energy for removing a link is minus the energy for adding a link) and then add a site.

Now we should derive the equation for $\eta_{\text{cav}}(\sigma)$. When $q/N \ll 1$, generically, the distance on the lattice between two generic cavity spins is large (it is of the order of the size of the loops, therefore diverges logarithmically in the large N limit). We will therefore assume that:

1. Different cavity variables become uncorrelated. This is true only if the Gibbs measure is a *pure state*, and the *clustering property*, stating that distant variables are uncorrelated, holds.
2. The states of the system before and after any of the previous graph operations (e.g. iteration) are related. Equivalently one should assume that the perturbation corresponding to the variation of one of the cavity spins remains *localized* and it does not propagate to the whole lattice. This is clearly a decorrelation hypothesis that is very similar to the previous one.

Under these hypotheses, which are reasonable for a non frustrated homogeneous phase, it is very simple to compute the free energy shifts defined above.

The important point is that our hypotheses imply that the joint probability of the cavity variables *factorizes*; we have $\eta_{\text{cav}}(\sigma_1, \dots, \sigma_q) = \eta_{\text{cav}}^1(\sigma_1) \cdots \eta_{\text{cav}}^q(\sigma_q)$. To simplify the problem, let us assume that the cavity distributions are identical, $\eta_{\text{cav}}^i(\sigma) = \eta_{\text{cav}}(\sigma)$, for all cavity variables because of our assumption that the local environment is the same everywhere in the graph (no fluctuations of connectivity and interactions). This is not an harmless assumption, because in general frustration might induce different biases on different variables; we will come back to this in next section.

Consider now an iteration where a new cavity variable is added and connected to $c - 1$ cavity variables. The new cavity variable has a probability distribution

$$\eta_{\text{cav}}(\sigma) = \frac{1}{z_{\text{cav}}} \sum_{\sigma_1, \dots, \sigma_{c-1}} \eta_{\text{cav}}(\sigma_1) \cdots \eta_{\text{cav}}(\sigma_{c-1}) \psi(\sigma, \sigma_1) \cdots \psi(\sigma, \sigma_{c-1}) ,$$

$$z_{\text{cav}} = \sum_{\sigma} \left(\sum_{\sigma'} \eta_{\text{cav}}(\sigma') \psi(\sigma, \sigma') \right)^{c-1} , \quad (204)$$

that must again be identical to the old ones; this is because we assumed that the local environment does not fluctuate and that, for large N , the state of the system remains the same after any of the above operations. Therefore (204) is a self-consistent equation that can be solved to obtain $\eta_{\text{cav}}(\sigma)$. We got back Eq. (194).

Once this is done, we can compute the free energy shifts for a link and site addition. Consider a link addition between two cavity spins σ_1 and σ_2 . Before addition, we have

$$Z_{\text{before}} = \sum_{\sigma} \prod_a \psi_a(\sigma_a) = \sum_{\sigma_1 \sigma_2} Z(\sigma_1, \sigma_2) ,$$

$$\eta_{\text{cav}}(\sigma_1, \sigma_2) = \eta_{\text{cav}}(\sigma_1) \eta_{\text{cav}}(\sigma_2) = \frac{Z(\sigma_1, \sigma_2)}{Z_{\text{before}}} , \quad (205)$$

where $Z(\sigma_1, \sigma_2)$ is the trace of the Gibbs measure over all variables except the two cavity ones. When we add a link (i.e. a constraint) connecting σ_1 and σ_2 , we have

$$Z_{\text{after}} = \sum_{\sigma} \psi(\sigma_1, \sigma_2) \prod_a \psi_a(\sigma_a) = \sum_{\sigma_1 \sigma_2} \psi(\sigma_1, \sigma_2) Z(\sigma_1, \sigma_2) = Z_{\text{before}} \sum_{\sigma_1 \sigma_2} \eta_{\text{cav}}(\sigma_1) \eta_{\text{cav}}(\sigma_2) \psi(\sigma_1, \sigma_2) , \quad (206)$$

and we obtain the final result

$$\log z^{(l)} = \log \frac{Z_{\text{after}}}{Z_{\text{before}}} = \log \sum_{\sigma_1 \sigma_2} \eta_{\text{cav}}(\sigma_1) \eta_{\text{cav}}(\sigma_2) \psi(\sigma_1, \sigma_2) , \quad (207)$$

which coincides with (196). With a very similar argument one can show that

$$\log z^{(s)} = \log \sum_{\sigma_0, \sigma_1, \dots, \sigma_c} \eta_{\text{cav}}(\sigma_1) \cdots \eta_{\text{cav}}(\sigma_c) \psi(\sigma_0, \sigma_1) \cdots \psi(\sigma_0, \sigma_c) = \log \sum_{\sigma} \left(\sum_{\sigma'} \eta_{\text{cav}}(\sigma') \psi(\sigma, \sigma') \right)^c . \quad (208)$$

which gives back (196). Putting these results in (203) we get back Eq. (198). Finally, note that from $\eta_{\text{cav}}(\sigma)$ we can reconstruct the true *marginal probability* of the variables $\eta(\sigma)$, defined as the trace of the Gibbs measure over all variables but σ . To do this we consider a graph with c cavity spin $\sigma_1, \dots, \sigma_c$ and perform a site addition to get the real graph; we get

$$P(\sigma) = \frac{1}{z^{(s)}} \sum_{\sigma_1, \dots, \sigma_c} \eta_{\text{cav}}(\sigma_1) \cdots \eta_{\text{cav}}(\sigma_c) \psi(\sigma, \sigma_1) \cdots \psi(\sigma, \sigma_c) = \frac{1}{z^{(s)}} \left(\sum_{\sigma'} \eta_{\text{cav}}(\sigma') \psi(\sigma, \sigma') \right)^c . \quad (209)$$

which is (195). This concludes our derivation; we have then presented two slightly different but equivalent derivations of the cavity method.

A very important property of the free energy (198) is that it is *variational*²²: one can easily show (\Rightarrow **Ex.III.8**) that the functional equation $\frac{df}{d\eta_{\text{cav}}(\sigma)} = 0$ gives back Eq. (204). In particular, this allows for a simple computation of

²² However, it cannot be proven that the extremum is a minimum in general.

the energy $e = \frac{d(\beta f)}{d\beta}$ and entropy $s = -\frac{df}{dT}$, because it is enough to compute the explicit derivative with respect to T without deriving with respect to $\eta_{\text{cav}}(\sigma)$. The result is²³:

$$\begin{aligned} s &= \log z^{(s)} - c/2 \log z^{(l)} + \beta e , \\ e &= e^{(s)} - c/2 e^{(l)} , \\ e^{(l)} &= \frac{1}{z^{(l)}} \sum_{\sigma_1 \sigma_2} \eta_{\text{cav}}(\sigma_1) \eta_{\text{cav}}(\sigma_2) \psi(\sigma_1, \sigma_2) E(\sigma_1, \sigma_2) , \\ e^{(s)} &= \frac{1}{z^{(s)}} \sum_{\sigma_0, \sigma_1, \dots, \sigma_c} \eta_{\text{cav}}(\sigma_1) \cdots \eta_{\text{cav}}(\sigma_c) \psi(\sigma_0, \sigma_1) \cdots \psi(\sigma_0, \sigma_c) [E(\sigma_0, \sigma_1) + \cdots + E(\sigma_0, \sigma_c)] . \end{aligned} \quad (210)$$

The equations above can be applied to many problems on random graphs, such as the Ising ferromagnet (\Rightarrow **Ex.III.3**), the SK model (\Rightarrow **Ex.III.4**) and the q -COL problem (\Rightarrow **Ex.III.5**).

In the case of un-frustrated ferromagnetic models it has been shown rigorously [82] that the assumption we made on the way are correct, the predictions of the cavity method being exact in the thermodynamic limit, both for the local magnetizations and for the free-energy per site.

5. Fluctuations of the local environment: distributions of cavity probabilities

We will now allow for the presence of local fluctuations, in the form of quenched random couplings, and fluctuations of the variable connectivity. We show here how to take the average over this quenched disorder. We will still restrict to $k = 2$ for simplicity. In this more general setting, the cavity variables are not equivalent: they do not have the same distribution, because of the explicit disorder present in the Hamiltonian, or in the graph, or both.

In principle we could take a given realization of the disorder (graph and couplings) for finite (but large) N , and try to find a solution of (183). This can be done in some cases numerically, but it is not very practical. If we are interested in computing the free energy averaged over the disorder, we can introduce a *distribution of cavity distributions*, $\mathcal{P}[\eta_{\text{cav}}(\sigma)]$, that gives the probability (over the links $i \rightarrow j$) that variable σ_i has a cavity probability distribution:

$$\mathcal{P}[\eta_{\text{cav}}(\sigma)] = \text{Prob}[\eta_{i \rightarrow j}(\sigma_i) = \eta_{\text{cav}}(\sigma_i)] . \quad (211)$$

If we take the average over the disorder (both the couplings and the random graph), then this distribution must be the same for all sites, since all sites are statistically equivalent.

The equation for \mathcal{P} is deduced by using Eq. (183) and imposing that the probability distribution of $\eta_{i \rightarrow j}$ is the same as that of the $\eta_{k \rightarrow i}$. Defining

$$\eta_{\text{cav}}^0(\sigma_0) = \frac{1}{z_{\text{cav}}} \sum_{\sigma_1, \dots, \sigma_{c-1}} \eta_{\text{cav}}^1(\sigma_1) \cdots \eta_{\text{cav}}^{c-1}(\sigma_{c-1}) \psi_1(\sigma_0, \sigma_1) \cdots \psi_{c-1}(\sigma_0, \sigma_{c-1}) = \mathcal{F}_J[\eta_{\text{cav}}^1, \dots, \eta_{\text{cav}}^{c-1}] , \quad (212)$$

where the interactions $\psi_1 \cdots \psi_{c-1}$ may contain one realization of the disorder, one obtains

$$\mathcal{P}[\eta_{\text{cav}}^0] = \overline{\int d\mathcal{P}[\eta_{\text{cav}}^1] \cdots d\mathcal{P}[\eta_{\text{cav}}^{c-1}] \delta[\eta_{\text{cav}}^0 - \mathcal{F}_J[\eta_{\text{cav}}^1, \dots, \eta_{\text{cav}}^{c-1}]]}^{\{c, J\}} , \quad (213)$$

where the overline denotes an average over the couplings J and over the distribution of c . This equation has the following interpretation: one must extract the η_{cav}^i from \mathcal{P} , and produce a new η_{cav}^0 that must also be typical of \mathcal{P} . The function \mathcal{F}_J may depend on the couplings that appear in the constraints; these have to be extracted from their distribution at each iteration.

Moreover c might also be a random variable, and an important remark on the distribution of c is in order. Suppose that $P(c)$ is the distribution of the connectivity of the variables of the random graph. We *should not* use $P(c)$ to take the average in Eq. (213). The reason is the following. The cavity distributions $\eta_{i \rightarrow j}$ are defined on the links of the graph. When we perform a cavity iteration using Eq. (183), we fix an oriented link $i \rightarrow j$ and consider all the other links $k \rightarrow i$ that are connected to site i . Since $\mathcal{P}[\eta_{\text{cav}}(\sigma)]$ is the histogram over the links of cavity distributions, to

²³ Recall that we defined $\psi(\sigma_1, \sigma_2) = \exp[-\beta E(\sigma_1, \sigma_2)]$.

derive Eq. (213) we must take a random link, not a random site. The average in Eq. (213) is taken over *the probability* $\tilde{P}(c)$ that, picking uniformly at random a link $i \rightarrow j$, the variable i has connectivity c . It is easy to show that

$$\begin{aligned}\tilde{P}(c) &= \frac{cP(c)}{\bar{c}}, \\ \bar{c} &= \sum_{c=0}^{\infty} cP(c),\end{aligned}\tag{214}$$

and the average over c in Eq. (213) must be taken with the distribution $\tilde{P}(c)$.

To compute the free energy one has to average (190) over the distribution \mathcal{P} that solves the previous equation. It is easy to see that the result is

$$f = \overline{f^{(s)}}^{\{\mathcal{P}, c, J\}} - \frac{\bar{c}}{2} \overline{f^{(l)}}^{\{\mathcal{P}, J\}},\tag{215}$$

where

$$\begin{aligned}\overline{f^{(s)}}^{\{\mathcal{P}, c, J\}} &= -T \int d\mathcal{P}[\eta_{\text{cav}}^1] \cdots d\mathcal{P}[\eta_{\text{cav}}^c] \log \left[\sum_{\sigma, \sigma_1, \dots, \sigma_c} \eta_{\text{cav}}^1(\sigma_1) \cdots \eta_{\text{cav}}^c(\sigma_c) \psi_1(\sigma, \sigma_1) \cdots \psi_c(\sigma, \sigma_c) \right]^{\{c, J\}} \\ \overline{f^{(l)}}^{\{\mathcal{P}, J\}} &= -T \int d\mathcal{P}[\eta_{\text{cav}}^1] d\mathcal{P}[\eta_{\text{cav}}^2] \log \left[\sum_{\sigma_1 \sigma_2} \eta_{\text{cav}}^1(\sigma_1) \eta_{\text{cav}}^2(\sigma_2) \psi(\sigma_1, \sigma_2) \right]^J.\end{aligned}\tag{216}$$

We note that here the site term must be averaged using $P(c)$, since it is an average over all sites, see Eq. (190).

6. The zero temperature limit

As we already discussed there are two ways of taking the zero-temperature limit. The first is to assume that the system is in the SAT phase and therefore the ground state has zero energy. In this case a solution to the constraints exist and we can just take infinitely hard constraints ($\beta \rightarrow \infty$). The energy is zero as can be seen from (210), and the entropy is simply $\frac{1}{N} \log Z$ and is given by the first of (210) without the last term βe .

On the other hand we might be interested in a situation where not all the constraints can be satisfied at the same time and the ground state energy is non-zero. In this case the limit $\beta \rightarrow \infty$ of Eq. (204) does not make sense since the normalization constant might vanish when a contradiction is met.

In this case one has to take care. For simplicity, let us focus on a spin glass Hamiltonian $H = -\sum_{(ij)} J_{ij} S_i S_j$ for Ising spins [44]. The denominator in (212) is given by $z_{\text{cav}} \sim e^{-\beta e_{\text{cav}}}$ at leading order for large β . We introduce a *cavity field* $h_{i \rightarrow j}$ by the parametrization, again at leading order for $\beta \rightarrow \infty$:

$$\eta_{i \rightarrow j}(S_i) \sim e^{\beta(h_{i \rightarrow j} S_i - |h_{i \rightarrow j}|)}.\tag{217}$$

The cavity equation becomes, substituting the previous parametrizations and taking the leading order for $\beta \rightarrow \infty$:

$$h_0 S_0 - |h_0| = e_{\text{cav}} + \sum_{i=1}^{c-1} (|h_i + J_{0i} S_0| - |h_i|).\tag{218}$$

We can write

$$\begin{aligned}|h_i + J_{0i} S_0| &= a(h_i, J_{0i}) + S_0 u(h_i, J_{0i}), \\ a(h_i, J_{0i}) &= \frac{1}{2}(|h_i + J_{0i}| + |h_i - J_{0i}|), \\ u(h_i, J_{0i}) &= \frac{1}{2}(|h_i + J_{0i}| - |h_i - J_{0i}|).\end{aligned}\tag{219}$$

Then we get

$$\begin{aligned}h_0 &= \sum_{i=1}^{c-1} u(h_i, J_{0i}), \\ e_{\text{cav}} &= -|h_0| + \sum_{i=1}^{c-1} [|h_i| - a(h_i, J_{0i})].\end{aligned}\tag{220}$$

Similarly we get

$$\begin{aligned} e^{(l)} &= |h_1| + |h_2| - \max_{S_1, S_2} [h_1 S_1 + h_2 S_2 + J_{12} S_1 S_2] , \\ e^{(s)} &= \sum_{i=1}^c [|h_i| - a(h_i, J_{0i})] + \left| \sum_{i=1}^c u(h_i, J_{0i}) \right| . \end{aligned} \quad (221)$$

If we assume that the J_{ij} are drawn from a given distribution $P(J)$, and we introduce the distribution of cavity fields $\mathcal{P}(h)$, we obtain [44] the zero-temperature limit of (213)

$$\mathcal{P}(h) = \overline{\int dh_i \mathcal{P}(h_i) \delta \left(h - \sum_{i=1}^{c-1} u(h_i, J_{0i}) \right)}^{\{c, J\}} , \quad (222)$$

where the overline is an average over $P(J)$ and, if one wishes, also on fluctuations of c . The ground state energy is

$$e_0 = \overline{e^{(s)}}^{\{P, c, J\}} - \frac{\bar{c}}{2} \overline{e^{(l)}}^{\{P, J\}} , \quad (223)$$

i.e. the site and link energies (221) have to be averaged over the distribution of J and c , and over $\mathcal{P}(h)$, as in Eq. (215).

The solution to these equations for the case $J = \pm 1$ with probability 1/2 can be found in [44]. Many other problems have been studied using this zero-temperature “energetic” formalism, including q -COL [83] and k -SAT [69, 70]. In the following we will focus more on the “entropic” limit in which one assumes to be in the SAT phase and studies the structure of the solutions.

7. On a factor graph

Let us conclude by generalizing the previous equations to the case of a factor graph. We will only briefly sketch the derivation, more details can be found in [84].

In this case we have two type of nodes, variables and constraints. It is convenient to introduce *cavity variables* as before: they are variables connected only to $c - 1$ constraints. We also introduce *cavity constraints*: they are constraints that are connected only to $k - 1$ variables.

To each cavity variable we associate its cavity distribution $\eta_{\text{cav}}(\sigma)$. To each cavity constraint, we associate a distribution $\eta_{\text{test}}(\sigma)$ that is defined as follows: imagine to add a k -th missing variable σ to the cavity constraint and *only to it*. Then $\eta_{\text{test}}(\sigma)$ is the distribution of this variable.

Recall that the number of constraints is $M = cN/k$. We denote by $\mathcal{G}_{N, M, p, q}$ a graph with N variables and M constraints, of which p are cavity variables and q are cavity constraints.

We have five possible operations:

1. *Variable iteration*: We add a new cavity variable and connect it to $c - 1$ cavity constraints.
2. *Constraint iteration*: We add a new cavity constraint and connect it to $k - 1$ cavity variables.
3. *Site addition*: We add a new variable and connect it to c cavity constraints.
4. *Constraint addition*: We add a new constraint and connect it to k cavity variables.
5. *Link addition*: We add a new link connecting a cavity constraint and a cavity variable.

We can start with a $\mathcal{G}_{N, M, 0, 0}$ graph and delete ck links. Now we get a graph $\mathcal{G}_{N, M, ck, ck}$ as each link deletion produces a cavity variable and a cavity constraint. To the latter graph we add k new variables, that have to be connected to the ck cavity constraints, and c new constraints, that have to be connected to the ck cavity variables. We thus produce a graph with $N + k$ variables and $M + c$ constraint (note that the relation $M = cN/k$ still holds), $\mathcal{G}_{N+k, M+c, 0, 0}$. Then we get

$$F(N + k) - F(N) = kf = k\Delta F^{(s)} + c\Delta F^{(c)} - ck\Delta F^{(l)} . \quad (224)$$

The iteration equation are the following. When we add a new cavity variable σ , we connect it to $c - 1$ constraints. The influence of each constraint on the new variable is independent from the others and given by $\eta_{\text{test}}(\sigma)$. Then we have

$$\eta_{\text{cav}}^0(\sigma_0) = \frac{1}{z_{\text{cav}}} \prod_{i=0}^{c-1} \eta_{\text{test}}^i(\sigma_0) = \mathcal{F}_{\text{cav}}[\eta_{\text{test}}^1 \cdots \eta_{\text{test}}^{c-1}] , \quad (225)$$

where in principle each constraint can produce a different distribution.

When we add a cavity constraint ψ_a , we connect it to $k - 1$ cavity variables $\sigma_1, \dots, \sigma_{k-1}$. To compute the cavity distribution we need to add also a fictitious variable σ that is connected only to the new constraint. Its distribution is then

$$\eta_{\text{test}}^0(\sigma_0) = \frac{1}{z_{\text{test}}} \sum_{\sigma_1, \dots, \sigma_{k-1}} \eta_{\text{cav}}^1(\sigma_1) \cdots \eta_{\text{cav}}^{k-1}(\sigma_{k-1}) \psi_a(\sigma_0, \sigma_1, \dots, \sigma_{k-1}) = \mathcal{F}_{\text{test}}[\eta_{\text{cav}}^1 \cdots \eta_{\text{cav}}^{k-1}] . \quad (226)$$

Finally we need to compute the free energy shifts. When we add a new constraint, k cavity variables become connected and

$$\log z^{(c)} = \log \sum_{\sigma_1, \dots, \sigma_k} \eta_{\text{cav}}^1(\sigma_1) \cdots \eta_{\text{cav}}^k(\sigma_k) \psi_a(\sigma_1, \dots, \sigma_k) . \quad (227)$$

When we add a new variable, c constraints are connected to it and give independent influence, then

$$\log z^{(s)} = \log \sum_{\sigma} \prod_{i=1}^c \eta_{\text{test}}^i(\sigma) . \quad (228)$$

When we add a link, we connect a cavity variable σ with distribution $\eta_{\text{cav}}(\sigma)$ with a cavity constraint whose influence on σ is $\eta_{\text{test}}(\sigma)$. Then

$$\log z^{(l)} = \log \sum_{\sigma} \eta_{\text{cav}}(\sigma) \eta_{\text{test}}(\sigma) . \quad (229)$$

It is easy to check that the equations above reduce to the ones for a normal graph for $k = 2$ (\Rightarrow **Ex.III.6**).

In presence of site fluctuations all the considerations we made in the $k = 2$ case can be easily generalized. The same holds for the zero temperature limit. The generalization of the formalism to the factor graph allows to discuss for instance the case of XORSAT (\Rightarrow **Ex.III.7**).

8. Summary

Before turning to the 1RSB equations, let's summarize this discussion. The replica symmetric cavity method works when the Gibbs measure is a single pure state. Under this assumption, cavity variables are uncorrelated for $N \rightarrow \infty$ since loops are very long. The equations derived on a tree can then be used to describe a factor graph:

- On a given system of finite (large) size N , one can use Eqs. (183) and (190).
- For a homogeneous system (such that locally there is no disorder in the couplings and the graph), in the thermodynamic limit all the cavity fields are equal and the RS cavity equations reduce to Eqs. (194) and (198).
- In presence of local disorder, one must introduce a distribution of cavity fields over the disorder; the cavity equation for this object is given by Eq. (213), and the free energy can be obtained from Eq. (215).

Similar equations are obtained for systems defined on factor graphs, and in the zero temperature limit.

D. 1-step replica symmetry breaking

In the one-step replica symmetry breaking scenario, we will assume that the Gibbs state is split in a large number of states, as we obtained for the spherical p -spin model. Each state has a weight $w_\alpha \propto \exp(-\beta N f_\alpha)$ in the partition function. As discussed in section IIB 3, in such a situation we wish to compute

$$Z_m = \sum_a e^{-\beta N m f_\alpha} = \int df e^{N[\Sigma(f) - \beta m f]} , \quad (230)$$

from which the thermodynamics of the system can be reconstructed.

Recall that the central hypothesis of the RS cavity method is that (distant) cavity spins are uncorrelated and the Gibbs state is stable (for $N \rightarrow \infty$) under the operations on the graph defined above. Both these properties are false in

the presence of many states, because *i*) the Gibbs state is not a pure state and the decorrelation (clustering) property does not hold, and *ii*) the free energy of the states are shifted when operating on the graph, and this might change the relative weight of the states in the partition function, therefore changing the nature of the Gibbs state. The treatment of the free energy shift is quite complicated [43]. Therefore in the following we will not use the derivation of the 1RSB cavity equations based on the graph operation of section III C 4. This derivation can be found in [43]. We will present instead a derivation based on the idea of first writing the recurrence equations on the tree and then justify its use on the random graph by a decorrelation assumption [85]. This derivation has also the advantage that it is formulated for a single graph and choice of the couplings, so one does not need to take the average over the disorder.

In the RS treatment, the key property is the factorization of the joint distribution of the cavity variables, expressed by Eq. (192), that leads to the closed equations (183) for the cavity messages. Based on the discussion above, in presence of many pure states we can only assume that Eq. (192) is true for the messages $\eta_{i \rightarrow j}^\alpha$ restricted to one pure state. A precise formalization of this hypothesis is the following. By definition, we must be able to select one state by acting on each spin with infinitesimal field h_i^α . If we take *first* the limit $N \rightarrow \infty$ and *then* the limit $h_i^\alpha \rightarrow 0$, we will end up in the state α . For $N \rightarrow \infty$ in presence of h_i^α , we have a single pure state and we can use the RS cavity equations to obtain a set of messages $\eta_{i \rightarrow j}^\alpha$. Then we can take the limit h_i^α , and the resulting messages will describe the state α in absence of the external field. Therefore the $\eta_{i \rightarrow j}^\alpha$ are a fixed point of the RS cavity equation (183). The free energy of a state is given by equation (190), calculated in the fixed point $\eta_{i \rightarrow j}^\alpha$. While finding the fixed points analytically is not possible, we could hope to determine them numerically. The problem is that often, in presence of many fixed points, an iterative solution of equation (183) is not possible because the recursion will not converge if one starts with random messages. Still, in many cases we do not need to know the full set of fixed points. We only want to count how many solutions have a given free energy f , to compute the complexity, and this can be done by mean of Eq. (230).

1. The auxiliary model

Let's summarize the situation, and rewrite once again the relevant equations (183) and (190), in the case $k = 2$ (simple graph) for simplicity. We should find all the solutions of the RS equations

$$\eta_{i \rightarrow j}(\sigma_i) = \frac{\psi_i(\sigma_i)}{z_{i \rightarrow j}} \prod_{k \in \partial i \setminus j} \left(\sum_{\sigma_k} \eta_{k \rightarrow i}(\sigma_k) \psi_{ik}(\sigma_i, \sigma_k) \right) = \mathcal{F}_{i \rightarrow j}[\eta_{k \rightarrow i}, k \in \partial i \setminus j] , \quad (231)$$

and make use of the Bethe free energy to obtain the free energy of each state:

$$-\beta F_{\text{Bethe}}[\{\eta_{i \rightarrow j}\}] = \sum_i \log z_i - \sum_{\langle i, j \rangle} \log z_{ij} , \quad (232)$$

where

$$\begin{aligned} z_{i \rightarrow j} &= \sum_{\sigma_i} \psi_i(\sigma_i) \prod_{k \in \partial i \setminus j} \left(\sum_{\sigma_k} \eta_{k \rightarrow i}(\sigma_k) \psi_{ik}(\sigma_i, \sigma_k) \right) , \\ z_i &= \sum_{\sigma_i} \psi_i(\sigma_i) \prod_{j \in \partial i} \left(\sum_{\sigma_j} \eta_{j \rightarrow i}(\sigma_j) \psi_{ij}(\sigma_i, \sigma_j) \right) , \\ z_{ij} &= \sum_{\sigma_i, \sigma_j} \eta_{j \rightarrow i}(\sigma_j) \eta_{i \rightarrow j}(\sigma_i) \psi_{ij}(\sigma_i, \sigma_j) = \frac{z_j}{z_{j \rightarrow i}} = \frac{z_i}{z_{i \rightarrow j}} . \end{aligned} \quad (233)$$

In the equations above, we also added a local term $\psi_i(\sigma_i)$, which may represent a local field $\psi_i(\sigma_i) = e^{\beta h_i \sigma_i}$. One can easily understand how to place this factor by doing the calculation on the tree. The solution of the equations above gives the free energy of a generic statistical mechanics model having the partition function

$$Z = \sum_{\{\sigma_i\}} \prod_i \psi_i(\sigma_i) \prod_{\langle i, j \rangle} \psi_{\langle i, j \rangle}(\sigma_i, \sigma_j) . \quad (234)$$

Note that on random graphs, the cavity messages $\eta_{i \rightarrow j}^\alpha$ play the role of the local magnetizations in fully connected

models: they fully specify a given state α of the system. We can write the partition function (230) as an integral²⁴ over the messages $\eta_{i \rightarrow j}$:

$$Z_m = \sum_{\alpha} e^{-\beta m F_{\text{Bethe}}[\eta_{i \rightarrow j}^{\alpha}]} = \int \mathcal{D}\eta_{i \rightarrow j} e^{-\beta m F_{\text{Bethe}}[\eta_{i \rightarrow j}]} \prod_{\langle i, j \rangle} \delta[\eta_{i \rightarrow j} - \mathcal{F}_{i \rightarrow j}] \delta[\eta_{j \rightarrow i} - \mathcal{F}_{j \rightarrow i}] \quad (236)$$

where on each link $\langle i, j \rangle$ we have two messages, $\eta_{i \rightarrow j}$ and $\eta_{j \rightarrow i}$, and the two delta functions enforce the RS cavity equations (231). Using (232), we get

$$\begin{aligned} Z_m &= \int \mathcal{D}\eta_{i \rightarrow j} \prod_i z_i^m \prod_{\langle i, j \rangle} z_{ij}^{-m} \delta[\eta_{i \rightarrow j} - \mathcal{F}_{i \rightarrow j}] \delta[\eta_{j \rightarrow i} - \mathcal{F}_{j \rightarrow i}] \\ &= \int \mathcal{D}\eta_{i \rightarrow j} \prod_i \left(z_i^m \prod_{j \in \partial i} \delta[\eta_{i \rightarrow j} - \mathcal{F}_{i \rightarrow j}] \right) \prod_{\langle i, j \rangle} z_{ij}^{-m} \\ &= \int \mathcal{D}\eta_{i \rightarrow j} \prod_i \Psi_i(\{\eta_{i \rightarrow j}, \eta_{j \rightarrow i}\}_{j \in \partial i}) \prod_{\langle i, j \rangle} \Psi_{ij}(\eta_{i \rightarrow j}, \eta_{j \rightarrow i}) \end{aligned} \quad (237)$$

To simplify the notations we will often omit the arguments of the different functions. There are two interaction terms in the last equation above. The first term is a product over all the sites i of a term Ψ_i that depends on all the messages involving site i . The second term is a product over all the links of a term Ψ_{ij} that depends only on the messages living on that link.

We can therefore interpret Eq. (237) as the partition function of a statistical mechanics model, where the variables are the messages. On each link of the original graph, we have a variable made by the two messages $\{\eta_{i \rightarrow j}, \eta_{j \rightarrow i}\}$ with a local field z_{ij}^{-m} ; on each site of the original graph, we have a *many-body* interaction $z_i^m \prod_{j \in \partial i} \delta[\eta_{i \rightarrow j} - \mathcal{F}_{i \rightarrow j}]$. We can therefore re-interpret the original graph as a factor graph, where on each link there is a variable node, and the original variable nodes act as interaction nodes.

2. RS cavity equations for the auxiliary model: the 1RSB equations

We can write the RS cavity equations for the auxiliary model in a compact way by introducing the message $Q_{i \rightarrow j}(\eta_{i \rightarrow j}, \eta_{j \rightarrow i})$, which is the probability distribution of the two messages sitting on $\langle i, j \rangle$ when the connection between this link and node j is absent.

A quite straightforward calculation, similar to the one of section III C 1, leads to

$$Q_{i \rightarrow j}(\eta_{i \rightarrow j}, \eta_{j \rightarrow i}) = \frac{\Psi_{ij}(\eta_{i \rightarrow j}, \eta_{j \rightarrow i})}{\mathcal{Z}_{i \rightarrow j}} \sum_{\{\eta_{i \rightarrow k}, \eta_{k \rightarrow i}\}_{k \in \partial i \setminus j}} \Psi_i(\{\eta_{i \rightarrow l}, \eta_{l \rightarrow i}\}_{l \in \partial i}) \prod_{k \in \partial i \setminus j} Q_{k \rightarrow i}(\eta_{k \rightarrow i}, \eta_{i \rightarrow k}) \quad (238)$$

²⁴ For continuous messages, it is not completely clear what is the correct integration measure $\mathcal{D}\eta_{i \rightarrow j}$ in Eq. (236). In principle, the delta functions require the introduction of a determinant of the second derivatives since one should write

$$\begin{aligned} Z_m &= \sum_{\alpha} e^{-\beta m F_{\text{Bethe}}[\eta_{i \rightarrow j}^{\alpha}]} = \int d\eta_{i \rightarrow j} e^{-\beta m F_{\text{Bethe}}[\eta_{i \rightarrow j}]} \sum_{\alpha} \prod_{i, j} \delta[\eta_{i \rightarrow j} - \eta_{i \rightarrow j}^{\alpha}] \\ &= \int d\eta_{i \rightarrow j} e^{-\beta m F_{\text{Bethe}}[\eta_{i \rightarrow j}]} \left(\prod_{i, j} \delta[\eta_{i \rightarrow j} - \mathcal{F}_{i \rightarrow j}] \right) \det \left[\frac{\partial(\eta_{i \rightarrow j} - \mathcal{F}_{i \rightarrow j})}{\partial \eta_{k \rightarrow l}} \right] \end{aligned} \quad (235)$$

Here we don't discuss this issue in details and just neglect the determinant. A discussion, based on a discretization of the cavity distributions, can be found in [85, pag.436] (thanks to P.Urbani for pointing out this problem).

Using the explicit expressions of Ψ_i and Ψ_{ij} we obtain

$$\begin{aligned}
Q_{i \rightarrow j}(\eta_{i \rightarrow j}, \eta_{j \rightarrow i}) &= \\
&= \frac{z_{ij}(\eta_{i \rightarrow j}, \eta_{j \rightarrow i})^{-m}}{\mathcal{Z}_{i \rightarrow j}} \sum_{\{\eta_{i \rightarrow k}, \eta_{k \rightarrow i}\}_{k \in \partial i \setminus j}} z_i(\{\eta_{k \rightarrow i}\}_{k \in \partial i})^m \prod_{l \in \partial i} \delta[\eta_{i \rightarrow l} - \mathcal{F}_{i \rightarrow l}] \prod_{k \in \partial i \setminus j} Q_{k \rightarrow i}(\eta_{k \rightarrow i}, \eta_{i \rightarrow k}) \\
&= \frac{z_{ij}(\eta_{i \rightarrow j}, \eta_{j \rightarrow i})^{-m}}{\mathcal{Z}_{i \rightarrow j}} \sum_{\{\eta_{k \rightarrow i}\}_{k \in \partial i \setminus j}} z_i(\{\eta_{k \rightarrow i}\}_{k \in \partial i})^m \delta[\eta_{i \rightarrow j} - \mathcal{F}_{i \rightarrow j}[\{\eta_{k \rightarrow i}\}_{k \in \partial i \setminus j}]] \prod_{k \in \partial i \setminus j} Q_{k \rightarrow i}(\eta_{k \rightarrow i}, \mathcal{F}_{i \rightarrow k}) \\
&= \frac{1}{\mathcal{Z}_{i \rightarrow j}} \sum_{\{\eta_{k \rightarrow i}\}_{k \in \partial i \setminus j}} z_{i \rightarrow j}(\{\eta_{k \rightarrow i}\}_{k \in \partial i \setminus j})^m \delta[\eta_{i \rightarrow j} - \mathcal{F}_{i \rightarrow j}[\{\eta_{k \rightarrow i}\}_{k \in \partial i \setminus j}]] \prod_{k \in \partial i \setminus j} Q_{k \rightarrow i}(\eta_{k \rightarrow i}, \mathcal{F}_{i \rightarrow k})
\end{aligned} \tag{239}$$

where in the second step we used the delta functions to integrate over the $\eta_{k \rightarrow i}$, and in the third step we used the identity $z_i/z_{ij} = z_{i \rightarrow j}$, see Eq. (233). This last simplification makes $\eta_{j \rightarrow i}$ disappear from the last line of the equation above. The only point where $\eta_{j \rightarrow i}$ appears in the right hand side of the above equations is in the argument of $\mathcal{F}_{i \rightarrow k}$ inside the function Q . Therefore, a consistent choice is to assume that $Q_{i \rightarrow j}$ does not depend on $\eta_{j \rightarrow i}$, or in other word Q does not depend on its second argument. Using this assumption, we finally obtain

$$Q_{i \rightarrow j}(\eta_{i \rightarrow j}) = \frac{1}{\mathcal{Z}_{i \rightarrow j}} \sum_{\{\eta_{k \rightarrow i}\}_{k \in \partial i \setminus j}} z_{i \rightarrow j}(\{\eta_{k \rightarrow i}\}_{k \in \partial i \setminus j})^m \delta[\eta_{i \rightarrow j} - \mathcal{F}_{i \rightarrow j}[\{\eta_{k \rightarrow i}\}_{k \in \partial i \setminus j}]] \prod_{k \in \partial i \setminus j} Q_{k \rightarrow i}(\eta_{k \rightarrow i}). \tag{240}$$

Note that $Q_{i \rightarrow j}$ is the probability distribution of $\eta_{i \rightarrow j}$ over the states, with weight $e^{-\beta m F_\alpha}$, or in formula:

$$Q_{i \rightarrow j}(\eta_{i \rightarrow j}) = \sum_{\alpha} e^{-\beta m F_{\text{Bethe}}[\eta_{i \rightarrow j}^\alpha]} \delta[\eta_{i \rightarrow j} - \eta_{i \rightarrow j}^\alpha]. \tag{241}$$

Following the same steps as in section III C 1 (the details are slightly different because of the different graph structure of the auxiliary partition function), we find that the “replicated” free energy is

$$\begin{aligned}
-\beta N \Phi(m, T) &= \log Z_m = \sum_i \log \mathcal{Z}_i - \sum_{ij} \log \mathcal{Z}_{ij}, \\
\mathcal{Z}_i &= \sum_{\{\eta_{k \rightarrow i}\}_{k \in \partial i}} z_i(\{\eta_{k \rightarrow i}\}_{k \in \partial i})^m \prod_{k \in \partial i} Q_{k \rightarrow i}(\eta_{k \rightarrow i}) = \langle z_i^m \rangle_\alpha, \\
\mathcal{Z}_{ij} &= \sum_{\eta_{i \rightarrow j}, \eta_{j \rightarrow i}} z_{ij}(\eta_{i \rightarrow j}, \eta_{j \rightarrow i})^m Q_{i \rightarrow j}(\eta_{i \rightarrow j}) Q_{j \rightarrow i}(\eta_{j \rightarrow i}) = \langle z_{ij}^m \rangle_\alpha,
\end{aligned} \tag{242}$$

Eq. (240) and Eq. (242) constitute the set of 1RSB cavity equations for a given graph and choice of the couplings. The reader has probably already guessed that 2RSB equations could in principle be obtained by performing a 1RSB calculation on the auxiliary model, and so on. Unfortunately the complexity of the calculation is already prohibitive at 2RSB so we will not explore further this possibility.

3. Homogeneous 1RSB equations

As we did in the RS case, we can now consider a system where there are no spatial fluctuations: the graph is regular and the coupling are all equal (an important example is the coloring of random regular graphs, that as we already said corresponds to the Potts antiferromagnetic model).

In that case, it is natural to assume that the distribution $Q_{i \rightarrow j}$ does not depend on the particular site. Even if in a given glass state α the local fields are different, once we take the average over the states, all the sites must be statistically equivalent in the thermodynamic limit. Then we have $Q_{i \rightarrow j}(\eta_{i \rightarrow j}) \rightarrow Q_{\text{cav}}(\eta_{\text{cav}})$ for $N \rightarrow \infty$, and Eq. (240) becomes:

$$\begin{aligned}
Q_{\text{cav}}[\eta_{\text{cav}}] &= \frac{1}{\mathcal{Z}_{\text{cav}}} \int dQ[\eta_{\text{cav}}^1] \cdots dQ[\eta_{\text{cav}}^{c-1}] \delta[\eta_{\text{cav}} - \mathcal{F}[\eta_{\text{cav}}^1, \dots, \eta_{\text{cav}}^{c-1}]] \{z_{\text{cav}}[\eta_{\text{cav}}^1, \dots, \eta_{\text{cav}}^{c-1}]\}^m \\
&= \mathbb{E}\{Q[\eta_{\text{cav}}^1] \cdots Q[\eta_{\text{cav}}^{c-1}]\},
\end{aligned} \tag{243}$$

where the function \mathcal{F} is defined in (212).

Now we can compute the free energy. This is done by noting that in Eq. (242) all the terms are equal if $Q_{i \rightarrow j} \rightarrow Q$. We get

$$\begin{aligned} \mathcal{Z}^{(l)} &= \int dQ[\eta_{\text{cav}}^1] dQ[\eta_{\text{cav}}^2] \{z^{(l)}[\eta_{\text{cav}}^1, \eta_{\text{cav}}^2]\}^m, \\ z^{(l)} &= \sum_{\sigma_1 \sigma_2} \eta_{\text{cav}}^1(\sigma_1) \eta_{\text{cav}}^2(\sigma_2) \psi(\sigma_1, \sigma_2). \end{aligned} \quad (244)$$

and similarly

$$\mathcal{Z}^{(s)} = \int dQ[\eta_{\text{cav}}^1] \cdots dQ[\eta_{\text{cav}}^c] \{z^{(s)}[\eta_{\text{cav}}^1, \dots, \eta_{\text{cav}}^c]\}^m, \quad (245)$$

with $z^{(s)}$ given in (197). The free energy $\Phi(m, T) = -\frac{T}{N} \log Z_m$ is given by

$$\Phi(m, T) = -T \left[\log \mathcal{Z}^{(s)} - \frac{c}{2} \log \mathcal{Z}^{(l)} \right]. \quad (246)$$

The equation above is still variational; differentiating it with respect to $Q[\eta_{\text{cav}}]$ leads to the self-consistency equation (243).

A final remark is in order to conclude this discussion. Eq. (243) is dangerously reminiscent of equation (213), that corresponds to the RS case in presence of local fluctuations (indeed, the two equations are formally equivalent at $m = 0$). These two equations should not be confused. There is a deep physical difference between the two distributions $Q[\eta]$ and $\mathcal{P}[\eta]$: the former describes the fluctuations over the many states for a given sample, while the latter describes the fluctuations over the samples of a single pure state. For this reason, in (213) the weight z_{cav}^m is absent. The physical difference between these equations is better seen if we compare the free energy (215) with the one we derived here, Eq. (246). In the former case, the average over $\mathcal{P}[\eta]$ represents an average over the disorder and is taken *outside* the logarithm. In the latter case, the average over $Q[\eta]$ is over states for a given sample, and therefore it is taken *inside* the logarithm.

4. Complications: spatial fluctuations, factor graphs

Now it should be clear how to introduce spatial fluctuations. Instead of considering a single $Q[\eta_{\text{cav}}]$, we must introduce a distribution *over the sites*, $\mathcal{P}[Q[\eta_{\text{cav}}]]$, defined as the probability that a cavity variable has distribution of cavity fields $Q[\eta_{\text{cav}}]$ *over the states*. The equation (243) now depends on the disorder, i.e. \mathbb{F}_J depends on the coupling and the number c might fluctuate. Similarly to (213) we get

$$\mathcal{P}[Q] = \overline{\int d\mathcal{P}[Q^1] \cdots d\mathcal{P}[Q^{c-1}] \delta[Q - \mathbb{F}_J[Q^1, \dots, Q^{c-1}]]}^{\{c, J\}}. \quad (247)$$

The free energy has now to be computed according to (246) taking an external average over c, J, \mathcal{P} .

In the case of a factor graph all these considerations are easily generalized along the lines of section III C 7. We must introduce a $Q_{\text{cav}}[\eta_{\text{cav}}]$ and a $Q_{\text{test}}[\eta_{\text{test}}]$, with recursions

$$\begin{aligned} Q_{\text{cav}}[\eta_{\text{cav}}] &= \frac{1}{\mathcal{Z}_{\text{cav}}} \int dQ_{\text{test}}[\eta_{\text{test}}^1] \cdots dQ_{\text{test}}[\eta_{\text{test}}^{c-1}] \delta[\eta_{\text{cav}} - \mathcal{F}_{\text{cav}}[\eta_{\text{test}}^1, \dots, \eta_{\text{test}}^{c-1}]] \{z_{\text{cav}}[\eta_{\text{test}}^1, \dots, \eta_{\text{test}}^{c-1}]\}^m \\ &= \mathbb{F}_{\text{cav}}\{Q_{\text{test}}[\eta_{\text{test}}^1] \cdots Q_{\text{test}}[\eta_{\text{test}}^{c-1}]\}, \\ Q_{\text{test}}[\eta_{\text{test}}] &= \frac{1}{\mathcal{Z}_{\text{test}}} \int dQ_{\text{cav}}[\eta_{\text{cav}}^1] \cdots dQ_{\text{cav}}[\eta_{\text{cav}}^{k-1}] \delta[\eta_{\text{test}} - \mathcal{F}_{\text{test}}[\eta_{\text{cav}}^1, \dots, \eta_{\text{cav}}^{k-1}]] \{z_{\text{test}}[\eta_{\text{cav}}^1, \dots, \eta_{\text{cav}}^{k-1}]\}^m \\ &= \mathbb{F}_{\text{test}}\{Q_{\text{cav}}[\eta_{\text{cav}}^1] \cdots Q_{\text{cav}}[\eta_{\text{cav}}^{k-1}]\}. \end{aligned} \quad (248)$$

The free energy $\Phi(m, T)$ is computed as in (224) by replacing $z \rightarrow \mathcal{Z}$ as in the $k = 2$ case:

$$\Phi(m, T) = \Delta F^{(s)} + \frac{c}{k} \Delta F^{(c)} - c \Delta F^{(l)} = -T \left[\log \mathcal{Z}^{(s)} + \frac{c}{k} \log \mathcal{Z}^{(c)} - c \log \mathcal{Z}^{(l)} \right]. \quad (249)$$

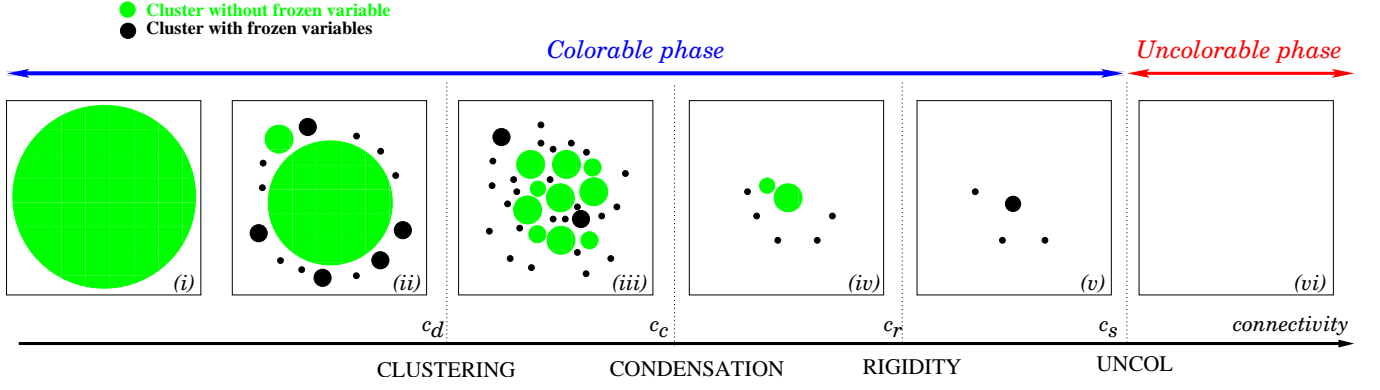


FIG. 16: (From [68]; replace c_c by c_K in the figure) Sketch of the space of solutions —colored points in this representation— in the q -coloring problem on random graphs when the connectivity c is increased. (i) At low c , all solutions belong to a single cluster. (ii) For larger c , other clusters of solutions appear but a giant cluster still contains almost all solutions. (iii) At the clustering transition c_d , it splits into an exponentially large number of clusters. (iv) At the condensation transition c_K , most colorings are found in the few largest of them. (v) The rigidity transition c_r ($c_r < c_K$ and $c_r > c_K$ are both possible depending on q) arises when typical solutions belong to clusters with frozen variables (that are allowed only one color in the cluster). (vi) No proper coloring exists beyond the COL/UNCOL threshold c_s .

In presence of external disorder one introduces distributions $\mathcal{P}_{\text{cav}}[Q[\eta_{\text{cav}}]]$, $\mathcal{P}_{\text{test}}[Q[\eta_{\text{test}}]]$, of these fields and equations like (247),

$$\begin{aligned} \mathcal{P}_{\text{cav}}[Q_{\text{cav}}] &= \int d\mathcal{P}_{\text{test}}[Q_{\text{test}}^1] \cdots d\mathcal{P}_{\text{test}}[Q_{\text{test}}^{c-1}] \delta[Q_{\text{cav}} - \mathbb{F}_{J,\text{cav}}[Q_{\text{test}}^1, \dots, Q_{\text{test}}^{c-1}]]^{\{J,c\}}, \\ \mathcal{P}_{\text{test}}[Q_{\text{test}}] &= \int d\mathcal{P}_{\text{cav}}[Q_{\text{cav}}^1] \cdots d\mathcal{P}_{\text{cav}}[Q_{\text{cav}}^{k-1}] \delta[Q_{\text{test}} - \mathbb{F}_{J,\text{test}}[Q_{\text{cav}}^1, \dots, Q_{\text{cav}}^{k-1}]]^{\{J\}}, \end{aligned} \quad (250)$$

and the free energy (249) has to be averaged over J , c , and \mathcal{P} .

The explicit solution of the 1RSB cavity equations is possible for the case of k -XORSAT (\Rightarrow **Ex.III.9**). This is a very useful exercise that will allow to familiarize with 1RSB cavity equations, and to check that we can obtain in this way the same result that we already obtained by mean of the leaf removal algorithm and the replica method (\Rightarrow **Ex.III.1**).

E. Phase transitions in q -COL

We wish to conclude the discussion of the cavity method by presenting the spectacular results that have been obtained for the q -coloring of random graphs. These results are particularly interesting because, at variance with XORSAT, q -COL has a nontrivial $\Sigma(s)$ which seems to be common also to other optimization problems [68, 71, 84]. In this case the 1RSB equations have to be solved numerically. As we already discussed, q -COL corresponds to an antiferromagnetic Potts model. There is no disorder in the coupling and one has only two-body interactions, hence there is no need to introduce a factor graph representation. For regular random graphs, there is no local disorder at all. At the 1RSB level, one can use therefore Eq. (243) and (246) to compute the free energy. For Erdős-Rényi graphs, there is local disorder due to the fluctuations of the connectivity and one needs to solve Eq. (247). There are several tricks that help the numerical resolution of these complicated equations. We do not discuss here the details and we refer to the original paper [68], from which the following discussion is reprinted.

Consider that we have $q \geq 4$ colors (the $q = 3$ case being a bit particular [68, 71], as we shall see) and a large Erdős-Rényi random graph whose average connectivity c we shall increase continuously. Different phases are encountered that we will now describe (and enumerate) in order of appearance (the corresponding phase diagram is depicted in figure 16).

- (i) **A unique cluster exists:** For low enough connectivities, all the proper colorings are found in a single cluster, where it is easy to “move” from one solution to another. The 1RSB equation reduce to the RS ones and the

cavity fields are uniform. The entropy can be computed and reads in the large graph size N limit

$$s_{tot} = \frac{\log \mathcal{N}}{N} = \log q + \frac{c}{2} \log \left(1 - \frac{1}{q}\right). \quad (251)$$

This corresponds to the region $T > T_{TAP}$ in figure 2.

- (ii) **Some (irrelevant) clusters appear:** As the connectivity is slightly increased, a 1RSB solution appears and the phase space of solutions decomposes into a large (exponential) number of different clusters. It is tempting to identify that as the clustering transition, but it happens that all (but one) of these clusters contain relatively very few solutions—as compare to the whole set—and that almost all proper colorings still belong to one single giant cluster. Clearly, this is not a proper clustering phenomenon and in fact, for all practical purpose, there is still only one single cluster. Equation (251) still gives the correct entropy at this stage. This corresponds to $T_{TAP} > T > T_d$ in figure 2.
- (iii) **The clustered phase:** For larger connectivities, the large single cluster also decomposes into an exponential number of smaller ones: this now defines the genuine clustering threshold c_d . Beyond this threshold, a local algorithm that tries to move in the space of solutions will remain trapped in a cluster of solutions [77]. Interestingly, as in the case of the fully connected p -spin model and of k -XORSAT, it can be shown that the total number of solutions is still given by equation (251) in this phase. This is because, as we already discussed for the p -spin, the free energy has no singularity at the dynamical transition (which is therefore not a true transition, but rather a dynamical or geometrical transition in the space of solutions). This region corresponds to $T_K < T < T_d$ in figure 2.
- (iv) **The condensed phase:** As the connectivity is further increased, a new sharp phase transition arises at the condensation threshold c_K where most of the solutions are found in a finite number of clusters (the largest). From this point, equation (251) is not valid anymore and becomes just an upper bound. The entropy is non-analytic at c_K , therefore this is a genuine static phase transition. This correspond to $T < T_K$ in figure 2.
- (v) **The rigid phase:** Recall that in XORSAT there was a finite fraction of frozen variables (the backbone) in each cluster. Here the situation is different and two different types of clusters exist: in the first type, that we shall call the *unfrozen* ones, all spins can take at least two different colors. In the second type, however, a finite fraction of spins are allowed only one color within the cluster and are thus “frozen” into this color. It follows that a transition exists, that we call *rigidity*, when frozen variables appear inside the dominant clusters (those that contain most colorings). If one takes a proper coloring at random beyond c_r , it will belong to a cluster where a finite fraction of variables is frozen into the same color. Depending on the value of q , this transition may arise before or after the condensation transition.
- (vi) **The UNCOL phase:** Eventually, the connectivity c_s is reached beyond which no more solutions exist. The ground state energy (as sketched in figure 7) is zero for $c < c_s$ and then grows continuously for $c > c_s$. The values c_s computed within the cavity formalism are in perfect agreement with the rigorous bounds derived using probabilistic methods and are widely believed to be exact (although this remains to be rigorously proven).

Precise values of all threshold connectivities corresponding to all these transitions are reported in [68] for the regular and the Poissonian (*i.e.* Erdős-Rényi) random graphs ensembles. The peculiarity of 3-coloring is that $c_d = c_K$ so that the clustered phase is always condensed in this case.

F. Exercises

1. **XORSAT with replicas:** The aim of this (long) exercise is to re-obtain the results on the clustering in XORSAT discussed in section IIIB by means of the replica method discussed in section IIB3. Consider k -XORSAT on an Erdős-Rényi graph of mean connectivity $c = \alpha k$. Recall that this means just that the variables entering in each equation are taken independently at random. It is convenient here to use boolean variables, $X = (x_1, \dots, x_N)$, and the form of the constraints is $x_{i_1} + \dots + x_{i_k} = b_i$, with b_i a random boolean variable. In the following we discuss the problem for general k but one might first try to do the exercise for $k = 3$ for simplicity.

In the replica method (section IIB3) we wish to compute the entropy of m coupled replicas $\mathcal{S}(m)$. The partition function of one replica is $Z = \mathcal{N} = \sum_X \mathbb{I}(X)$, *i.e.* the number of solutions. Based on the discussion of

sections II B 4 and II B 5, we have:

$$\mathcal{S}(m) = \frac{1}{N} \overline{\log \mathcal{N}_m} = \frac{1}{N} \lim_{n \rightarrow 0} \partial_n \overline{(\mathcal{N}_m)^n} = \frac{1}{N} \lim_{n \rightarrow 0} \partial_n \overline{\mathcal{N}^{mn}}, \quad (252)$$

where the $\nu = mn$ replicas are divided in blocks of m coupled replicas. Then we want to compute all the moments of \mathcal{N} . Note that the computation of the first two moments has already been discussed in section III B.

- Following the same route than for the second moment, show that

$$\overline{\mathcal{N}^\nu} = \sum_{X^1, \dots, X^\nu} \overline{\prod_{a=1}^M \mathbb{I}(X^a)} = \sum_{X^1, \dots, X^\nu} [p(X^1, \dots, X^\nu)]^M, \quad (253)$$

where $p(X^1, \dots, X^\nu)$ is the probability that all configurations X^a are solutions of a randomly drawn equation.

- Denote $\vec{X} = (X^1, \dots, X^\nu)$ and $\vec{x} = (x^1, \dots, x^\nu)$; denote by $\vec{0}$ and $\vec{1}$ the vectors of all 0 and 1 respectively. Define $\vec{x} + \vec{y} = (x^1 + y^1, \dots, x^\nu + y^\nu)$. Show that, for large N ,

$$p(\vec{X}) \sim \frac{1}{N^k} \sum_{i_1, \dots, i_k}^{1, N} \mathcal{E}(\vec{x}_{i_1}, \dots, \vec{x}_{i_k}), \quad (254)$$

$$\mathcal{E}(\vec{x}_1, \dots, \vec{x}_k) = \frac{1}{2} \left[\delta(\vec{x}_1 + \dots + \vec{x}_k = \vec{0}) + \delta(\vec{x}_1 + \dots + \vec{x}_k = \vec{1}) \right].$$

Introduce the function

$$\rho(\vec{x} | \vec{X}) = \frac{1}{N} \sum_{i=1}^N \delta(\vec{x} = \vec{x}_i), \quad (255)$$

note that it is normalized to 1 when summed over \vec{x} , and show that

$$p(\vec{X}) = \sum_{\vec{x}_1, \dots, \vec{x}_k} \rho(\vec{x}_1 | \vec{X}) \cdots \rho(\vec{x}_k | \vec{X}) \mathcal{E}(\vec{x}_1, \dots, \vec{x}_k). \quad (256)$$

- Using the previous results, denote by $r(\vec{x})$ a generic normalized function, and show that

$$\overline{\mathcal{N}^\nu} = \int D\vec{x} \mathcal{M}[r(\vec{x})] \left[\sum_{\vec{x}_1, \dots, \vec{x}_k} r(\vec{x}_1) \cdots r(\vec{x}_k) \mathcal{E}(\vec{x}_1, \dots, \vec{x}_k) \right]^M, \quad (257)$$

where $\mathcal{M}[r(\vec{x})]$ is the number of replicated configurations \vec{X} giving rise to the same $\rho(\vec{x} | \vec{X}) = r(\vec{x})$. Show that the latter is given by the multinomial factor

$$\mathcal{M}[r(\vec{x})] = \frac{N!}{\prod_{\vec{x}} (Nr(\vec{x})!)} . \quad (258)$$

- Take the large N limit with $M = \alpha N$ and deduce that

$$\overline{\mathcal{N}^\nu} = \exp \left\{ N \max_{r(\vec{x})} \left[- \sum_{\vec{x}} r(\vec{x}) \log r(\vec{x}) + \alpha \log \sum_{\vec{x}_1, \dots, \vec{x}_k} r(\vec{x}_1) \cdots r(\vec{x}_k) \mathcal{E}(\vec{x}_1, \dots, \vec{x}_k) \right] \right\} \quad (259)$$

- Make the following ansatz for $r(\vec{x})$:

$$r(\vec{x}) = \frac{1-b}{2^\nu} + b \prod_{k=1}^n \left[\frac{1}{2} \left(\delta(\vec{x}_k = \vec{0}) + \delta(\vec{x}_k = \vec{1}) \right) \right], \quad (260)$$

where $\vec{x}_k = (x_{1+m(k-1)}, \dots, x_{mk})$ is the vector of the replicas in the k -th block. Compute the overlap between two replicas; using spin notations, $S = (-1)^x$,

$$Q_{ab} = \langle (-1)^{x_a} (-1)^{x_b} \rangle = \sum_{\vec{x}} r(\vec{x}) (-1)^{x_a} (-1)^{x_b} . \quad (261)$$

Show that it is equal to b if the two replicas are in the same block, and zero otherwise. Based on the results of section III B, give a justification of this ansatz and interpret b as the fraction of variables in the backbone.

- Substitute this ansatz in (259); show that $\overline{\mathcal{N}^{mn}} = \exp\{N \max_b S(m, n; b)\}$ with

$$S(m, n; b) = -2^n \left(\frac{b}{2^n} + \frac{1-b}{2^{mn}} \right) \log \left(\frac{b}{2^n} + \frac{1-b}{2^{mn}} \right) - (2^{mn} - 2^n) \frac{1-b}{2^{mn}} \log \left(\frac{1-b}{2^{mn}} \right) \\ + \alpha \log \left(\frac{1}{2^{mn}} (1 - b^k) + \frac{1}{2^n} b^k \right) \quad (262)$$

and deduce that (for the interesting case $m < 1$):

$$\mathcal{S}(m) = \min_b \lim_{n \rightarrow 0} \partial_n S(m, n; b) \\ = \log(2) \min_b \{ b + m(1-b) + b^k(m-1)\alpha - m\alpha - (m-1)(1-b) \log(1-b) \} . \quad (263)$$

- Write the equation for b and check that it does not depend on m . Using Eq. (139), deduce the expressions of $s(m)$ and $\Sigma(m)$. Note that $\mathcal{S}(m)$ is linear in m , therefore for each value of α , $s(m)$ and $\Sigma(m)$ do not depend on m . Show that this gives back Eq.(176) and (172).
2. **The Bethe equations and the transfer matrix method:** Adapt the reasoning of section III C 1 to the case of a one dimensional chain with open boundaries, and show that it is equivalent to the transfer matrix method.
 3. **The Ising ferromagnet:** Consider the Ising model on the fixed connectivity random lattice. The cavity probability can be parametrized as $\eta_{\text{cav}}(S) = \frac{1+m_c S}{2}$. Show that the recurrence equation (204) in terms of the magnetization m_c becomes

$$m_c = \tanh[(c-1) \operatorname{atanh}[m_c \tanh(\beta J)]] . \quad (264)$$

Show that there is a phase transition from a paramagnetic to a ferromagnetic phase; compute the critical temperature T_c . Express the real magnetization m that enters in $P(S) = \frac{1+mS}{2}$ in terms of m_c ; compute the critical exponent β associated to $m \sim |T - T_c|^\beta$.

Now, in order to mimic a finite-dimensional system of dimension d , choose $c = 2d$ and $J = 1/(2d)$. Show that for $d \rightarrow \infty$ one recovers the mean field equation of the fully-connected model and that $T_c = 1$ in this limit. Compute numerically T_c from the cavity method as a function of d . Find in the literature data for the exact T_c in dimension $d = 2, 3, 4, 5, 6, 7, 8$ (at least) and compare it with the cavity method result and from the fully-connected result.

4. **A cavity derivation of the reaction term:** Consider the SK model with N spins and think about it as a spin glass model on the fully connected graph.

- Show, using the same parametrization of Exercise 3, that the cavity equations can be written as

$$m_c^{i \rightarrow j} = \tanh \left[\sum_{k \neq \{i, j\}} \operatorname{atanh}[m_c^{k \rightarrow i} \tanh(\beta J_{ik})] \right] , \\ m_i = \tanh \left[\sum_{k \neq i} \operatorname{atanh}[m_c^{k \rightarrow i} \tanh(\beta J_{ik})] \right] , \quad (265)$$

where $m_c^{i \rightarrow j}$ are the cavity magnetizations and m_i are the true magnetizations.

- Recall that in the SK model $J_{ij} \sim N^{-1/2}$ and therefore the couplings are small. Using this, show that at the leading order

$$m_c^{i \rightarrow j} - m_i \sim -m_j \beta J_{ij} (1 - m_i^2) . \quad (266)$$

- Plug this result in the second Eq. (265) and show that

$$m_i = \tanh \left[\sum_{k \neq i} \beta J_{ik} m_k - m_i \sum_{k \neq i} (\beta J_{ik})^2 (1 - m_k^2) \right] . \quad (267)$$

Show that this is exactly the same result obtained in Eq. (42) through the high temperature expansion.

Discuss why this derivation justifies the name “reaction term” that is used for the correction term.

5. **RS solution of q -COL:** Consider the q -coloring of fixed connectivity random graphs at zero temperature.
 - Assume that the replica symmetric solution is uniform over all possible colors, $\eta_{\text{cav}}(\sigma) = 1/q$; show that this is indeed a solution. Compute the entropy $s(c, q) = \log q + c/2 \log((q-1)/q)$; note that it vanishes for a given value of $c \sim q \log q$ for large q .
 - Consider solving the cavity equation by iteration, at each step using the right hand side to compute a new estimate to the solution until convergence. Study the stability of the uniform solution under this process. In other words, consider a small perturbation of the uniform solution, $\eta_{\text{cav}}(\sigma) = 1/q + \delta\eta_{\text{cav}}(\sigma)$, $\sum_{\sigma} \delta\eta_{\text{cav}}(\sigma) = 0$. Linearize the cavity equation to obtain a linear equation for $\delta\eta_{\text{cav}}(\sigma)$. Show that the perturbation decays exponentially under iteration for $c < q$ while it grows exponentially for $c > q$. Then the uniform solution is unstable for $c \geq q$. See [76] for an interpretation of this instability.
6. **A consistency check:** Show that for $k = 2$ the factor graph cavity equations reduce to (204) and the free energy reduces to (198).
7. **XORSAT:** Consider the 3-XORSAT problem with fixed or fluctuating connectivity, at zero temperature in the SAT phase (“entropic” cavity method). Show that the uniform solution $\eta_{\text{cav}}(S) = \eta_{\text{test}}(S) = 1/2$ is indeed a solution of the iteration equations on a factor graph. Deduce that the zero-temperature entropy is $s = (1-\alpha) \log 2$ as found using the leaf removal algorithm.
8. **Variational principle:** Show that differentiation of (198) with respect to $\eta_{\text{cav}}(\sigma)$ gives back (204). Keep in mind that $\eta_{\text{cav}}(\sigma)$ must be normalized! Repeat the calculation also in the factor graph case.
9. **Explicit solution of 1RSB equations for XORSAT:** Consider k -XORSAT on an Erdős-Rényi graph of mean connectivity $c = \alpha k$. Variables are represented by Ising spins and the form of the constraint is $\psi_a(S_1, \dots, S_k) = \delta(J_a S_1 \cdots S_k = 1)$, where $J_a = \pm 1$ with uniform probability.

Solve the iteration equation as follows:

- For a given graph, variables may be in the backbone or not. According to the analysis of section III B, this depends only on the topological structure of the graph. Then the cavity fields η (for both cavity spins and cavity tests) can be of three different types: $\eta(S) = 1/2$, if the variable is not in the backbone; $\eta(S) = \delta_{S,1}$ or $\eta(S) = \delta_{S,-1}$ if the variable is in the backbone.
- If the variable is not in the backbone, then for all states α it is free; the distribution

$$Q[\eta(S)] = \delta[\eta(S) = 1/2] \equiv \Delta_{1/2} . \quad (268)$$

If the variable is in the backbone, then it is frozen to ± 1 with uniform probability,

$$Q[\eta(S)] = \frac{1}{2} \delta[\eta(S) = \delta_{S,1}] + \frac{1}{2} \delta[\eta(S) = \delta_{S,-1}] \equiv \Delta_{\pm 1} . \quad (269)$$

Show that the latter statement is a consequence of the symmetries of the problem.

- Assume that the 1RSB distribution over the sites of $Q[\eta_{\text{cav}}]$ has the form

$$\mathcal{P}[Q[\eta_{\text{cav}}]] = b \delta[Q[\eta_{\text{cav}}] = \Delta_{\pm 1}] + (1-b) \delta[Q[\eta_{\text{cav}}] = \Delta_{1/2}] , \quad (270)$$

where b is the probability (over the sites) that a variable is in the backbone.

- Plug the equation above into the second Eq.(250); show that

$$\mathcal{P}[Q[\eta_{\text{test}}]] = b^{k-1}\delta[Q[\eta_{\text{test}}] = \Delta_{\pm 1}] + (1 - b^{k-1})\delta[Q[\eta_{\text{test}}] = \Delta_{1/2}] , \quad (271)$$

- Now plug the latter expression in the first Eq.(250); show that for a given c one has

$$\mathcal{P}[Q[\eta_{\text{cav}}]] = (1 - (1 - b^{k-1})^{c-1})\delta[Q[\eta_{\text{cav}}] = \Delta_{\pm 1}] + (1 - b^{k-1})^{c-1}\delta[Q[\eta_{\text{cav}}] = \Delta_{1/2}] . \quad (272)$$

Show that the average over $\ell = c - 1 \geq 0$ must be taken using a Poissonian of average αk ; for this follow the reasoning before Eq. (214). Take the average over c and show that one gets back

$$\mathcal{P}[Q[\eta_{\text{cav}}]] = (1 - f(b))\delta[Q[\eta_{\text{cav}}] = \Delta_{\pm 1}] + f(b)\delta[Q[\eta_{\text{cav}}] = \Delta_{1/2}] , \quad (273)$$

with $f(b) = e^{-\alpha k b^{k-1}}$. Then b must satisfy the equation

$$1 - b = f(b) = e^{-\alpha k b^{k-1}} , \quad (274)$$

that gives back Eq. (162) obtained with the leaf removal. Show that for $\alpha \leq \alpha_d$ only the solution $b = 0$ exist, and show that it gives back the RS solution. For $\alpha > \alpha_d$, there is a solution $b^* \neq 0$. Note that b^* does not depend on m .

Compute the free entropy (139) from Eq.(249) (just drop the $-T$ to get the free entropy, and take the average of the different terms over J, c, \mathcal{P} . The result is

$$\begin{aligned} \mathcal{S}^{(l)} &= \log \mathcal{Z}^{(l)} = -(\log 2)[b^k + m(1 - b^k)] , \\ \mathcal{S}^{(c)} &= \log \mathcal{Z}^{(c)} = -(\log 2)[b^k + m(1 - b^k)] , \\ \mathcal{S}^{(s)} &= \log \mathcal{Z}^{(s)} = -(\log 2)[m(\alpha k - 1 + b - \alpha k b^{k-1}) + \alpha k b^{k-1} - b] . \end{aligned} \quad (275)$$

Then $\mathcal{S}(m) = -\lim_{T \rightarrow 0} \beta \Phi(m, T)$ is linear in m and one gets a single value of Σ and s for all m . This gives back Eq.(176) and (172).

IV. CONCLUSIONS AND PERSPECTIVES

The main message of these notes was that *mean field spin glasses are characterized by the existence of many pure states*, among which some are stable equilibrium states and others are metastable. We discussed different models (spherical p -spin, SK model, optimization problems such as XORSAT and q -COL) that share this feature, and some methods (the replica and cavity method, and in the case of XORSAT the rigorous leaf-removal method) to compute the complexity and other properties of these states.

This particular property of spin glasses (that is *not* shared by all disordered systems) raises many intriguing questions. For instance, what is the influence of the presence of these states on the dynamics? This question is also relevant for the analysis of search algorithms in optimization, that can be regarded as (non-equilibrium) dynamics for the corresponding physical system.

And what about non mean-field models? Are so many states present also in finite dimensional models? And how can they be described?

These questions did not receive a complete and satisfactory answer at present and are active research topics. Still, many important advances have been made. Here it follows a list of references that may be consulted to go deeper into these fascinating problems. The list is very incomplete and strongly biased towards mean-field inspired work; it is intended only to stimulate the curiosity, and the reader is strongly encouraged to look for further references. The articles cited below have also been chosen because they are useful sources of more references on the same subject.

1. The *equilibrium* dynamics of the spherical p -spin model can be completely solved in the paramagnetic phase, and it can be shown that a *dynamical transition* takes place at the temperature T_d where states first appear. The transition is characterized by the divergence of the relaxation time. These results are reviewed in [12, 13, 46]. The same can be proven for the equilibrium dynamics of XORSAT, see [77, 86].
2. In optimization problems one wants to find the ground state of the system. The simplest way to do that is to consider a dynamics satisfying detailed balance at temperature T_i , and then reduce the temperature down to $T = 0$ (or a low temperature $T = T_f$) at a given rate γ (*classical annealing*). In the limit $\gamma \rightarrow \infty$ one just instantaneously *quenches* the system from T_i to T_f . For the spherical p -spin one can show that if $T_f < T_d$, the system falls out of equilibrium and starts to *age*; its energy decreases but approaches the energy of the threshold states. Therefore classical annealing cannot find the ground state for this system, as it is always trapped by higher energy metastable states. The *aging* dynamics of this and many other models is reviewed in [12]; for the specific case of the SK model see [87]. In some cases it is not at all obvious to understand which states dominate the aging dynamics, see [88] and in particular [89] for a very detailed discussion of this point using the cavity method.
3. More generally, one can consider dynamics that do not satisfy detailed balance. In the case of optimization problems, many algorithms designed to search for solutions falls in this class. These algorithms are known to undergo *algorithmic transitions*: the probability (over formulas and randomness built in the algorithm) to find a solution decreases abruptly from 1 to 0 ($N \rightarrow \infty$) when the density of constraints is increased over a value α_a . Is α_a related to some property of the equilibrium states (their existence, the presence of frozen variables, \dots)? This is mainly an open problem. See [90] for a review of algorithms that have been studied with methods borrowed from physics, and [91] for an original perspective on the general connection between (free)energy landscapes and algorithms.
4. The 1RSB spin glass transition has been conjectured to describe the glass transition in finite-dimensional particle systems. This is based on the following observations:
 - The equations that describe the equilibrium dynamics of the spherical p -spin closely resemble the *Mode-Coupling equations* that describe liquids close to the glass transition. See e.g. [12].
 - The existence of an exponential number of states between T_d and T_K at the mean field level is impossible in finite-dimensional systems. Therefore one has to re-discuss the definition of these states. This leads to very important ideas, such as *entropic-driven nucleation*, that might explain the dynamics of liquids at temperatures below the Mode-Coupling regime. A pedagogical discussion of the definition of states in finite dimension can be found in [7] and [92], as well as in Appendix A of [93]. A very successful theory of glasses based on the adaptation of the mean-field scenario has been developed by Wolynes and goes under the name of *Random First Order Theory*; a review is [94], see also [18, 19]. Quantitative replica calculations of the thermodynamics are reviewed in [93, 95].
 - A detailed investigation of the dynamics of liquids close to the glass transition revealed the existence of *dynamical heterogeneities*, namely of regions of the sample that are more mobile than others. This defines

a *dynamical correlation length*, related to the typical size of the heterogeneities, that seems to diverge at the glass transition. Different theories account for heterogeneity; in particular mean-field like equations predict the existence of such a correlation length and its divergence at T_d [96–98].

- The aging dynamics of glasses is very similar to the mean-field one [12, 13].
- This mean-field-like scenario has been derived also for Kac versions of 1RSB spin glasses in finite dimension; see in particular [99–101].

It is important to keep in mind that, as the transition is first-order in mean-field, its understanding in finite dimension is mostly related to nucleation phenomena.

5. On the contrary, the fRSB transition of the SK model is a true second-order critical point. A natural question is whether finite-dimensional spin glass models on cubic lattices with nearest-neighbor two body interactions, like the Edward-Anderson model, also undergo a fRSB spin glass transition. This is very much debated; a classical alternative picture is presented in [102]. Recent reviews of the status of the mean-field approach are in [6, 103, 104]. In this case one would like to apply to the problem the whole machinery of standard second order phase transition, like scaling, renormalization group, computation of upper/lower critical dimensions, etc. Unfortunately, this is very difficult, see e.g. [50], and for the moment most of the results come from numerical simulations.
6. It is very important to understand how glassy systems respond to external drives. For instance, one can shear a liquid close to the glass transition, or consider a granular driven by an external tapping, etc. This situations are often met in experiments and in many practical applications. A seminal paper in this respect is [105], where it was shown that the structure of states of the spherical p -spin model gives rise to a complex behavior of the system when subject to an external drive. This led to the prediction of a “complex rheology” in liquids close to the glass transition and colloidal systems [106] that is able to explain most of the phenomenology of these materials subject to external drives.
7. Finally, the role of quantum fluctuations for the glass transition has to be elucidated. Is it possible to have many pure states in a quantum system? Quantum versions of the spherical p -spin model have been solved in [107] using the replica method, and quantum TAP equations have been discussed in [108]. It was shown that the spin glass transition becomes first order at low temperature (and down to $T = 0$) as a function of the quantum fluctuations parameter (e.g. a transverse field). However, much less is known for non-mean field models; already on random graphs, the development of a quantum version of the cavity method is a very recent achievement [109, 110].

-
- [1] S. Edwards and P. Anderson, *Phys. F: Metal Phys* **5**, 965 (1975).
 - [2] S. Edwards and P. Anderson, *Journal of Physics F: Metal Physics* **6**, 1927 (1976).
 - [3] G. Parisi, in *Complex Systems*, edited by J.-P. Bouchaud, M. Mézard, and J. Dalibard (Elsevier, Les Houches, France, 2007), [arXiv:0706.0094](https://arxiv.org/abs/0706.0094).
 - [4] C. Newman and D. Stein, *Journal of Statistical Physics* **82**, 1113 (1996).
 - [5] G. Parisi, *Statistical Field Theory* (Perseus Books Group, 1998).
 - [6] E. Marinari, G. Parisi, F. Ricci-Tersenghi, J. Ruiz-Lorenzo, and F. Zuliani, *Journal of Statistical Physics* **98**, 973 (2000).
 - [7] J. P. Bouchaud and G. Biroli, *J. Chem. Phys.* **121**, 7347 (2004).
 - [8] K. Binder and A. Young, *Reviews of Modern Physics* **58**, 801 (1986).
 - [9] M. Mézard, G. Parisi, and M. A. Virasoro, *Spin glass theory and beyond* (World Scientific, Singapore, 1987).
 - [10] K. Fischer and J. Hertz, *Spin Glasses* (Cambridge University Press, 1991).
 - [11] L. F. Cugliandolo and J. Kurchan, *Phys. Rev. Lett.* **71**, 173 (1993).
 - [12] L. Cugliandolo, in *Slow relaxations and nonequilibrium dynamics in condensed matter*, edited by J. Barrat, M. Feigelman, J. Kurchan, and J. Dalibard (Springer-Verlag, Les Houches, France, 2003), [arXiv.org:cond-mat/0210312](https://arxiv.org/abs/cond-mat/0210312).
 - [13] J. Bouchaud, L. Cugliandolo, J. Kurchan, and M. Mezard, in *Spin glasses and random fields*, edited by A. Young (World Scientific Pub Co Inc, 1998), [arXiv.org:cond-mat/9702070](https://arxiv.org/abs/cond-mat/9702070).
 - [14] F. Guerra, *Communications in mathematical physics* **233**, 1 (2003).
 - [15] M. Talagrand, *Spin glasses: a challenge for mathematicians: cavity and mean field models* (Springer, 2003).
 - [16] S. Franz and F. Tria, *Journal of Statistical Physics* **122**, 313 (2006).
 - [17] L. Leuzzi and T. Nieuwenhuizen, *Thermodynamics of the glassy state* (Taylor & Francis, 2007).
 - [18] A. Cavagna, *Physics Reports* **476**, 51 (2009).
 - [19] G. Biroli and J. Bouchaud, [arXiv.org:0912.2542](https://arxiv.org/abs/0912.2542) (2009).

- [20] K. A. Dawson, G. Foffi, F. Sciortino, P. Tartaglia, and E. Zaccarelli, *Journal of Physics: Condensed Matter* **13**, 9113 (2001).
- [21] M. Müller and L. Ioffe, *Physical Review Letters* **93**, 256403 (2004).
- [22] Y. Kohsaka, C. Taylor, K. Fujita, A. Schmidt, C. Lupien, T. Hanaguri, M. Azuma, M. Takano, H. Eisaki, H. Takagi, et al., *Science* **315**, 1380 (2007).
- [23] M. Tarzia and G. Biroli (2008), [arXiv.org:0802.2653](https://arxiv.org/abs/0802.2653).
- [24] L. Fallani, C. Fort, and M. Inguscio (2008), [arXiv.org:0804.2888](https://arxiv.org/abs/0804.2888).
- [25] S. Balibar and F. Caupin, *Journal of Physics: Condensed Matter* **20**, 173201 (2008).
- [26] L. Angelani, C. Conti, G. Ruocco, and F. Zamponi, *Physical Review Letters* **96**, 65702 (2006).
- [27] A. Mehta (Ed.), *Granular Matter: An Interdisciplinary Approach* (New York: Springer, 1994).
- [28] J. Amit, *Modeling brain function* (Cambridge University Press New York, 1989).
- [29] J. D. Bryngelson and P. G. Wolynes, *Proceedings of the National Academy of Sciences* **84**, 7524 (1987).
- [30] S. Takada and P. G. Wolynes, *Phys. Rev. E* **55**, 4562 (1997).
- [31] P. G. Wolynes, *Philosophical Transactions of the Royal Society A: Mathematical, Physical and Engineering Sciences* **363**, 453 (2005).
- [32] S. Cocco, S. Leibler, and R. Monasson, *Proceedings of the National Academy of Sciences* **106**, 14058 (2009).
- [33] V. Sessak and R. Monasson, *Journal of Physics A: Mathematical and Theoretical* **42**, 055001 (2009).
- [34] M. Weigt, R. White, H. Szuromant, J. Hoch, and T. Hwa, *Proceedings of the National Academy of Sciences* **106**, 67 (2009).
- [35] T. Mora, A. Walczak, W. Bialek, and C. Callan Jr, *Proceedings of the National Academy of Sciences* (2010).
- [36] N. Halabi, O. Rivoire, S. Leibler, and R. Ranganathan, *Cell* **138**, 774 (2009).
- [37] R. Monasson, in *Complex Systems*, edited by J. Bouchaud, M. Mézard, and J. Dalibard (Elsevier, Les Houches, France, 2007), [arXiv:0704.2536](https://arxiv.org/abs/0704.2536).
- [38] C. Papadimitriou and K. Steiglitz, *Combinatorial Optimization: Algorithms and Complexity* (Courier Dover Publications, 1998).
- [39] G. Santoro and E. Tosatti, *Journal of Physics A: Mathematical and General* **39**, R393 (2006).
- [40] E. Farhi, J. Goldstone, S. Gutmann, J. Lapan, A. Lundgren, and D. Preda, *Science* **292**, 472 (2001).
- [41] D. Sherrington and S. Kirkpatrick, *Physical Review Letters* **35**, 1792 (1975).
- [42] L. Viana and A. Bray, *Journal of Physics C: Solid State Physics* **18**, 3037 (1985).
- [43] M. Mézard and G. Parisi, *Eur. Phys. J. B* **20**, 217 (2001).
- [44] M. Mézard and G. Parisi, *J. Stat. Phys.* **111**, 1 (2003).
- [45] S. Franz and M. Leone, *Journal of Statistical Physics* **111**, 535 (2003).
- [46] T. Castellani and A. Cavagna, *Journal of Statistical Mechanics: Theory and Experiment* **2005**, P05012 (2005).
- [47] J. Langer, *Annals of Physics*, 54 (1969).
- [48] G. Gallavotti, *Statistical Mechanics. A short treatise* (Springer Verlag, Berlin, 2000).
- [49] D. Thouless, P. Anderson, and R. Palmer, *Philosophical Magazine* **35**, 593 (1977).
- [50] C. De Dominicis and I. Giardinà, *Random Fields and Spin Glasses: A Field Theory Approach* (Cambridge University Press, 2006).
- [51] A. Georges and J. S. Yedidia, *Journal of Physics A: Mathematical and General* **24**, 2173 (1991).
- [52] T. Plefka, *Europhysics Letters* **58**, 892 (2002).
- [53] A. Crisanti and H.-J. Sommers, *Zeitschrift für Physik B Condensed Matter* **87**, 341 (1992).
- [54] L. Cugliandolo and D. Dean, *Journal of Physics A: Mathematical and General* **28**, 4213 (1995).
- [55] G. Biroli, *Journal of Physics A: Mathematical and General* **32**, 8365 (1999).
- [56] R. Monasson, *Phys. Rev. Lett.* **75**, 2847 (1995).
- [57] M. Mézard, *Physica A* **265**, 352 (1999).
- [58] J. Kurchan, G. Parisi, P. Urbani, and F. Zamponi, *J. Phys. Chem. B* **117**, 12979 (2013).
- [59] J. de Almeida and D. Thouless, *Journal of Physics A: Mathematical and General* **11**, 983 (1978).
- [60] T. Rizzo, in preparation (2013).
- [61] U. Ferrari, L. Leuzzi, G. Parisi, and T. Rizzo, *Phys. Rev. B* **86**, 014204 (2012).
- [62] A. Bray and M. Moore, *Journal of Physics C: Solid State Physics* **13**, L469 (1980).
- [63] G. Parisi, in *Mathematical statistical physics*, edited by A. Bovier, F. Dunlop, A. V. Enter, F. D. Hollander, and J. Dalibard (Elsevier, Les Houches, France, 2005), [arXiv.org:cond-mat/0602349](https://arxiv.org/abs/cond-mat/0602349).
- [64] B. Derrida, *Phys. Rev. B* **24**, 2613 (1981).
- [65] A. J. Bray and M. A. Moore, *Journal of Physics C: Solid State Physics* **12**, 79 (1979).
- [66] S. Janson, *Random graphs* (John Wiley New York, 2000).
- [67] N. Wormald, *Surveys in Combinatorics* **276**, 239 (1999).
- [68] F. Krzakala and L. Zdeborová, *EPL (Europhysics Letters)* **81**, 57005 (2008).
- [69] M. Mézard and R. Zecchina, *Phys. Rev. E* **66**, 056126 (2002).
- [70] S. Mertens, M. Mézard, and R. Zecchina, *Random Struct. Algorithms* **28**, 340 (2006).
- [71] F. Krzakala, A. Montanari, F. Ricci-Tersenghi, G. Semerjian, and L. Zdeborova, *Proceedings of the National Academy of Sciences* **104**, 10318 (2007), <http://www.pnas.org/cgi/reprint/104/25/10318.pdf>.
- [72] M. Mézard, F. Ricci-Tersenghi, and R. Zecchina, *J. Stat. Phys.* **111**, 505 (2003).
- [73] S. Cocco, O. Dubois, J. Mandler, and R. Monasson, *Phys. Rev. Lett.* **90**, 047205 (2003).
- [74] O. Dubois and J. Mandler, *Comptes rendus-Mathématique* **335**, 963 (2002).
- [75] F. Ricci-Tersenghi, M. Weigt, and R. Zecchina, *Phys. Rev. E* **63**, 026702 (2001).

- [76] L. Zdeborová and F. Krzakala, *Physical Review E (Statistical, Nonlinear, and Soft Matter Physics)* **76**, 031131 (pages 29) (2007).
- [77] A. Montanari and G. Semerjian, *J. Stat. Phys.* **125**, 23 (2006).
- [78] G. Semerjian, *J. Stat. Phys.* **130**, 251 (2008).
- [79] F. R. Kschischang, B. J. Frey, and H.-A. Loeliger, *IEEE Trans. Inf. Theory* **47**, 498 (2001).
- [80] J. S. Yedidia, W. T. Freeman, and Y. Weiss, *Advances in Neural Information Processing Systems* **13**, 689 (2001).
- [81] G. Biroli and M. Mézard, *Phys. Rev. Lett.* **88**, 025501 (2001).
- [82] A. Dembo and A. Montanari, *Ann. Appl. Probab.* **20**, 565 (2010).
- [83] A. Braunstein, R. Mulet, A. Pagnani, M. Weigt, and R. Zecchina, *Physical Review E* **68**, 36702 (2003).
- [84] A. Montanari, F. Ricci-Tersenghi, and G. Semerjian, *Journal of Statistical Mechanics: Theory and Experiment* **2008**, P04004 (41pp) (2008).
- [85] M. Mézard and A. Montanari, *Information, Physics and Computation* (Oxford University Press, 2009).
- [86] A. Montanari and G. Semerjian, *J. Stat. Phys.* **124**, 103 (2006).
- [87] L. Cugliandolo and J. Kurchan, *Journal of Physics A: Mathematical and General* **41**, 4018 (2008).
- [88] A. Montanari and F. Ricci-Tersenghi, *Phys. Rev. B* **70**, 134406 (2004).
- [89] L. Zdeborová and F. Krzakala, *Phys. Rev. B* **81**, 224205 (2010).
- [90] F. Altarelli, R. Monasson, G. Semerjian, and F. Zamponi, in *Handbook of Satisfiability, Frontiers in Artificial Intelligence and Applications*, edited by A. Biere, M. Heule, H. van Maaren, and T. Walsh (IOS Press, 2009), [arXiv:0802.1829](https://arxiv.org/abs/0802.1829).
- [91] F. Krzakala and J. Kurchan, *Physical Review E (Statistical, Nonlinear, and Soft Matter Physics)* **76**, 021122 (pages 13) (2007).
- [92] M. Mézard and G. Parisi, *Journal of Physics: Condensed Matter* **12**, 6655 (2000).
- [93] G. Parisi and F. Zamponi, *Rev. Mod. Phys.* **82**, 789 (2010).
- [94] V. Lubchenko and P. G. Wolynes, *Annual Review of Physical Chemistry* **58**, 235 (2007), [arXiv.org:cond-mat/0607349](https://arxiv.org/abs/cond-mat/0607349).
- [95] M. Mézard and G. Parisi, *The Journal of Chemical Physics* **111**, 1076 (1999).
- [96] S. Franz and G. Parisi, *Journal of Physics: Condensed Matter* **12**, 6335 (2000).
- [97] L. Berthier, G. Biroli, J. Bouchaud, W. Kob, K. Miyazaki, and D. Reichman, *The Journal of chemical physics* **126**, 184503 (2007).
- [98] L. Berthier, G. Biroli, J. Bouchaud, W. Kob, K. Miyazaki, and D. Reichman, *The Journal of chemical physics* **126**, 184504 (2007).
- [99] S. Franz, *Journal of Statistical Mechanics: Theory and Experiment* **2005**, P04001 (2005).
- [100] S. Franz, *Journal of Statistical Physics* **126**, 765 (2007).
- [101] S. Franz and A. Montanari, *Journal of Physics A: Mathematical and Theoretical* **40**, F251 (2007).
- [102] D. S. Fisher and D. A. Huse, *Phys. Rev. B* **38**, 386 (1988).
- [103] G. Parisi, *Journal of Physics A: Mathematical and Theoretical* **41**, 324002 (2008), [arXiv:0711.0369](https://arxiv.org/abs/0711.0369).
- [104] G. Parisi, *Physica A: Statistical Mechanics and its Applications* **386**, 611 (2007), ISSN 0378-4371, proceedings of the Pan American Scientific Institute (PASI) Conference *Disorder and Complexity*, Mar del Plata, Argentina, 11–20 December 2006, [arXiv:0710.1091](https://arxiv.org/abs/0710.1091).
- [105] L. Berthier, J. Barrat, and J. Kurchan, *Physical Review E* **61**, 5464 (2000).
- [106] L. Berthier and J. Barrat, *The Journal of Chemical Physics* **116**, 6228 (2002).
- [107] L. F. Cugliandolo, D. R. Grempel, and C. A. da Silva Santos, *Phys. Rev. B* **64**, 014403 (2001).
- [108] G. Biroli and L. F. Cugliandolo, *Phys. Rev. B* **64**, 014206 (2001).
- [109] C. Laumann, A. Scardicchio, and S. L. Sondhi, *Phys. Rev. B* **78**, 134424 (2008).
- [110] F. Krzakala, A. Rosso, G. Semerjian, and F. Zamponi, *Phys. Rev. B* **78**, 134428 (2008).